Targeting Schlemm's canal endothelium to modulate aqueous humour outflow facility as a potential treatment for glaucoma

ESTER REINA-TORRES

SUPERVISOR: DR. DARRYL R. OVERBY

IMPERIAL COLLEGE OF SCIENCE, TECHNOLOGY AND MEDICINE
DEPARTMENT OF BIOENGINEERING

DATE: 19TH OF FEBRUARY 2016

Submitted in fulfillment of the requirements for the award of Doctor of Philosophy in Bioengineering and the Diploma of the Imperial College.

Abstract

Glaucoma is an ocular neurodegenerative disease generally associated to sustained elevated intraocular pressure (IOP). Lowering IOP is the only suitable therapeutic strategy for glaucoma but current treatments do not target the root cause of elevated IOP: increased aqueous humour outflow resistance.

The mechanisms involved in outflow resistance generation are not fully understood. It is thought that resistance is generated at the vicinity of the juxtacanalicular connective tissue, the inner wall of Schlemm's canal (SC) and its basement membrane. We hypothesise that the continuity of SC endothelium, and especially its pores, are key regulators of outflow resistance. To test this hypothesis, we assessed the role of physiological processes known to be relevant for pore formation by measuring changes in outflow facility (C) using the newly developed iPerfusion system.

First, we showed that vascular endothelial growth factor (VEGF) is involved in C regulation and that steroid-treated mice have altered VEGF signaling, potentially contributing to outflow dysfunction and ocular hypertension. Second, we demonstrated that down regulation of plasmalemmal vesicle-associated protein results in reduced C, probably because of impaired ability to form intracellular pores. Third, we proved that the inhibition of tight junction related proteins results in increased C and lower IOP. Additionally, we also examined the effects of anesthetics on IOP and we propose a new protocol to measure IOP by rebound tonometry.

Altogether, these studies support the idea that the inner wall of SC plays a crucial regulatory role in aqueous humour outflow resistance. Therefore, targeting SC endothelium and more precisely the mechanisms of pore formation may provide a new therapeutic approach for ocular hypertension.

(*Word Count: 263*)

Tingues sempre al cor la idea d'Ítaca.

Keep Ithaka always in your mind.

Konstantinos Kavafis (1911)

TO MY PARENTS AND BROTHER, MY ROLE MODELS.

Acknowledgements

I am very thankful to Dr. Darryl Overby, first, for giving me the opportunity to do a PhD with him when I was about to give up. And second, for his constant support, guidance and enthusiasm during these years, he has been very encouraging.

I would also like to thank Prof. Ernst Tamm (University of Regensburg) and Prof. Pete Humphries (Trinity College Dublin) for their implication in the projects we worked together as well as Dr. Leonie Herrnberger (University of Regensburg), Dr. Lawrence Tam and Mr. Paul Cassidy (Trinity College Dublin), it has been a pleasure working with them. Moreover, I would also like to thank Prof. Dan Stamer (Duke University) for his always valuable comments.

I am infinitely thankful to all former and current members of the Overby lab for their help and support in the lab and for every lunch and beer we have had together:

• To Dr. Alexandra Boussommier-Calleja for initiating me into mouse eye perfusions.
• To Dr. Sietse Braakman for all those discussions about any possible topic.
• To Dr. Cristoforo Silvestri for sharing the status of ”these weird biologists” with me.
• To Dr. Joseph Sherwood for all I have learnt from him because of the adventure that has been the *iPerfusion*.
• To Dr. Jason Chang for sharing the pain of writing a thesis and for challenging my optimism all the time.
• To Jacques Bertrand for always having everything under control.
• To Alice Spenlehauer and Anabela Cepa Areias for the light they bring to our windowless office.
• To Michael Madekurozwa for sharing my passion for football and always being so considerate.
• To Kathy (Pei-Jung) Wu for always having a smile ready.
• To my dearest bubbles, for making me even more patient and perseverant.

London would not have been the same without Carla, Francesc, Gerard and Pol, having them around feels like being at home. And specially to Anna, we definitely managed to domesticate this wild city.

Equally important had been my friends back home. A big thank you to my favorite biotechnologists; Adriana, Cristina and Gemma, for always being so close. And to Francesc, Moni, Eli, Sergi, Mariona, Santi, Roger and Jordi, for being there for me after more than 15 years.

Last but not least, I could not have arrived here without my family. Specially my parents, for the efforts they made to support my brother and me during our education and because they always prioritise our happiness, even though it implies having us away.

Contribution Statement

Several researchers have contributed to the work presented in this thesis. Their contributions have been acknowledged below:

Chapters 2 to 5: All perfusions done in these chapters were carried out using the iPerfusion system designed and developed by Dr. Joseph M. Sherwood. He also analysed the data and generated the figures.

Chapter 2: Dr. Jason Chang assisted with confocal microscopy.

Chapter 3: Mr. Jacques Bertrand trained me on how to implant the osmotic mini-pumps and assisted with the cohort of mice treated with 0.1 mg/kg/day.

Chapter 4: Mr. Jacques Bertrand did the genotyping of the mice and did initial IOP measurements. Dr. Herrnberger (Regensburg University) provided assistance importing the PLVAP transgenic mice into Imperial College London.

Chapter 5: Dr. Lawrence Tam (Trinity College Dublin) trained me on how to perform intracameral injections and participated in the injections of the first cohort of mice. Mr. Paul Cassidy (Trinity College Dublin) has assisted on all siRNA injections and measurements of outflow facility. Moreover, he collaborated with the IOP measurement performed at Trinity College Dublin. Dr. Jason Chang assisted with the siRNA injections performed to measure IOP under isoflurane anesthesia and helped generating the tracers maps. Dr. Joseph M. Sherwood analysed the data regarding the IOP measurements under isoflurane anesthesia and generated Figure.5.1, Figure.5.4 and Figure.5.5.

Chapter 6: Mr. Paul Cassidy (Trinity College Dublin) collaborated with the IOP decays performed with the iPerfusion system, which were carried out at Trinity College Dublin.

Copyright and Financial Disclosure

I hereby declare that the studies presented in this thesis are my own work, performed in Dr. Overby's laboratory between October 2012 and December 2015. All data, results and figures from third party works have been referenced. Contributions by other researchers are specified in the Contribution Statement. I certify that this thesis complies with copyright laws and does not contain any instance of plagiarism. I have granted permission to reprint Figures 1.1, 1.2, 1.3, 1.4, 1.5, 1.6, 1.7 and 1.8 in this thesis. Transcripts of all permissions are included in Appendix II.

This study was supported by a PhD scholarship Fight for Sight (Ref 1385) and a National Glaucoma Research Grant, Bright Focus Foundation, formerly AHAF (G2013-0248) obtained by Dr. Overby. Moreover, financial support was also provided by Professor Peter Humphries (Trinity College Dublin) under the European Research Council Advanced Grant 2012.

The Academic Regulations 2015/16 from Imperial College London state:
The copyright of this thesis rests with the author and is made available under a Creative Commons Attribution-Non Commercial-No Derivatives licence. Researchers are free to copy, distribute or transmit the thesis on the condition that they attribute it, that they do not use it for commercial purposes and that they do not alter, transform or build upon it. For any reuse or distribution, researchers must make clear to others the license terms of this work.

Associated Publications

Refereed Journal Publications:

- Sherwood JM, **Reina-Torres E**, Bertrand JA, Rowe B, Overby DR (2016) Measurement of Outflow Facility Using *iPerfusion*. *PLoS ONE* 11(3): e0150694. doi:10.1371/journal.pone.0150694
- **Reina-Torres E**, Wen JC, Liu K, Li G, Sherwood JM, Stamer WD, Allingham RR, Overby DR. Anti-VEGF Therapy Causes Ocular Hypertension by Reducing Aqueous Humor Outflow Facility. In preparation, to be submitted to *Journal of Clinical Investigation*
- Tam LCS, **Reina-Torres E**[1], Sherwood JM, Cassidy P, Crosbie D, Perkuma K, Humphries MM, Kiang AS, Read T, Ethier CR, Lutjen-Drecöll E, Callahan S, O'Brien C, Lawrence M, Campbell M, Stamer WD, Overby DR, Humphries P. Dynamic remodeling of Schlemm's canal endothelial cell tight junctions in glaucomatous eye disease. In submission.

Conference Presentations:

- **Reina-Torres E**, Sherwood JM, Overby DR **(2016)**. The role of VEGF on outflow facility in mice with glucocorticoid-induced ocular hypertension. *The Association of Research in Vision and Ophthalmology Conference*, Seattle, USA; Oral presentation.
- Madekurozwa M, Sherwood JM, **Reina-Torres E**, Bertrand JA, Overby DR **(2016)**. Pressure-independent outflow in ex vivo mouse eyes. *The Association of Research in Vision and Ophthalmology Conference*, Seattle, USA
- Sherwood JM, **Reina-Torres E**, Bertrand J, Ethier CR, Overby DR **(2015)** Extracting mechanical properties of the cornoescleral shell from whole eye perfusion. *Summer Biomechanics, Bioengineering and Biotransport Conference*, Utah, USA
- **Reina-Torres E**, Herrnberger L, Sherwood JM, Tamm ER, Overby DR **(2015)**. The Influence of Plasmalemma Vesicle-Associated Protein on Conventional Outflow Facility in Mice. *The Association of Research in Vision and Ophthalmology Conference*, Denver, USA; Oral presentation. Awarded with an ARVO International travel grant.
- Overby DR, **Reina-Torres E**, Wen JC, Liu K, Li G, Sherwood JM, Allingham RR, Stamer WD **(2015)**. The Effects of VEGF and anti-VEGF on Outflow Facility in Mice

[1] co-first author

and Humans. *The Association of Research in Vision and Ophthalmology Conference*, Denver, USA

- **Reina-Torres E**, Sherwood JM, Stamer WD, Overby DR **(2014)**. Role of Vascular Endothelial Growth Factor (VEGF) in the regulation of conventional outflow facility in mice. *Medical Engineering Centres Annual Meeting and Bioengineering14*, London, UK; Poster presentation

- **Reina-Torres E**, Sherwood JM, Stamer WD, Overby DR **(2014)**. Role of Vascular Endothelial Growth Factor (VEGF) in the regulation of conventional outflow facility in mice. *The Association of Research in Vision and Ophthalmology Conference*, Orlando, USA; Poster presentation

Contents

Abbreviations ii

1 Introduction and background 1

1.1 Introduction . . . 2

1.2 Background . . . 3

1.2.1 Glaucoma . . . 3

1.2.2 Anatomy of the Eye . . . 4

1.2.3 Outflow pathways . . . 6

1.2.4 The inner wall of Schlemm's canal . . . 10

1.2.5 Aqueous humour dynamics . . . 12

1.2.6 Outflow resistance generation . . . 13

1.2.7 Mouse model for aqueous humour dynamics . . . 16

1.2.8 Vascular Endothelial Growth Factor physiology . . . 20

1.3 Motivation of Thesis . . . 29

1.4 Specific Aims . . . 29

2 The Role of Vascular Endothelial Growth Factor in Murine Conventional Outflow Physiology 31

2.1 Introduction . . . 32

2.2 Materials and Methods . . . 33

2.2.1 Reagents . . . 33

2.2.2 Immunostaining . . . 34

2.2.3 Animal Husbandry . . . 34

2.2.4 *Ex vivo* mouse eye perfusion . . . 35
2.2.5 Outflow facility analysis for *ex vivo* perfusions and statistics . . . 36
2.3 Results . . . 38
2.3.1 Endogenous VEGF Signaling within the Conventional Outflow Pathway. . . . 38
2.3.2 VEGF-A_{164}a Modulates Outflow Facility. . . . 39
2.3.3 Blockade of VEGFR-2 Decreases Outflow Facility. . . . 39
2.3.4 Vegf-D Increases Facility through VEGFR-2. . . . 41
2.3.5 The Facility-Increasing Effect of $Vegf_{164}$a is mediated through both NO and Rac1. . . . 42
2.4 Discussion . . . 44

3 The role of VEGF on outflow facility in mice with glucocorticoid-induced ocular hypertension 47
3.1 Introduction . . . 48
3.2 Materials and Methods . . . 49
3.2.1 Experimental design . . . 49
3.2.2 Animal husbandry and mini-pump implantation . . . 50
3.2.3 IOP measurement . . . 52
3.2.4 *Ex vivo* mouse eye perfusion . . . 52
3.2.5 Statistical analysis . . . 53
3.3 Results . . . 54
3.3.1 Mice treated with 0.1 mg/kg/day DEX . . . 54
3.3.2 Mice treated with 2 mg/kg/day DEX . . . 58
3.3.3 IOP and R correlation . . . 62
3.4 Discussion . . . 64

4 Influence of plasmalemmal vesicle-associated protein on conventional outflow facility in mice 68
4.1 Introduction . . . 69
4.2 Materials and Methods . . . 71

4.2.1 Experimental Design . . . 71
4.2.2 Animal Husbandry . . . 71
4.2.3 IOP measurements. . . . 72
4.2.4 *Ex vivo* Mouse Eye Perfusion . . . 73
4.2.5 Statistical Analysis . . . 74
4.3 Results . . . 75
4.3.1 Effect of PLVAP depletion on outflow facility and IOP in mice . . . 75
4.3.2 Effect of PLVAP-depletion on the outflow facility response to Latrunculin in mice . . . 77
4.3.3 Pore imaging in the inner wall of SC of PLVAP depleted mice . . . 77
4.4 Discussion . . . 78

5 Targeting tight junctions in the inner wall of Schlemm's canal endothelium to modulate outflow facility 81

5.1 Introduction . . . 82
5.2 Materials and Methods . . . 84
5.2.1 Experimental Design . . . 84
5.2.2 Animal Husbandry . . . 85
5.2.3 Pulled Glass micro needles . . . 85
5.2.4 Intracameral Injections . . . 86
5.2.5 *Ex vivo* mouse eye Perfusions . . . 87
5.2.6 IOP measurements . . . 88
5.2.7 Fluorescent tracers patterns . . . 93
5.3 Results . . . 93
5.3.1 *Ex vivo* mouse eye Perfusions . . . 93
5.3.2 IOP measurements . . . 94
5.3.3 Fluorescent tracers patterns . . . 97
5.4 Discussion . . . 99

6 Effects of anesthesia on intraocular pressure in mice 103

6.1 Introduction . . . 104

6.2 Materials and Methods . . . 106
6.2.1 Experimental design . . . 106
6.2.2 Animal Husbandry . . . 106
6.2.3 Tonometric IOP measurement . . . 106
6.2.4 IOP measurements using the iPerfusion system . . . 107
6.3 Results . . . 108
6.3.1 Effect of isoflurane anesthesia on IOP . . . 108
6.3.2 Effect of ketamine/Domitor® anesthesia on IOP . . . 110
6.3.3 Effect of ketamine/xylazine anesthesia on IOP . . . 110
6.4 Discussion . . . 112

7 Conclusions **115**

7.1 Summary . . . 116
7.2 Future work . . . 117
7.2.1 How is VEGF expression controlled? . . . 117
7.2.2 How does VEGF affect the ultrastructure of inner wall of SC? . . . 118
7.2.3 What is the response to long-time exposure to VEGF? . . . 118
7.2.4 Is the effect seen in DEX-treated mice a representation of POAG? . 118
7.2.5 Future applications for the iPerfusion system. . . . 119

Bibliography **120**

Appendices . . . 139
Appendix I: Representative elecrophoresis gel for PLVAP transgenic mice genotyping. . . . 139
Appendix II: Permission Documents for Reprint. . . . 139

List of Figures

1.1 Representation of the human eye. 5

1.2 Representation of the outflow pathways. 7

1.3 The trabecular outflow pathway. 8

1.4 Transmission electron micrograph of Schlemm's canal. 9

1.5 Pores in the inner wall of SC. 11

1.6 TJs and fenestrae in the inner wall of SC. 12

1.7 Funneling model. 15

1.8 VEGFs and VEGFRs interactions. 23

2.1 iPerfusion system set up and perfusion trace 36

2.2 Q *vs.* P and C *vs.* P representative plot 37

2.3 VEGF-A_{164} and CD31 staining in the mouse outflow pathway 39

2.4 Effect of $Vegf_{164}a$ on outflow facility 40

2.5 Effect of VEGFR inhibitors on outflow facility 41

2.6 Effect of Vegf-D on outflow facility 42

2.7 Effect of inhibiting eNOS and Rac1 on outflow facility 43

3.1 IOP evolution during 0.1 mg/kg/day DEX treatment 55

3.2 Weight evolution during DEX treatment 56

3.3 Facility values of eyes from controls and DEX treated mice. 57

3.4 Eyes from 0.1 mg/kg/day DEX treated mice perfused with 500 mg/ml $Vegf_{164}a$ . . 58

3.5 Eyes from 0.1 mg/kg/day DEX treated mice perfused with 500 ng/mL $VEGF_{165}b$. 59

3.6 IOP evolution during 2 mg/ kg/ day DEX treatment 60

3.7 Weight evolution during 2 mg/kg/day DEX treatment 60

3.8 Eyes from 2 mg/kg/day DEX treated mice perfused with 500 mg/ml $Vegf_{164}a$ 61

3.9 Eyes from 2 mg/kg/day DEX treated mice perfused with 1 µg/ml Vegf-D 62

3.10 IOP and outflow resistance correlation. 64

3.11 Effect of all forms of VEGF on eyes from DEX treated mice compared to naïve mice. 66

4.1 Facility values for *Plvap*$^{+/+}$ and *Plvap*$^{+/-}$ mice. 76

4.2 IOP values for *Plvap*$^{+/+}$ and *Plvap*$^{+/-}$ mice. 76

4.3 Effect of Lat-B on facility on *Plvap*$^{+/+}$ and *Plvap*$^{+/-}$ mice. 78

4.4 Scanning electron micrograph of the inner wall of SC 79

5.1 Representative pressure trace to measure sIOP. 91

5.2 Effect of ZO-1 and Tricellulin down regulation on outflow facility of enucleated mouse eyes. 94

5.3 Effect of ZO-1 and Tricellulin down regulation on IOP measured by rebound tonometry under ketamine/xylazine anesthesia. 95

5.4 IOP decays under isoflurane anesthesia. 97

5.5 Effect of ZO-1 and Tricellulin down regulation on IOP measure by rebound tonometry under isoflurane anesthesia. 98

5.6 Fluorescent tracers patterns 99

6.1 IOP decay under isoflurane anesthesia. 109

6.2 IOP decay under ketamine/Domitor® anesthesia. 110

6.3 IOP decay under ketamine/xylazine anesthesia. 111

7.1 Representative gel electrophoresis for PLVAP transgenic mice genotyping. 141

7.2 Permission for reproduction Figure.1.1 143

7.3 Permission for reproduction Figure.1.2 144

7.4 Permission for reproduction Figure.1.3 145

7.5 Permission for reproduction Figure.1.4 146

7.6 Permission for reproduction Figure.1.5 147

7.7 Permission for reproduction Figure.1.6a and Figure.1.7 148

7.8 Permission for reproduction Figure.1.6b 149

7.9 Permission for reproduction Figure.1.8 150

List of Tables

1.1 VEGF concentrations in human aqueous humour 27

3.1 Averaged IOP, R and C values for 3 different groups of mice 64

4.1 IOP and C measurements on *Plvap*$^{+/+}$ and *Plvap*$^{+/-}$ mice 75

5.1 Groups of mice used in this chapter. 85

5.2 Averaged IOP measurements for eyes injected with t-siRNA or nt-siRNA measured by cannulation 96

6.1 Individual tonometric IOP readings for IOP decay under isoflurane anesthesia . . . 109

Abbreviations list

AC	Anterior chamber
AH	Aqueous humour
B-pore	Border pore (paracellular)
C	Outflow facility
C_r	Reference outflow facility
DBG	PBS including divalent cations and 5.5 mM glucose
DEX	Dexamethasone
EVP	Episcleral venous pressure
GCs	Glucocorticoids
IOP	Intraocular pressure
IP	Intraperitoneal injection
I-pore	Intracellular pore
JCT	Juxtacanalicular connective tissue
Lat-B	Latrunculin B
NO	Nitric Oxide
OHT	Ocular hypertension
P	Pressure
PFA	Paraformaldehyde
PLVAP	Plasmalemmal vesicle-associated protein
POAG	Primary open-angle glaucoma
Q	Flow rate
Q_c	Conventional outflow rate
Q_p	Aqueous humour production rate
Q_u	Unconventional outflow rate
R	Outflow resistance
R_c	Conventional pathway outflow resistance
Rac1	Ras-related C3 botulinum toxin substrate 1
SC	Schlemm's canal
SD	Standard deviation
siRNA	Small interfering RNA
TJs	Tight junctions
TM	Trabecular Meshwork

VEGF	Vascular endothelial growth factor
VEGFR	Vascular endothelial growth factor receptor
ZO-1	Zonula occludens 1

Chapter 1

Introduction and background

1.1 Introduction

Glaucoma is a neurodegenerative ocular disease characterised by optic nerve damage that, if left untreated, can lead to irreversible blindness. Sustained elevation in intraocular pressure (IOP) is the principal risk factor for glaucoma and the only feature that can be treated since optic nerve damage is irreversible[172]. Clinically, there is a need for better and early detection of glaucoma in order to reduce IOP before the optic nerve is damaged. Furthermore, more effective treatments are also need. These treatments should target the root cause of elevation in IOP, increased outflow resistance and, ideally, overcome the unknown cause leading to increased outflow resistance[70]. To achieve this objective, it is still necessary to gain an understanding on how outflow resistance and IOP are regulated. IOP is defined by the rate of production of aqueous humour (AH) and the resistance opposed to its drainage by the tissues of the outflow pathway[276]. It is known that the elevation in IOP observed in glaucoma is due to an increase in resistance to AH outflow[117]. However, the exact factors causing the increase in outflow resistance still remain unknown.

The AH exits the eye at the iridocorneal angle, in the anterior chamber, mostly through the conventional outflow pathway. The conventional outflow pathway consist of the trabecular meshwork (TM), juxtacanalicular connective tissue (JCT), Schlemm's canal (SC) and post-trabecular pathway. AH percolates through the filter-like tissue of the TM and JCT into SC, where it flows circumferentially until it drains to blood circulation via the post-trabecular pathway[141]. The exact component of the outflow pathway that confers resistance to AH outflow are not clear, but it is though to be in the vicinity of JCT, inner wall of SC and its basement membrane[148,210,277]. The physical proximity of these three components make it difficult to discern which one is responsible for the increased resistance observed in glaucoma. Nevertheless, evidence seem to indicate that SC endothelium plays an important role. The inner wall of SC is a continuous endothelium containing tight junctions (TJs) and micron-sized pores[95], pore formation seems to be impaired in glaucomatous eyes, which may contribute to their increased resistance[151,211]. However, the mechanism of pore formation are not fully understood.

Two types of pores are found in the inner wall endothelium of SC: paracellular

(B-pores) and intracellular pores (I-pores)[91]. The nature of each type of pore appears to be different. While B-pores may form from disassembly of cellular junctions, I-pores may form from pre-existing ”mini-pores” similar to the fenestra found in other vascular tissues. Theoretically, the modulation of pore formation should modify the hydraulic conductance of SC endothelium and affect outflow resistance[210].

Vascular endothelial growth factor (VEGF) is an important cytokine known to enhance hydraulic conductivity in endothelial linings[28] by promoting the formation of both paracellular[110] and intracellular spaces[233]. VEGF receptors (VEGFR) are expressed by SC cells[16,220,242], VEGF is found in the AH[69,288] and TM cells can produce VEGF[104]. These evidence lead to think that VEGF may play a role regulating outflow resistance.

1.2 Background

1.2.1 Glaucoma

Glaucoma is a group of chronic neurodegenerative diseases characterised by visual field loss because of damage of the optic nerve head. Glaucoma is asymptomatic at early stages until the disease is very advanced and vision loss already affects the patient's normal life, for this reason, it is still under diagnosed. Optic nerve damage can be prevented but once the retinal ganglion cells in the optic nerve head are dead vision loss is irreversible. Therefore, an early diagnosis of the disease is crucial. The National Health Service estimates that around 500,000 people suffer from it in the United Kingdom (2015), while it is thought to affect 60 million people worldwide[227], being the second leading cause of blindness after cataracts[231].

Different forms of glaucoma are classified according to the anatomy of the irido-corneal angle. Glaucoma is defined as open-angle if the angle is normally open and the AH can access the outflow pathways whereas it is defined as closed-angle if the outflow pathway is physically blocked because the angle is abnormally closed. Both open and closed angle can then be divided between primary or secondary depending on the origin

of the problem, it is secondary when glaucoma is caused by another existing pathology, this is the case of neovascular glaucoma, pigmentary glaucoma and exfoliation glaucoma, among others[172]. Glaucomas are characterised by elevated IOP. However, in a few cases, the optic nerve is found to be damaged without IOP elevation, this form of the disease is known as normal-tension glaucoma. Nevertheless, all these forms have in common that biomechanical insult lead to apoptosis of the retinal ganglion cells (RGC) at the lamina cribrosa resulting in ”cupping” of the optic nerve head[172].

Primary open angle glaucoma (POAG) is the most common form of glaucoma. POAG is a multifactorial disease where elevated IOP is the primarily risk factor and the only treatable feature, in fact, reduction of IOP has been shown to improve visual field[281]. POAG is characterised by a sustained and gradual IOP elevation. Elevated IOP is a consequence of increased AH outflow resistance[117]. Although studies have reported that the pore density in SC is reduced in both human glaucomatous eyes[146,150] and cultured SC cells from patients suffering glaucoma[211] the underlying reasons for impaired pore formation in glaucoma and the link to increased outflow resistance are not fully understood. Nevertheless, current research indicated that cellular stiffness is a key factor[211].

Current treatments aiming to reduce IOP include reduction of AH production and promotion of alternative drainage routes either by pharmacological or surgical means[70]. The most effective drugs are prostaglandins analogues (commercially known as latanoprost, bimatoprost or travaprost, to mention a few), these compounds are known to enhance both the uveoscleral and the trabecular pathways[306]. Other medications reduce AH production, these are β blockers (timolol, betaxolol or carteolol), α-2 selective α agonists (apraclonidine or brimonidine) and carbonic anhydrase inhibitors (brinzolamide or acetazolamide diamox). Moreover, IOP can be lowered surgically, using laser therapies, or implanting drainage devices[70].

1.2.2 Anatomy of the Eye

The eye is a complex organ that enables sight. For vision to occur, light has to cross a number of transparent tissues and fluids through the eye and reach the retina at the back. There, the photoreceptors convert light into electric signals that are transmitted

to the brain through the optic nerve[164]. For this function to succeed, the shape and the correct function of every individual part of the eye is essential.

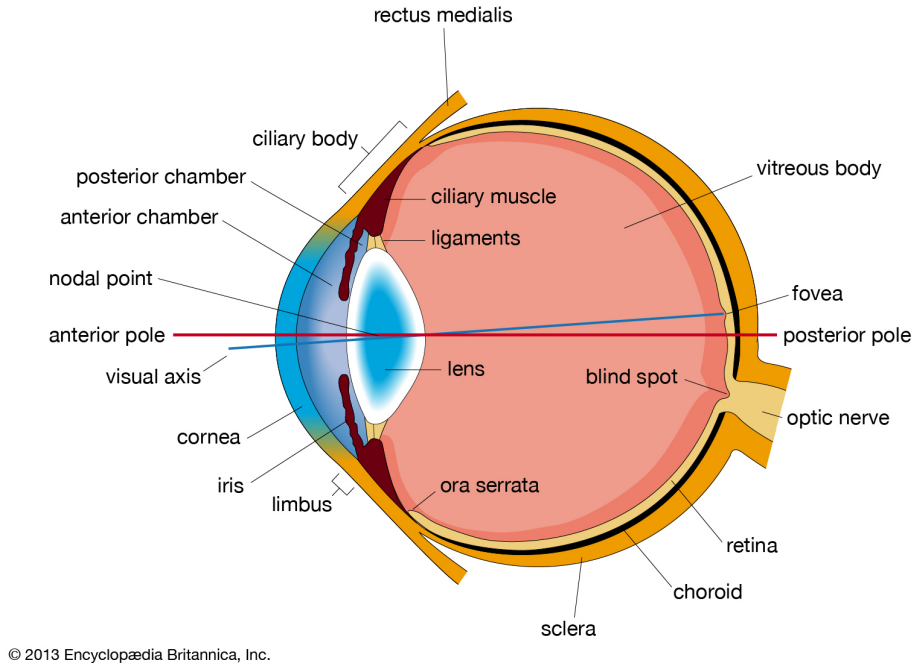


Figure 1.1: Representation of the human eye. Schematic representation of a cross-section of the human eye. Reproduced with permission from *"eye, human: horizontal section"*. *Encyclopædia Britannica Online. 20 Oct. 2015.*

As can bee seen from Figure.1.1, the outer part of the eye is composed of the sclera and the cornea. The sclera is the opaque white shell that forms the majority of the eye ball, while the cornea is the transparent frontal part that allows light into the eye. The place where the cornea and the sclera converge is known as the limbus. The space between the cornea and the iris is defined as the anterior chamber (AC). The AC is filled with AH that nourishes the anterior tissues and pressurises the eye. Between the iris and the lens there is the posterior chamber, delimited at the edges by the ciliary body. Behind the iris, there is the lens, responsible for focusing the light. Posteriorly, there is the vitreous, a transparent gel that occupies almost 80% of the eye, although it is not strictly necessary for vision, it contributes to maintain the shape of the eye by, for example, keeping the retina attached to the choroid. The choroid is a vascular layer that supplies oxygen and nutrients to the retina. The retina is a complex multi-layered structure, including the photoreceptors (cones and rods) responsible for sensing the light by transforming light into electrical signals. The fovea (or macula lutea) is a particular area

of the retina populated exclusively with cones where accurate vision takes place. From the retina emerges the optic nerve, which carries electric pulses to the visual centers in the brain. Because in mammals the nerve fibers are located before the photoreceptors, there are no photoreceptors in the optic nerve head, where the fibers converge to exit the eye ball, for this reason, the optic nerve head is considered a blind spot. The optic nerve head consists mostly of axons from RGC, which transduce the electric signals to the brain[160,164,219].

The eye receives supply of nutrients and oxygen from the ophthalmic artery, which branches into the retinal and the uveal vascular system. The retinal vascular system supplies the inner retina through the central retinal artery. The uveal vascular system can be divided between the anterior uveal circulation, which nourishes the iris and ciliary body, and the posterior uveal circulation, which supplies the choroid and, hence, the outer retina[92,164].

1.2.3 Outflow pathways

There is a constant circulation of AH in the anterior segment of the eye. Its function is to provide nutrients and oxygen to the tissues forming the AC as well as clear out residues and cell waste. Moreover, it is also responsible for keeping the eye pressurised at around 15 mmHg (physiological IOP, 15 ± 2.6 mmHg[92]), essential for maintaining the curvature of the cornea, thus preserving the refractive properties of the eye. AH is produced by the non-pigmented epithelium of the ciliary process in the posterior chamber[63], it flows between the iris and the lens and enters the AC through the pupil. There, it exits the eye at the iridocorneal angle (where the iris and inner part of the cornea meet) either through the trabecular or the uveoscleral pathway to the episcleral vein (See Figure.1.2). The outflow pathways are described in more detail below.

Trabecular outflow pathway

The trabecular outflow pathway (also known as the conventional pathway) drains most of the AH from the anterior chamber[92,112,152]. To leave the eye, the AH crosses the

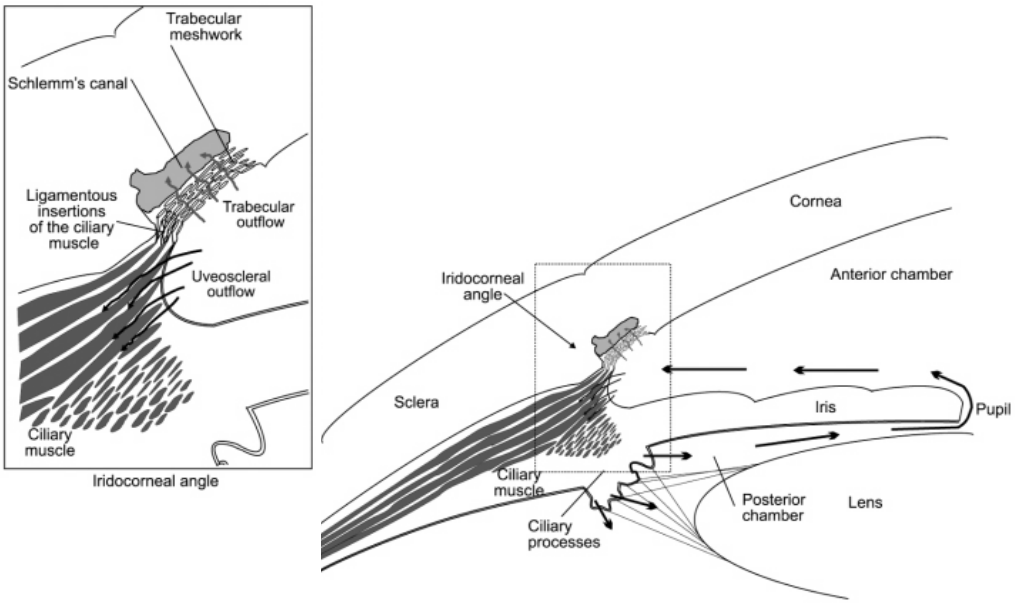


Figure 1.2: Representation of the AH circulation and the outflow pathways. Schematic representation of the AH circulation in the anterior segment, being produced by the ciliary precesses and drained in the iridocorneal angle. The insert represents the iridocorneal angle at greater detail, differentiating the trabecular pathway from the uveoscleral and showing the main structures involved in each one. Reproduced with permission from Llobet *et al.* (2003)[178].

sieve-like tissue that is the trabecular meshwork (TM) as bulk flow and it flows through the inner wall of Schlemm's canal (SC) to enter its lumen where AH circulates circumferentially. The AH is then drained through the collector channels into blood circulation (post-trabecular pathway). This drainage route is considered pressure dependent since the outflow rate increases in response to elevated IOP. As it is described in detail in the section "Resistance generation" (1.2.6), the resistance to outflow conferred by these tissues define IOP.

Trabecular Meshwork

The TM is the tissue that connects the anterior chamber with the inner wall of SC and extends between the stroma of the iris, ciliary body, sclera spur and the Schwalbe's line at the interior edge of the cornea. The TM has a depth of 100 - 200 µm and three layers can be differentiated: the inner one is the **uveal meshwork**, the central one is the **cornoescleral meshwork** and the outer one, which is in contact with SC, is the **juxtacanicular connective tissue** (JCT, or cribriform meshwork)[114,275]. The spacings between these structures become narrower as they approach the SC, this allows filtering

of the AH and avoid that impurities (e. g. cell debris or pigment granulates from the iris) clog further tissues that have smaller spaces for AH to flow. The TM has phagocytic properties[53] and it is considered to be a ”self-cleaning” filter.

The uveal and cornoescleral meshwork are made of lamellae positioned perpendicularly to the flow (see Figure.1.3). These lamellae, composed by collagen, elastin and proteoglycans, are covered with a continuos layer of vascular-derived TM cells, which have a continuous basement membrane rich in collagen type IV, laminin and fibronectin[178,275,312]. The JCT is slightly different in terms of cells and extracellular matrix (ECM) arrangements. JCT cells do not grow on lamellae, are more tight and cells are embedded in an ECM of collagen type IV, laminin, fibronectin, proteoglycans and glycosaminoglycans (GAGs)[114,210], this, makes the JCT a more irregular connective tissue with narrower spaces for AH to flow than the layers below. The JCT and the inner wall of SC are connected through tangentially arranged elastic fibers (cribriform plexus)[237]. The connection between the JCT and SC is believed to be key for outflow resistance generation[243,275].

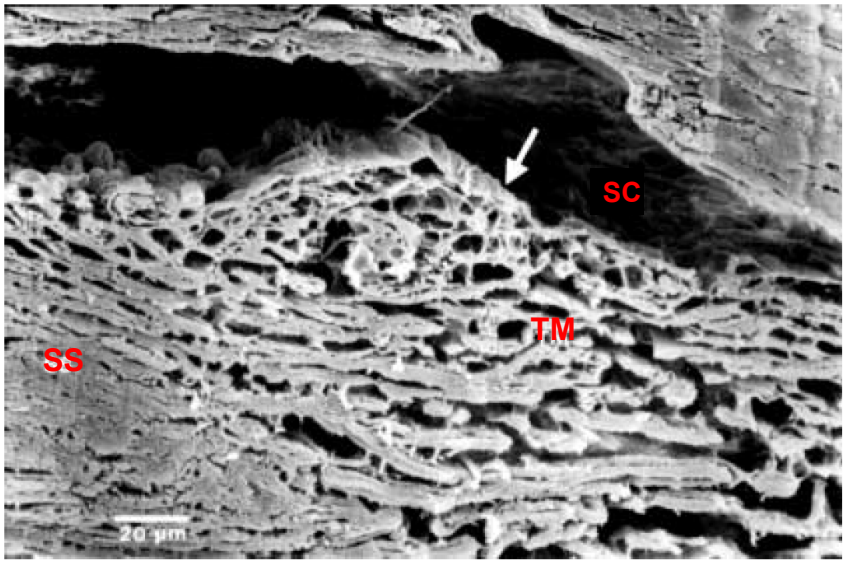


Figure 1.3: The trabecular outflow pathway. Scanning electron micrograph of a cross-section of human trabecular outflow tissues. Arrow: inner wall of SC; SS: scleral spur; SC: Schlemm's canal lumen; TM; trabecular meshwork. Reproduced with permission from Ethier *et al.* (2002)[95].

Schlemm's canal

SC is a vessel made of a monolayer of endothelial cells that encircles the eye

at the limbus. SC has two well differentiated parts: the **inner wall** and the **outer wall**. The inner wall is in contact with the JCT and at the opposite side there it the outer wall. Collector channels emerge from the outer wall. SC receives the AH filtered through the TM driven by pressure gradient. Once AH is in the lumen of the canal, it circulates circumferentially until it drains through the collector channels and aqueous vein.

As can be seen from Figure.1.4, the distinctive forces that the inner and outer wall are subjected to, give them a very different appearance. The inner wall experiences the bulk of AH crossing it in a basal-to-apical direction, the pressure drop associated with it and shear stress from the circumferential flow[93]. Such forces increase with elevated IOP because the SC collapses narrowing the lumen, which results in increased circumferential flow and shear stress. The outer wall doses not have to undergo such stress since AH leaves SC through collector channels and it does not have to cross the endothelium.

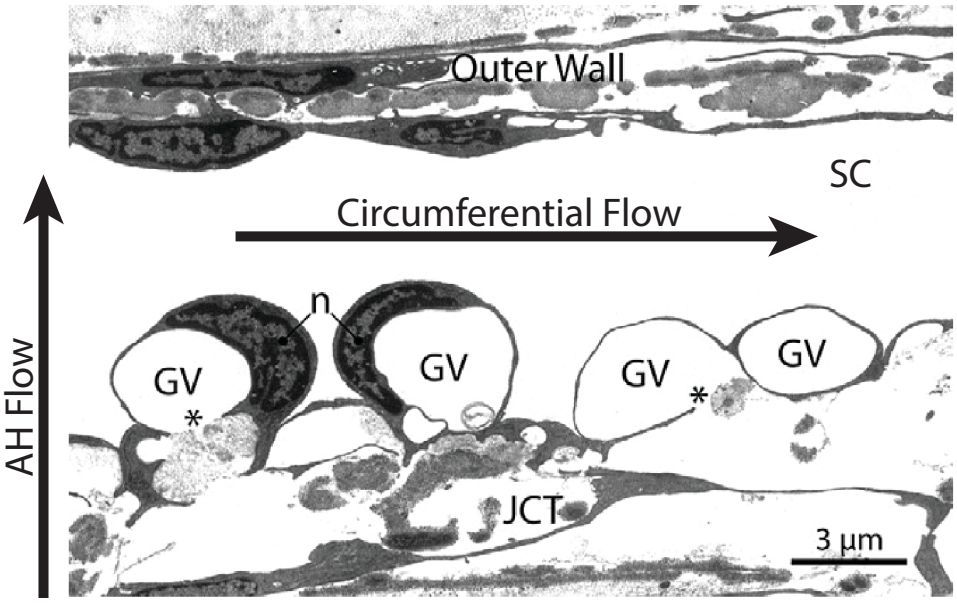


Figure 1.4: Transmission electron micrograph of Schlemm's canal. Cross section of the JCT and SC. AH flows from the anterior chamber in a basal-to-apical direction crossing the JCT and inner wall of SC, because of the pressure drop SC cells deform forming giant vacuoles (GV). In the lumen of SC, AH circulates circumferentially. The outer wall of SC exhibits a flat appearance. SC: Schlemm's canal lumen; n: cell nuclei; $*$: meshwork pores; JCT: juxtacanicular connective tissue. Adapted with permission from Pedrigi *et al.* (2011)[216].

Uveoscleral outflow pathway

The uveoscleral outflow pathway (also known as the unconventional pathway) is thought to contribute less to outflow drainage than the trabecular pathway, despite the fact that there is not an agreement on the percentage of AH exiting the eye trough this route[11,154,286]. Because of the pressure drop between the anterior chamber and the suprachoroidal spaces ($\approx$ 3.5 mmHg)[215] AH is driven through the fibers of the ciliary muscle in the iris root into the suprachoroidal spaces where it is reabsorbed by the sclera[11,201]. The uveoscleral pathway is considered to be pressure independent, since the flow through it does not change significantly with changes in IOP[37].

1.2.4 The inner wall of Schlemm's canal

The inner wall of SC is made of vascular-derived endothelial cells sitting on a discontinuous basement membrane[115]. SC cells in the inner wall allow AH to flow in a basal-to-apical direction while maintaining the blood-aqueous barrier[45]. Flow crossing SC pushes the endothelial cells away from their basement membrane forming extracellular outpouchings known as giant vacuoles (GVs), giving the inner wall a peculiar undulated appearance (Figure.1.4).

A special characteristic of SC endothelium is that it has both blood and lymphatics endothelial features[159,228]. For example, SC cells express all vascular endothelial growth factor receptors (VEGFR): VEGFR-1, -2 and -3[16,220,242]. VEGFR-1 and -2 are blood vascular markers while VEGFR-3 is a lymphatic marker. In addition, other vascular markers expressed by SC cells are CD31[47], PECAM-1 and VE-Cadherin[123] (blood) and PROX-1[16] (lymphatic).

It is known that SC endothelium expresses plasmalemma vesicle-associated protein (PLVAP or PV1)[126]. PLVAP is the structural protein forming the diaphragm that bridges some fenestra[142,266]. Moreover, it is necessary and sufficient for fenestra formation and its expression correlates with increased permeability[308].

Pores in the inner wall of SC

The inner wall is a continuous endothelium forming TJs and containing micron-sized transendothelial pores where the AH flows through[148]. Two types of pores are found in SC, pores that form in between cells (known as paracellular pores, border pores or **B-pores**) and pores that cross the entire cell (known as transcellular pores, intracellular pores or **I-pores**)[84,91,136,251] (see Figure.1.5). About 70% of pores in human eyes are I-pores[91] although B-pores seem to provide the predominant flow pathway[47]. I- and B-pores also seem to be regulated independently[47,94] and their dimensions are slightly different, I-pores have a diameter of 0.9 µm whereas B-pores are larger with a diameter of 1.6 µm on average[91,95].

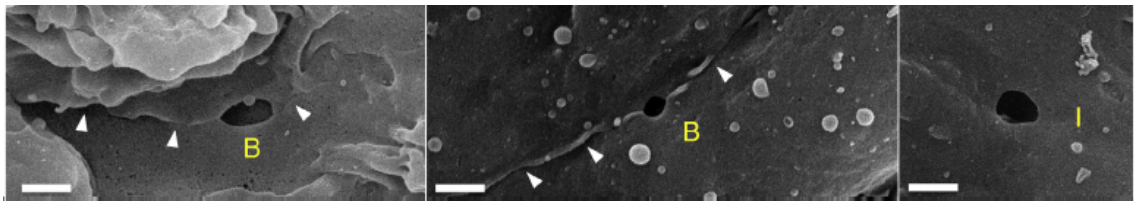


Figure 1.5: Pores in the inner wall of SC. Scanning electron micrograph of the inner wall of SC from a human eye showing both B- and I-pores. Arrow heads show cell borders. Scale bars represent 1µm. Reproduced with permission from Braakman *et al.* (2014)[46].

Pores in the inner wall of SC are very difficult to study. It is known that pore densities can be affected by fixation conditions and post-mortem times when observed *in situ*[91,150,251]. Moreover, SC is not very porous (0.07%)[91,151] and pores are not distributed uniformly, which complicates its visualization. Nevertheless, several studies report the importance of pores on outflow resistance regulation. Mostly, because the number of pores is reduced in glaucoma[150,151,211] and their distribution correlates with active areas of flow[47]. However, the mechanisms of pore formation and why pore density is reduce in glaucomatous eyes, is still under investigation.

The hypothesis, however, is that pores form from pre-existing ”mini-pores” due to tension generated by AH flow, this theory was first proposed by Anders Bill in 1972[40]. Apart from the micron-sized pores, smaller openings are found in the inner wall of SC: apertures in between TJs (Figure.1.6a) and fenestrae-like structures containing a diaphragm (Figure.1.6b)[36,126,275]. Flow crossing the inner wall causes tension that stretch

SC cells which may rupture these initial structures, in fact, pores are more often found in GVs, where the cell is deformed putting more strain on it. In line with this, it has been shown that SC cells in culture form more pores under stretching conditions[46]. It appears that cell stiffness is also key to pore formation, stiffer SC cells (like those from glaucomatous eyes) form less pores[211], which can explain the reduced pore density observed in glaucoma.

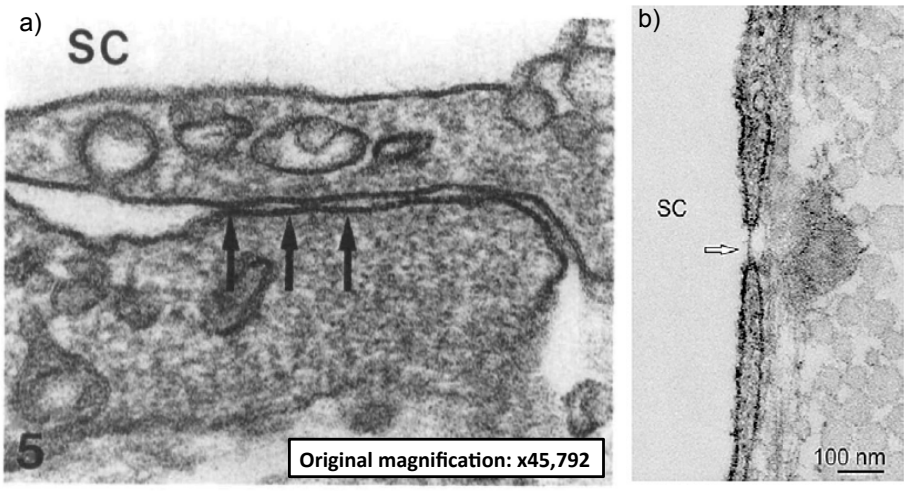


Figure 1.6: TJs and fenestrae in the inner wall of SC. a) Transmission electron microscopy of the inner wall of SC showing TJ (arrows). b) Transmission electron microscopy of the inner wall of SC showing a fenestra-like opening containing a diaphragm (arrow). Reproduced with permission from Bhatt *et al.* (1995)[36] and Herrnberger *et al.* (2012)[126].

1.2.5 Aqueous humour dynamics

The AH is in constant circulation and its dynamics can be defined by the principle of mass conservation, such that at steady state the rate of AH production (Q_p) equals the rate of AH drainage. As has been described previously, the AH drainage is divided into two routes: the conventional (Q_c) and the unconventional (Q_u) pathways, therefore,

$$Q_p = Q_c + Q_u \tag{1.1}$$

Taking into account the pressure dependency of the conventional (trabecular) pathway, influenced by IOP, conventional outflow resistance (R_c) and the downstream episcleral venous pressure (EVP), the relationship is defined by the modified Goldmann's

equation[52]:

$$Q_p = \frac{(IOP - EVP)}{R_c} + Q_u \tag{1.2}$$

The Goldmann's equation can also be expressed as a function of conventional outflow facility (C), which is the inverse of the conventional outflow resistance ($C = 1/R_c$):

$$Q_p = (IOP - EVP) \times C + Q_u \tag{1.3}$$

If this equation is rearranged to be a function of IOP it leads to:

$$IOP = \frac{(Q_p - Q_u)}{C} + EVP \tag{1.4}$$

These relationships are physiologically accurate if Q_c is pressure dependent and Q_u is pressure independent for a given IOP and the eye is at steady state.

1.2.6 Outflow resistance generation

As can be deduced from Equation.1.4 IOP depends on C or, which leads to the same, if resistance of the conventional outflow pathway increases so does IOP. This mathematical relationship has also been proven empirically[9,117,146,148]. Early in 1951, Grant[117] observed that elevated IOP measured in glaucoma patients was due to an increased outflow resistance and no, for instance, to an increase in AH production. Although these measurements were carried out before the uveoscleral pathway was discovered, one may consider that it does not contribute to the overall resistance generation because the magnitude of fluid leaving the eye through this route is insignificant in the healthy eye[201]. Despite these observations, what regulates AH outflow resistance is still not fully understood.

As it has been described previously (1.2.3), the trabecular pathway is made of three layers of TM, SC and the post-trabecular pathway, therefore, all theses elements

could contribute to outflow resistance generation. Here, they will be analysed individually.

The components of the conventional pathways that are considered not to contribute to resistance generation are the two first layers of the TM (the uveal and the cornoescleral meshwork)[118,188], the lumen of SC, even if it is collapsed at high IOP[149], and the post-trabecular pathway. The resistance generated by these structures is neglected because the space that the AH has to flow through them is sufficiently big to not confer any resistance[148,210]. However, the implication of the post-trabecular pathway is not clear since Grant (1963)[118] still measured a 25% of resistance after a trabeculotomy[1]. Then, there is only the JCT and the inner wall of SC left to generate resistance. Several studies confirmed that the the bulk of resistance is found in the vicinity of JCT and inner wall of SC, but their physical proximity makes it very difficult to discern the implication of each tissue. Moreover, these studies also demonstrated that the abnormal high resistance detect in glaucoma occurs within this area[117,118,258].

The JCT forms gaps smaller than the previous layers (micron-sized) and it is not thought to be compact enough to generate much resistance. Even so, the ECM is so rich that it hinders the flow of AH. Important elements of the ECM are GAGs, which have been associated with outflow resistance generation[48,210]. However, studies carried out in different species are not conclusive neither regarding its visualization nor to the effect that its inhibition has in facility. Thus, JCT cannot represent the totality of resistance generation but it seems that GAGs in its ECM contribute to it.

The inner wall of SC has a discontinuous basement membrane, which leads to think that, on its own, it should not oppose significant resistance to AH outflow[210]. However, mice treated with systemic dexamethasone (DEX) develop an enlarged basement membrane of SC, which could contribute to the rise in outflow resistance that these mice exhibit after DEX treatment[207].

The endothelial cells of the SC's inner wall form a continuous endothelium with pores of around 1 µm in diameter at a pore density that may range between 600 and 2500 pores/mm^2 depending on the study[10,40,47,151,251]. While these variations in pore density

[1] Surgical removal of the TM and inner wall of SC.

make it challenging to estimate the resistance attributable to the inner wall, hydrodynamic models assessed that it would contribute to a 5-10%[10,40,89,198,272]. Nevertheless, Johnson *et al.* (2002)[150] detected lower pore density in glaucomatous eye as well as an increased resistance, which suggests that pores might contribute to resistance generation. Other studies showed that when the integrity of the inner wall is compromised by perfusing eyes with chelating agents (EDTA, EGTA) or proteolytic enzymes (α-chymotrypsin) outflow resistance decreases significantly[120].

The individual analysis of each component of the trabecular outflow pathway leads to a paradox as the addition in series of each one is much smaller than the total resistance measured experimentally[210]. For this reason, a **synergic model** of outflow resistance generation based on the funneling model was proposed. The **funneling model**, first theorised by Johnson and colleagues (1992)[153], states that the interaction between the JCT and pores in the inner wall of SC determine the resistance of the outflow pathway. The rationale is that the AH is forced to flow through small pores when it comes from a wider area in the TM, as it happens with fluid passing through a funnel (See Figure.1.7). Mathematically, this models ends up being a function dependent on pore density, their diameter and the depth of JCT. Applying this model, Johnson *et al.* predicted a 30-fold increment in resistance compared to the addition of each individual resistance[153]. Further revision of this model taking into account the impact of giant vacuoles (where pores are more frequently found) reduced the original "funneling" effect by half[210]. According to this model, although pore density itself only accounts for about 10% of the generation of resistance, a change in pore density would have a huge impact on outflow resistance.

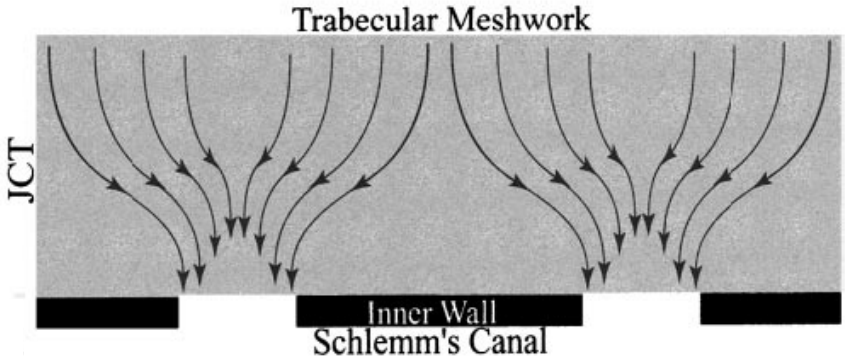


Figure 1.7: Funneling model. Schematic representation of the funneling model. Reproduced with permission from Overby *et al.* (2002)[209]

An additional factor that can contribute to outflow resistance generation is **segmental outflow**. Perfusion of eyes with tracers show that outflow is not uniformly distributed along the outflow pathway[47,59,74,180] but there are areas of active flow and other where apparently there is no flow going through. It is not clear how this discontinuity contributes to resistance modulation but it has been shown that when drugs that increase facility (like Y-27632) are perfused with tracers, the tracer distribution is more uniform[180]. In addition, Braakman *et al.* (2015)[47] recently reported that active flow areas strongly correlate with the presence of B-pores.

Altogether, empirical data suggests that resistance to AH outflow is generated within the JCT, the inner wall of SC and its basement membrane but its proximity and interconnection makes it hard to discern the role played by each component. Everything leads to think, however, that the ECM of JCT, discontinuity of SC's basement membrane, pores in the inner wall of SC and specially the connection between them are extremely important. It is necessary, then, a strong physical connection, both at tissue and cellular level, between the elements in the outflow pathway to maintain their integrity, specially because they are subject to high pressures and flows[148,210].

1.2.7 Mouse model for aqueous humour dynamics

In the past decades, the use of mice as animal model for human diseases has grown exponentially. The main reasons for this increment are that they are cost-effective, easy to handle and their tissues can be used within very short postmortem times. Moreover, their relatively short life spam allows the comparison between generations. But mostly because of the facility to manipulate its genome to the researcher's needs.

Despite the small size of the mouse eyes, which makes them technically demanding to work with, they are a useful tool to study the eye[189]. In glaucoma, most of the studies focus on optic nerve damage and less research has been done on the anterior segment because the abnormal increase in AH outflow resistance characteristic of glaucoma is not observed in mice. Nevertheless, because of great anatomic similarities with the human eye and the easy accessibility to fresh tissues, the use of mouse eyes to understand normal AH dynamics is growing in comparison to monkey, porcine, bovine and

even human eyes that have been traditionally used.

Anatomy and aqueous humour dynamics of the mouse eye

Mouse eyes are anatomically similar to human eyes, although the lens is much bigger and rounded in mice, occupying 75% of the intraocular space[253]. Obviously, dimensions are substantially smaller. The axial length of an adult mouse eye is about 3.3 mm, the anterior chamber has a depth of round 0.45 mm[246] and the AH volume is about 6 µl[6]. A structural difference between the human and mouse is that the ciliary body in humans is located posterior to the TM while it covers the TM in mice[278]. Nevertheless, similarly to human and non-human primate eyes, the TM and SC is tethered to the ciliary muscle by a tendinous elastic net[206]. The TM of mice is similar to the human since it has a distinctive lamellae, although narrower. Mice also have a mature and continuos SC than encircles the eyes containing giant vacuoles and pores[253,254,278,293]. The post-trabecular pathway is simpler in mice, which has direct link between SC and superficial limbal vasculature through aqueous vessels[293]. In mice, like humans, AH is produced in the ciliary body and enters the AC through the pupil to be drained through both the trabecular and uveoscleral pathway. Furthermore, both mice and humans have similar IOP.

AH dynamics is studied through perfusion experiments. Based on the modified Goldmann's equation (Equation.1.3), we can calculate C knowing both flow (Q) and pressure (P), which are measurable parameters. Different research groups use different techniques to acquire Q and P data at multiple pressure steps, then, C is defined as the slope of the linear regression between Q and P. In enucleated eyes, one can assume that there is no production of AH and there is no EVP, while for experiments *in vivo* it is necessary to estimate these parameters in order to discern the perfusion flow from Q_p and the influence of EVP. Because of the small size of the mouse eye, the little AH volume and low AH flow rates, the study of AH dynamics is technically more demanding than in humans. For comparison, on *ex vivo* perfusion experiments, the flow rate measured at 8 mmHg on human eyes is about 1.7 µl/min[118], while it is around 0.05 µl/min in mice[249], hence very precise instruments and techniques are required to assess AH dynamics in mice.

Several studies have estimated the facility of the outflow pathway in mice both *in vivo* and *ex vivo* with diverse results[6,174,191,249]. Experiments *in vivo*[6,56,71,191,317] reported C values between 5 and 18 nl/mim/mmHg whereas *ex vivo*[42,44,60,174,206,235,249,261] ranged from 6 to 30 nl/min/mmHg.

The contribution of the unconventional pathway in respect to the conventional is controversial as well, in *in vivo* studies, Millar *et al.* (2011)[191] reported that only 18% of the outflow occurs through the trabecular pathway while Aihara *et al.* (2003)[6] measured an 80%. Traditionally, on enucleated eyes, Q_u was defined as the intercept of Q *vs.* P linear regression obtained from perfusions data; however, since recently Sherwood *et al.* (2016)[249] measured no pressure independent outflow on enucleated mouse eyes and explained the presence of an intercept as an artefact due to the non-linearity of the Q - P relationship, previous data should be treated cautiously. In this work, where 66 enucleated eyes from C57BL/6 mice were perfused, we reported that C is a log-normally distributed parameter with a geometric mean of 6.15 nl/min/mmHg and 95% of the eyes laying in a range between 2.5 and 15.1 nl/min/mmHg. It is noteworthy that these parameters can be very variable within individuals and that different mice strains have different characteristics[44].

Another important fact that resembles mice to human eyes in the lack of "washout". Washout is an increase in facility observed after long term perfusions which has been reported to happen in bovine[209], monkey[21,161], and porcine[313] eyes but it does not happen in mouse eyes[174] as it does not occurs in perfused human eyes[87]. However, perfused mouse eyes do experience a phenomenon known as "anterior chamber deepening"[43,199], which occurs when perfusions are done into the AC and the pressure in the AC exceeds the pressure in the posterior chamber, this, pushes the iris and TM causing an artificial increase in outflow facility.

For simplicity, most of the studies performed are done *ex vivo* on enucleated eyes. However, as mentioned before, this neglects AH secretion and EVP. The only way to account for these parameters is doing the perfusions *in vivo*, which is an invasive technique that requires the anesthesia or sedation of the mouse. Therefore, it is crucial to investigate the effects that anesthetics have in the AH dynamics. It has been reported

that anesthetics reduce IOP[54,56,58,66,73,79,119,144,145,195,302] and that α-2 adrenoreceptor agonist compounds (e. g. xylazine) reduce AH production[61,111,186,286]. However, the *in vivo* studies present in the literature do not seem to take into consideration the effects of anesthesia or, at least, do not give details about it.

Pharmacological response

As mentioned before mice had been used to study normal AH dynamics. Seen the similarities between both species, mouse eyes are now used to test drugs that could either have clinical impact by increasing outflow facility thus lowering IOP or that would help gaining and understanding on resistance regulation and dysfunctions in glaucoma. Mice have been proven to be a good model for drug testing as well since, in most cases, they respond to drugs in a similar fashion than human eyes. Boussommier *et al.* (2012)[42] tested the effect of sphingosine-1-phosphate (S1P) and the prostanoid EP_4 3,7-dithia prostaglandin E_1 (PGE_1) which increase and reduce outflow facility in human eyes respectively, and found out that mouse eyes respond similarly and through the same mechanisms. However, it does not seem to happen the same with the IOP lowering drug Latanoprost. Even though it decreases outflow resistance in both human and mice, it does it through different mechanisms, while the target for Latanoprost is the unconventional outflow in humans, it affects the conventional in mice, probably because the ciliary muscle is less mature in murine eyes[191].

Glucocorticoid-induced ocular hypertension mouse model

Several techniques are used to induce ocular hypertension (OHT) such as photocoagulation of the limbus using argon lasers[7], injection of hypertonic saline into the episcleral veins[299] or genetic modification that lead to elevated IOP, for instance mutations in the α1 subunits of collagen type I[8] and Tyr437His mutation in myocilin[318]. These techniques are used to study the effect of OHT in the optic nerve but are not useful for outflow studies because they damage or alter the outflow pathway. A model that resembles to POAG has been developed by treating mice with glucocorticoids (GCs).

Like most humans, mice develop elevated IOP after systemic treatment with GCs such as DEX[207,304,319]. Interestingly, increased IOP is associated with an increase in conventional outflow resistance[207]. Moreover, mouse eyes treated with DEX have hallmarks that resemble to those observed in glaucomatous eyes. For instance, the TM presents plaque-like sheath deposits and the basement membrane of SC is more continuous[208], which may contribute to the increase in outflow resistance. Moreover, mice treated with topical DEX also experience optic nerve damage[319]. The glucocorticoid-induced OHT mouse model provides a potent platform to study several aspects of POAG despite the fact that it is not know if the cause of OHT is the same.

1.2.8 Vascular Endothelial Growth Factor physiology

Vascular endothelial growth factor (VEGF, or formerly known as vascular permeability factor, VPF) is a soluble protein that was independently described first by Senger *et al.* in 1983[248] and then by Connolly *et al.* in 1989[67]. It was later in 1989 when Keck *et al.*[162] and Leung *et al.*[175] conclude independently that VPF and VEGF were the same molecule, which has multiple functions, and published its sequence. Since then, we known that VEGF is a cytokine that acts on endothelial cells (both vascular and lymphatics) expressing VEGFRs inducing signaling cascades that lead to cell proliferation, migration and permeability necessary for angiogenesis. Furthermore, now it is also known that VEGF functions are broader than ”vascular” functions and it has been reported that VEGF confer neuroprotection[113] and prevents apoptosis of photoreceptors and Müller cells[240]. In this section, VEGF physiology and its known role in the eye will be described since a very important part of this thesis focuses on the role of VEGF and VEGFRs on hydraulic conductance of SC and outflow resistance regulation.

General VEGF physiology

Vascular Endothelial Growth Factors

In mammals, the VEGF family includes five structurally related members, each of which is encoded by a different gene: **VEGF-A, -B, -C, -D** and placental growth factor

(**PIGF**), these forms differ on their ability to bind the diverse VEGFRs. VEGF-A is the most common and most studied form, so it is usually, and hereafter, referred to as simply VEGF[205,218].

VEGF is a glycoprotein that forms dimers of about 40 kDa. There are currently 17 defined isoforms of VEGF[15,292] produced by differential mRNA exon splicing from a gene of eight exons[284]. Each isoform is defined by the number of amino acids, in this way, the most abundant isoform is made of 165 amino acids and it is known as $VEGF_{165}$ (the full name is VEGF-A_{165}a). Other important forms are $VEGF_{121}$, $VEGF_{189}$ and $VEGF_{206}$ (mouse forms are one amino acid shorter than human forms)[98]. Common exons in these forms include exons 1 to 5 and 8, responsible for signaling, dimerization and VEGFR-1 and -2 activation. Splicing of exons 6 and 7 characterises each isoform by their ability to bind different co-receptors[27]. There is a second group of isoforms that lack exon 8 and are known to be inactive forms of VEGF. These forms have the same number of amino acids than active forms and they are known as ”b” forms, for example, $VEGF_{165}$b. In this case, $VEGF_{165}$a and $VEGF_{165}$b are identical except for 6 amino acids in the C_t sequence. $VEGF_{165}$b was discovered by Bates *et al.* in 2002[28] and after that, $VEGF_{121}$b[230], $VEGF_{146}$b[221] and $VEGF_{189}$b[194] have been described. These ”b” isoforms bind VEGFRs with the same affinity than their corresponding ”a” form but can not fully activate them[217].

VEGF is a soluble cytokine expressed by almost all type of cells under hypoxia or stress conditions and during tissue remodeling that acts through VEGFR-1 and -2. The main role of VEGF is to promote angiogenesis in order to provide oxygen and nutrients to tissues that require them. In a healthy environment, this is the case of wound healing and woman reproductive cycle and in pathology it is expressed, for instance, by tumors that need to be nourished[128] or retinal pigmented epithelial (RPE) cells when blood supply is compromised by the presence of accumulated drusen[218]. VEGF can affect in an autocrine or paracrine manner, all depending on the solubility of the isoform, which depends on the affinity to heparin. Isoforms with high affinity to heparin (containing exon 7) are more easily bind to the ECM of the cell that synthesises them and are less soluble ($VEGF_{189}$ and $VEGF_{206}$), while forms with less heparin affinity can easily reach further endothelial cells ($VEGF_{165}$ and $VEGF_{121}$)[273]. $VEGF_{165}$ is a basic heparin-binding pro-

tein that it is secreted but a portion of it can stay bond to the ECM. Moreover, VEGF can also be secreted in vesicles[280].

Because SC has some lymphatics features it is interesting to talk about VEGF forms that are ligands for VEGFR-3 (VEGF-C and VEGF-D)(see Figure.1.8), that, as it is described later, is characteristic of lymphatic endothelial cells. More precisely, we will focus on VEGF-D (also known as c-fos-induced growth factor) because of its role in prostaglandins metabolism[158]. Endogenous VEGF-D experiences a series of proteolytic processing, it is secreted as full-length dimer containing a central VEGF homology domain (VHD), which has the receptor binding sites, surrounded by N_t and C_t propeptides ($\sim$ 53 kDa). Protease cleavage of the C_t propeptide leads to a partially processed form of VEGF-D and further N_t proteolysis results in the homodimeric mature form ($\sim$ 22 kDa). Depending on the availability of proteases the amount of each form of VEGF-D may vary and, with it, the effect that they exert on the endothelial cells that they target. While the full-length unprocessed VEGF-D can bind VEGFR-3 but has very low affinity for VEGFR-2 and the partially processed form binds VEGFR-2 and -3 and neuropilin-1 and -2, mature VEGF-D activates VEGFR-2, -3 and the heteroreceptor VEGFR-2/VEGFR-3[2,4]. The role of VEGF-D is wider then VEGF-A since it can affect both vascular and lymphatic endothelial cells leading to angiogenesis and lymphangiogenesis[232].

VEGF receptors and co-receptors

There are three main VEGFRs: **VEGFR-1** (or fms-like tyrosine kinase, Flt-1), **VEGFR-2** (or kinase insert domain-containing receptor, KDR, in humans and fetal liver kinase-1, Flk-1, in mice) and **VEGFR-3** (or Flk-4). VEGFRs belong to the receptor tyrosine kinase superfamily with similar macrostructure, they have an extracellular portion with seven immunoglobulin (Ig)-like domains ($\sim$ 750 amino acids), a single-span transmembrane fragment, a split tyrosine kinase domain connected through a 70 amino acids kinase insert and a C_t tail. However, VEGFR-3 has a disulfide bridge instead of the 5^{th} Ig-like domain[185,205,218]. A schematic representation can be seen in Figure.1.8. VEGFR-1[137] and -2[81] can be alternatively spliced as soluble receptors, the exact role of these forms are not fully elucidated but since they are direct antagonists of the full active receptor because they sequester VEGF, they are thought to control VEGFR function.

VEGFRs can be activated by more than one form of VEGF and a form of VEGF can activate more than one receptor, although with different affinities, giving to these interactions a divers and complex bioactivity. VEGFR-1 is activated by VEGF-A, -B and PlGF, VEGFR-2 by VEGF-A, -C, -D and -E and VEGFR-3 by VEGF-C and -D (Figure.1.8)[169,205,218]. Receptor dimerization (forming either homodimers or heterodimers) is necessary for autophosphorylation to occur, which will trigger signal transduction. The actual mechanisms that lead to endothelial permeability will be described in the next section.

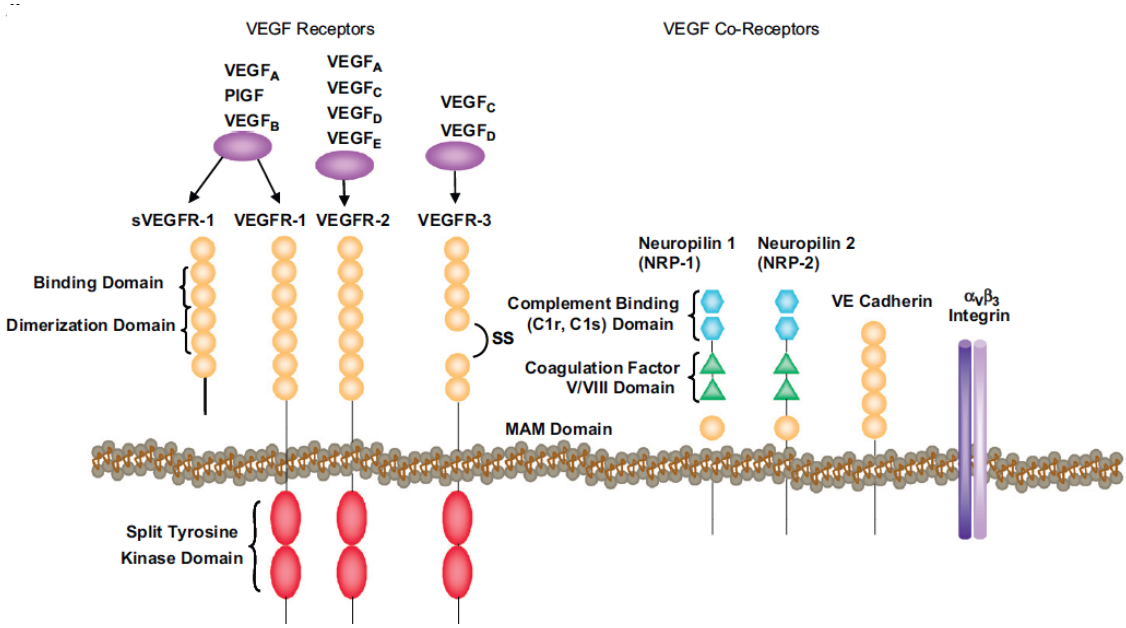


Figure 1.8: VEGFs and VEGFRs interactions. Schematic representation of VEGFRs (left) and VEGF co-receptors (right) structure expressed by endothelial cells and the VEGF family members that can activate them. Reproduced with permission from Penn *et al.* (2008)[218]

Apart from the VEGFRs mentioned above, VEGF can also interact with Neuropilins (NRP), a 120-130 kDa non-tyrosine kinase receptors with an inactive cytosolic domain that are necessary for VEGFR activation. NRP1 is a co-receptor for VEGFR-1 and -2 whereas NRP2 is a co-receptor for VEGFR-3[169,205,218]. NRP-1 interacts with axon 7 of VEGF$_{165}$a forming a ternary complex where VEGF bridges VEGFR-1/2 and NRP1[169], the lack of exon 7 in VEGF$_{165}$b impedes this interaction and the receptor is not activated[217]. In fact, it has been already shown that inhibition of NRP results in a suppression of VEGF$_{165}$a-mediated mitogenesis[204] and permeability activity[33].

Integrins are transmembrane proteins responsible for binding the cell to the ECM of the neighboring cell, it has been shown that integrins interact with VEGFRs as well.

The main role seems to be to enhance phosphorylation and prolong the receptor activity. For instance, they are essential for transmitting signaling cascades responsible for cell migration and proliferation through VEGFR-2[169]. Moreover, integrins can induce VEGFR-3 autophosphorylation in a VEGF-C/D independent manner[107] and interact with NRP in a VEGF dependent manner[169].

Interestingly, VEGFRs can also be activated by flow and shear stress without the presence of VEGF, although this process requires interaction with PECAM-1 (CD31) and Ve-Cadherin. Within this interactions, VEGFR-2 and PECAM-1 activate Src and PI(3)K signaling pathways respectively and Ve-Cadherin acts as an adaptor, where the transmembrane domain of both Ve-Cadherin and VEGFR-2 directly bind[68]. Without this protein complex, endothelial cells are insensitive to flow and, for example, they do not align with the direction of the flow[290]. In addition, it has recently been shown that VEGFR-3 form similar complexes and it can also behave as a mechanosensor[17,68].

Role of VEGF in hydraulic conductance

Although VEGF was first described as a permeability factor because of its ability to increase dye extravasation into the skin of guinea pigs[248], it is now known that its range of action is broader. It is involved in all aspects of angiogenesis: cell proliferation, migration and endothelial permeability. To date, VEGF has been shown to affect every signaling cascade in endothelial cells *in vitro*[316]. For this thesis, however, it is of great interest to understand how VEGF mediates endothelial hydraulic conductance.

The effects of VEGF on endothelial permeability (P_s) and hydraulic conductivity (L_p) have been studied in both intact vessels[22,25,103,311] and cultured endothelial cells monolayers[130,173,303]. Because of the difficulty to generate cell monolayers comparable to *in vivo* conditions in terms of endothelial tightness and expression of tight and adherent junctions it is more appropriate to perform these type of studies at tissue or organ level. Extensive studies have been carried out by Bates and colleagues[22,23,25,26,28,225] assessing the effects and mechanisms of action of VEGF in mesenteric microvessels of the frog. Their main fundings were that these vessels had an acute response (in about 1 minute) to continuous perfusion with 1nM VEGF with about 7-fold increase in L_p followed

by a drop returning to basal levels in 90 seconds, they also pointed out that a third of the vessels tested were non-responsive. In addition, it was reported that after a short exposure to VEGF, the vessels had an increased chronic L_p for up to 48 hours, which correlates in magnitude with the initial acute response. This chronic effect was found to be attenuated by perfusions with the nitric oxide synthase (NOS) inhibitor L-NAME, thus, it was suggested that VEGF may be acting through nitric oxide (NO).

At endothelium level, it is though that VEGF induction of hydraulic conductance is executed through the promotion of both intracellular openings and paracellular spaces[23]. It is important to bare in mind that this ultrastructural changes occur in different time frames and that the difference between studies performed *in vitro* and those done *in vivo* makes it very difficult to discern what is responsible for the acute and fast response and what is involved in the chronic effect of VEGF. It has been seen *in vivo* that after a few seconds of the addition of VEGF, there is formation of vacuolar organelles that connect the luminal with the abluminal sides of endothelial cells[97]. Moreover, transcellular gaps are also observed, mostly in a short distance of cell junctions[190]. At longer times (30 mins to 24 hours), it has been also shown that VEGF induces fenestration *in vivo*[233,234] and *in vitro*[90,142,244], most likely through up-regulation of PLVAP[57,135,167,270,307,309], even though there is a study claiming that PLVAP is down-regulated by VEGF[131]. Regarding cell-cell contacts, VEGF is believed to modulated adherent junctions as well as TJs. *In vitro* studies have shown that within 60 mins of exposure to VEGF, there is a reduction of junctional proteins like ZO-1, occludin and VE-cadherin[14,110,163]. Apart from the interactions between VEGFR-2 and VE-cadherin described before, it is also known that VEGF promote the internalization[110] and phosphorylation[75] of Ve-cadherin, the most prominent adherent junction. In addition, VEGF might modulate tight junction through ZO-1 phosphorylation, which has been shown to occur in rat retinas within 15 minutes and up to 45 minutes[14].

The signaling cascades involved in endothelial permeability are thought to be mediated through VEGFR-2[23,129,305], which gets phosphorylated after 2 minutes of addition of VEGF[300]. Signaling cascades leading into permeability have been studied *in vitro* and are well defined and happen to be diverse and complex[64,82,169,185,205,316]. A brief explanation of the main pathways and molecules involved will be given here. Once VEGFR-2

dimerises it gets autophosphorylated, for endothelial permeability, it is required phosphorylation of Tyrosines (Y) Y951 and Y1175 that activate Src, which triggers the PI_3K pathway[169]. Upon production of PIP_3, two main effectors come to the fore: nitric oxide (NO) and Ras-related C3 botulinum toxin substrate 1 (Rac1)[157]. **NO** is a product of NOS mediated through the Akt/PKB pathway, which is calcium dependent. The effects of NO in endothelial permeability are well known[80,105,298], although it can be stimulated and produced by other stimuli apart from VEGF, it seems clear that inhibition of NOS blunts considerably the effects of VEGF[26,35,311]. **Rac1** is responsible for cytoskeleton reorganization, essential for almost every aspect of cell dynamics. For instance, Rac activation is required for internalization of VE-cadherin[110] and VEGF-mediated fenestration[88].

VEGF in the eye

In an adult mammal, VEGFs are mostly involved in maintenance of the vasculature and in the eye, as an avascular organ with a blood barrier, has a very localised role to the choroid in the retina. Nevertheless, VEGF is also involved in maintaining the homeostasis of endothelial linings in the AC. In this section, the current knowledge of the role of VEGF in the eye will be described. Most of the literature available is relate to its role in the retinal vasculature, which will be summarised because of the implications that anti-VEGF therapies may have in IOP.

VEGF in the anterior segment

As it has been mentioned before, the anterior segment of the eye has no blood supply to nourish its inner tissues and has AH instead. Nevertheless, there are endothelial linings in this part of the eye that express VEGFRs and VEGF is a component of the AH. As can be seen from Table.1.1, there are some discrepancies in the reported VEGF concentrations in the AH, although, it seems to be to the magnitude of hundreds of pg/mL. One needs to be cautious when assessing these values for several reasons, first, there are technical reasons, most of these studies performed ELISAs to determine the VEGF concentration and the antibodies used may induce variability. Moreover, since samples are taken in clinical studies the sample sizes are generally small. A second problem is the experimental design itself, the antibodies used to carry out these experi-

ments recognise common sequences between isoforms, therefore, they can not discern between them, this is particularly a problem because of the known differences between $VEGF_{165}a$ and $VEGF_{165}b$, which have opposite effects and their balance could be key for the development of certain diseases.

Table 1.1: VEGF concentrations (mean ± SD, pg/mL) in human aqueous humour reported in the literature for different pathologies, patients with cataracts are considered as controls. POAG: primary open-angle glaucoma, ACG: angle-closured glaucoma, NVG: neovascular glaucoma, XFG: exfoliative glaucoma, AMD: age related macular degeneration, PDR: proliferative diabetic retinopathy. * denotes that a statistical significant change is reported compared to cataracts.

Cataracts	POAG	ACG	NVG	XFG	AMD	PDR	Reference
257 ± 47	726 ± 204*	–	29267 ± 7350*	–	–	–	Tripathi *et al.* (1998) [288]
102.7 ± 29.7	140.4 ± 51.0*	142.8 ± 40.2*	–	158.6 ± 58.9*	–	–	Hu *et al.* (2002) [139]
108.7 ± 72.3	–	–	–	–	668.9 ± 340.4*	–	Tong *et al.* (2006) [285]
146 ± 40	–	–	–	–	–	326 ± 125*	Sawada *et al.* (2007) [245]
81.8 ± 43.7	–	–	–	–	66.8 ± 35.1	–	Roh *et al.* (2009) [236]
533.1 ± 242.1	431.8 ± 197.2	–	–	722.9 ± 534.8	–	–	Takai *et al.* (2012) [274]
22.6 ± 16.1	–	–	–	–	–	146.2 ± 38.7*	Costagliola *et al.* (2013) [69]
14.4 ± 8.5	–	–	–	–	383 ± 155.5*	740.1 ± 267.7*	Hsu *et al.* (2014) [138]
233 ± 98	–	–	3698 ± 2105*	–	–	–	Wang *et al.* (2015) [301]

Certain endothelial linings in the anterior segment are VEGF dependent, for instance, the fenestrated capillaries of the ciliary processes, where VEGF is necessary for AH formation. Ford *et al.* (2012)[101] showed that VEGFR-2 is expressed in the ciliary body by the capillary endothelium and non-pigmented epithelium and VEGF is expressed by the adjacent pigmented epithelium. The role of VEGF in the ciliary body is to maintain the fenestrations of its capillaries, therefore, VEGF inhibition resulted in a reduction of both fenestrae and IOP, which the authors linked with an impaired AH formation.

In the outflow pathway, it has been described in a previous section that SC endothelial cells also express VEGFRs (1.2.4), previous studies by Sano *et al.* (2012)[242] reported that inhibition of either or both VEGFR-1 and VEGFR-2 resulted in buphthalmia[2] and elevated IOP. Moreover, it is also known that TM cells are capable to produce VEGF in culture and that its expression is enhanced by transforming growth factor β[104].

Abnormally high VEGF concentrations in the AH[288,301] (Table.1.1) are related with neovascular glaucoma, characterised by vessels growing in the surface of the iris and into the anterior chamber, this, can change the structure of the iridocorneal angle

[2]Buphthalmia is an enlargement of the eyeball because of increased IOP, it is associated with congenital glaucoma.

closing it and difficulting outflow. Moreover, blood leaking from these vessels interfere with vision and block the outflow pathway resulting in a further increased IOP[252].

VEGF in the posterior segment

Cells in the retina are nourished with oxygen and nutrients provided by the choroid, cells in the RPE form the ocular blood barrier and transfer these nutrients to the cells in the inner layers of the retina, like photoreceptors. Furthermore, RPEs also act on the opposite direction and clear waste products outside of the eye. Endothelial cells from the choroid express VEGFRs and RPE cells express VEGF in order to communicate with each other and keep this system in a healthy balance[102,239,241]. However, due to aging or metabolic diseases such as diabetes, drusen can accumulate in the Bruch's membrane (between the RPE and the choroid) and interfere with nutrients and oxygen supply to the RPE. In response to hypoxia, RPE over express VEGF and choriocapilaries grow uncontrolled into the retina. Therefore, the 3D structure of the retina is damaged and, eventually, the ocular blood barrier disrupted. Hence, malfunction of the communication between RPE cells and choroid endothelial cells leads to neovascular retinopathies such as exudative (or wet) age related macular degeneration and diabetic retinopathy[193,218]. As happens with glaucoma, retinal damage is irreversible. The only therapeutical option for these pathologies is to stop the progression of the disease by blocking VEGF. The most used treatments nowadays include intravitreal injections of antibodies (or fragments) against VEGF (bevacizumab and ranibizumab)[203] or drugs mimicking VEGF binding domains of VEGFRs (aflibercept)[122].

The administration of anti-VEGF therapies is growing and are very effective for retinal neovascularization. However, 3-11% of patients receiving repeated anti-VEGF injections suffer from sustained elevated IOP[5,18,62,116,132,184,247,255]. The reasons for this side effect are not clear, some studies postulate that impurities in the drug manufacture or protein agregates reach and block the outflow pathway[177], but studies showing reduced VEGF levels in the AH after intravitreal injection of anti-VEGF agents[69,202,236,245,301] suggest that these drugs may affect normal VEGF physiology within the outflow pathway.

1.3 Motivation of Thesis

This thesis is motivated for the need to find better treatments for glaucoma, current ones do not target the root of the problem (increased outflow resistance through the trabecular pathway) but they target either alternative outflow routes or inhibit AH production instead. The main hypothesis of this thesis is that **the continuity of SC endothelium plays a key role in conventional outflow resistance regulation, thus targeting components that maintain the continuity of the inner wall will modulate outflow facility**.

The principal objectives of this thesis are: **(1)** to determine the role of VEGF on AH outflow regulation in both normotensive and GC-induced hypertensive mice and **(2)** to assess the influence of PLVAP and TJs related proteins inhibition on outflow facility and IOP. In order to achieve these goals, four specific aims were formulated, each of which is addressed in a separate chapter of this thesis.

1.4 Specific Aims

Specific Aim 1: Determine the role of VEGF and VEGFRs on aqueous humour outflow regulation in normotensive mice. VEGF is well known to induce hydraulic conductance and permeability on endothelia. However, its role in outflow resistance regulation is unknown. We hypothesise that SC endothelium maintains its high hydraulic conductivity via VEGF signaling, which influences outflow. Therefore, we aim to understand the endogenous role of VEGF on the outflow pathway. Moreover, we also aim to identify signaling molecules involved in VEGF signaling. To achieve this, mouse eyes are perfused with different forms of VEGF, VEGFR inhibitors as well as Rac1 and endothelial NOS inhibitors.

Specific Aim 2: Determine the role of VEGF on aqueous humour outflow regulation in ocular hypertensive mice. A GC induced OHT mouse model is used to test the ability of VEGF to reduce outflow facility in mice with elevated IOP. With this purpose, mice are treated systemically with DEX for 4 weeks to induce OHT, the eyes are then perfused with different forms of VEGF to assess the effect on outflow facility.

Specific Aim 3: Assess the influence of PLVAP on outflow facility and IOP. PLVAP is known to be necessary for fenestra formation. We hypothesise that fenestrae are the precursors of I-pores, hence, reduced fenestration should result in impaired pore formation and reduced outflow facility. To test that, the outflow facility of PLVAP depleted mice is compared with their wild type littermates. Moreover, the role of the cytoskeleton is tested by perfusing eyes from both types of mice with latrunculin B, an actin disrupting drug.

Specific Aim 4: Assess the influence of TJs related proteins inhibition on outflow facility and IOP. B-pores form between neighboring SC cells. It is hypothesised that inhibiting TJs related proteins, the SC endothelium would become more permeable and outflow resistance would be reduced. To assess this, ZO-1 and tricellulin siRNA are injected into mouse eyes and outflow facility and IOP are measured 48 hours after.

Altogether, this thesis aims to assess the implication of SC endothelium on outflow resistance regulation by (1) targeting components of the inner wall of SC known to be important for pore formation and by (2) studying the role of VEGF, a cytokine known to regulate hydraulic conductivity and permeability of endothelia. This would be valuable information to gain an understanding on how outflow resistance is regulated and contribute to design better treatments for glaucoma.

Chapter 2

The Role of Vascular Endothelial Growth Factor in Murine Conventional Outflow Physiology

2.1 Introduction

Intravitreal anti-vascular endothelial growth factor (anti-VEGF) therapy, including bevacizumab, ranibizumab and aflibercept, are used to treat a number of retinal vascular disorders including neovascular age-related macular degeneration (NVAMD), diabetic macular edema, and retinal vein occlusion[122,203,238]. Injection of anti-VEGF into the eye is associated with a transient elevation of intraocular pressure (IOP) that is directly proportional to the injected volume, which typically resolves within 30-60 minutes[5,18,62,165]. However, a number of observational studies have reported sustained IOP elevation, or ocular hypertension (OHT), lasting several months or longer in 3-11% of patients receiving repeated anti-VEGF injections[116,132,133,155,177,179,184,247,255,315]. OHT is a major causative risk factor for glaucoma, a potentially blinding neurodegenerative disease that is caused by loss of retinal ganglion cells and damage to the optic nerve head. Vision loss in glaucoma is irreversible but further loss of vision can be prevented by reducing IOP[281]. With over 2 million intraocular injections of anti-VEGF administered annually in the United States alone[19], there is growing risk for secondary glaucoma in tens of thousands of patients who are already experiencing vision loss from retinal disease.

The mechanism for ocular hypertension following intravitreal anti-VEGF is unknown. Proposed mechanisms include obstruction of the aqueous humour outflow pathway by protein aggregates or foreign particles[177] or damage to the outflow pathway by local inflammation[155], mechanical trauma[256] or toxicity following repeated injections[155]. The aqueous humour outflow pathway includes the trabecular meshwork (TM), Schlemm's canal (SC) and downstream intrascleral vessels. This pathway is responsible for the bulk of aqueous humour drainage from the eye[39]. Decreased aqueous humour outflow facility (the mathematical inverse of outflow resistance) by a yet unidentified mechanism causes ocular hypertension in open-angle glaucoma[117].

Outflow facility is partly regulated by the inner wall endothelium of SC[181,183,210], a continuous cellular monolayer that provides the only functional barrier between aqueous humour and peripheral blood[45]. Aqueous humour crosses SC endothelium by flowing through micron-sized pores[47,91,141], and a reduction in pore density contributes to decreased outflow facility in glaucoma[10,151,211]. SC endothelium exhibits characteristics

of both vascular and lymphatic endothelia[16,159,166,228], and uniquely expresses all three VEGF receptor (VEGFR), including VEGFR-1 and 2 expressed by vascular endothelia and VEGFR-3 typical of lymphatic endothelia. VEGF-A (or simply VEGF) is a potent regulator of endothelial permeability[27,34,90,156,233] by inducing the formation of pore-like fenestrae[90,244] and focal disassembly of intercellular junctions[110,197]. Pigment-epithelium derived factor (PEDF), which functionally antagonises VEGF, decreases outflow facility in mice[235], and VEGF has been proposed as a potential regulator of outflow[104], but the effects of VEGF on conventional outflow facility have not been examined. We hypothesise that VEGF participates in the local, homeostatic regulation of aqueous humour outflow facility such that blockade of VEGF signaling leads to outflow dysregulation, which puts patients receiving anti-VEGF therapy at increased risk for ocular hypertension and secondary glaucoma.

2.2 Materials and Methods

2.2.1 Reagents

The following antibodies and reagents were used for immunostaining: formaldehyde (TAAB, #F017, UK), OCT (Bright instruments, Bright Cryo-m-Bed, UK), Dulbecco's Phosphate Buffered Saline (PBS, Gibco, Life Technologies, UK), normal horse serum (Stratech Scientific Limited, #008-000-121-JIR, UK), ProLong Diamond Antifade Mountant (Life technologies, #P36961, UK), rat anti-mouse CD31 antibody (1:100, BD biosciences, #550274, UK), goat anti-mouse $VEGF_{164}$ polyclonal antibody (15 µg/ml, R&D systems, #AF-493-NA, UK), anti-rat Alexa Fluor 594 (1:500, Life Technologies, #A-21213, UK) and anti-goat Alexa Fluor 488 (1:400, Life Technologies, #A-11055, UK).

The following reagents were used for *ex vivo* mouse eye perfusions: mouse $Vegf_{164}a$[1] (Sigma Aldrich, #V4512, UK), human $VEGF_{165}b$ (abcam, #ab104953, UK), Ki8751 (Selleckchem, #S1363, Germany), SU5416 (Sigma Aldrich, #S8442, UK), L-

[1] Sigma Aldrich names this mouse isoform as $Vegf_{165}a$ although they provided the sequence and we could verify that is 164 amino acids long and matches with the mouse sequence.

NAME (Cayman Chemicals, #80210, US), mouse Vegf-D (R&D Systems, #469-VD-025/CF, UK) and EHT1864 (Tocris, #3872, UK).

2.2.2 Immunostaining

To image the outflow system the whole eye was fixed in 4% formaldehyde in PBS for 2 hours immediately after enucleation and stored in 0.1% formaldehyde in PBS at 4℃ until needed. The eye was dissected as follows: the ocular muscles were removed and the eye cut equatorially using a surgical carbon steel blade (Swann-Morton, n°15, UK). The posterior segment and the lens were discarded, while the anterior segment was cleaned until free from uveal tissues being very careful not to damage the iris. When the anterior segment was isolated, it was submerged in a solution of 30% sucrose in PBS until it lost buoyancy (30 min approximately). The sample was then embedded in 1:1 OCT-30% sucrose solution and stored overnight at -80℃. Cryosections (8 µm) were cut and placed on micro-slides super-frost plus ground (VWR, # J1800AMNZ, UK) let air dry for 30 minutes and stored at -20℃ until stained.

Samples were defrosted for 1 hour at room temperature, permeabilised and blocked with 10% horse serum in 1% Triton-X solution for 30 min at room temperature. Both primary antibodies (CD31 + VEGF) were added to the blocking solution and incubated for 2 hours at 37℃ followed by 3 washes of 5 min in PBS. Both secondary antibodies were also diluted in blocking solution, incubated for 30 min at 37℃ and washed 3 times for 5 minutes in PBS. Samples were mounted on the glass microscope slide, embedded in anti-fade mountant and kept overnight at 4℃ to dry. Next day, they were imaged using a confocal microscope (Leica SP5) at 20x magnification.

2.2.3 Animal Husbandry

All animals were treated in compliance with the ARVO statement for the Use of Animals in Ophthalmologic and Vision Research under UK Home Office Project Licence 70/7306.

All mice were male C57BL/6 (Charles River Laboratories, UK) used between 9 and 13 weeks of age. Mice were kept in individually ventilated cages, fed *ad libitum* and maintained at 21℃ with 12 hours light/dark cycle.

2.2.4 *Ex vivo* mouse eye perfusion

Ex vivo mouse eye perfusions were done using the iPerfusion sytem according to Sherwood *et al.* (2016)[249]. Briefly, the eye was affixed to a support platform using cyanoacrylate glue (Loctite, UK) and submerged in a bath of PBS thermo regulated at 35℃. The anterior chamber was precisely cannulated with a 33-gauge needle (Nanofil, WPI, US) using a XYZ micro-manipulator (World Precision Instruments, USA). The eye was pressurised at 8mmHg for a 45 min acclimatization period and to allow for the drug to reach the outflow pathway. The eye was then perfused at 9 discrete pressure (P) steps between 4.5 and 21 mmHg[2] using an adjustable height reservoir controlled by a computerised linear actuator (L35; Nanotec, Germany). A wet-wet differential pressure transducer (PX409, Omegadyne, US) and flow sensor (SLG64-0075, Sensirion, Switzerland) were used to measure IOP and the flow rate (Q) into the eye at each pressure step in a custom system controlled using LabVIEW (National Instruments, US). The experimental set up and an example of the flow and pressure traces recorded can be seen in Figure.2.1.

The duration of each pressure step was determined by an stability criterion controlled by the iPerfusion software. When $Q(t)/P(t)$ did not change by more than 0.1 nl/min/mmHg/min over a period of a minute, Q and P data were considered to be stable, if stability was maintained for 6 minutes, the reservoir automatically rose to apply the next pressure step. The last 4 minutes of stable data were averaged to determine the Q and P for a given pressure step, this way, we ensured that the measured C changed by less than 0.4 nl/min/mmHg over the averaged period.

The perfusate for control eyes was Dulbecco's PBS including divalent cations + 5.5 mM glucose (referred to as "DBG") plus DMSO when it was the drug carrier. For

[2]Pressure steps applied: 4.5, 6, 7.5, 9, 10.5, 12, 15, 18 and 21 mmHg.

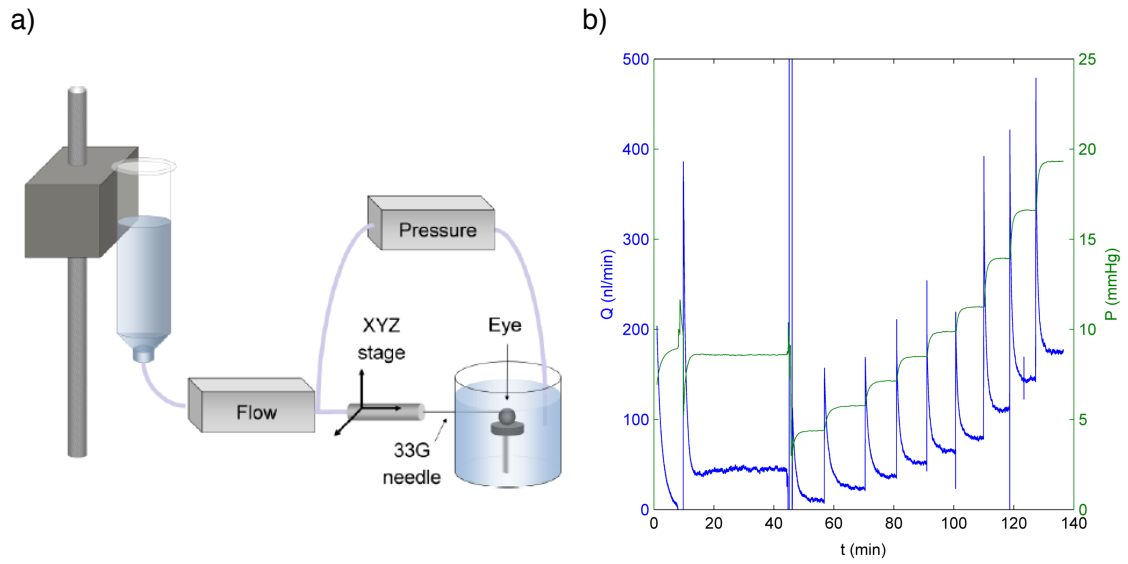


Figure 2.1: iPerfusion system set up and perfusion tracing. a) Schematic representation of the iPerfusion system done by Dr. Joseph M. Sherwood. b) Typical raw data from a control eye. The green trace represents the pressure and the blue the flow rate.

treated eyes, the drug was perfused dissolved in DBG. The perfusate was filtered (0.22 µm, #28145-477, VWR international, UK) prior to use and was backfilled through the needle.

Due to the development of the iPerfusion system, sets of perfusions corresponding to $Vegf_{164}a$ (all concentrations), $VEGF_{165}b$ and SU5416 were done using only one perfusion system. For theses sets of experiments, one eye was perfused first (randomizing whether it was control or treated) and the other one was perfused afterwards. The second eye awaited perfusion for a maximum of 4 hours after enucleation stored in PBS at 4 ℃. All other perfusions were done using 2 perfusion systems in parallel, so both eyes were perfused simultaneously between 10 and 30 minutes after enucleation.

2.2.5 Outflow facility analysis for *ex vivo* perfusions and statistics

Outflow facility is determined and analysed according to Sherwood *et al.* (2016)[249]. In summary, for each pressure step, the last four minutes of stable Q and P data are averaged and plotted. The data is then fitted to a model that assumes that there is no unconventional outflow in enucleated eyes[3] ($Q_u = 0$) and that Q *vs.* P data are not linear,

[3] Based on empirical data showing that there is no flow at P = 0 mmHg[249].

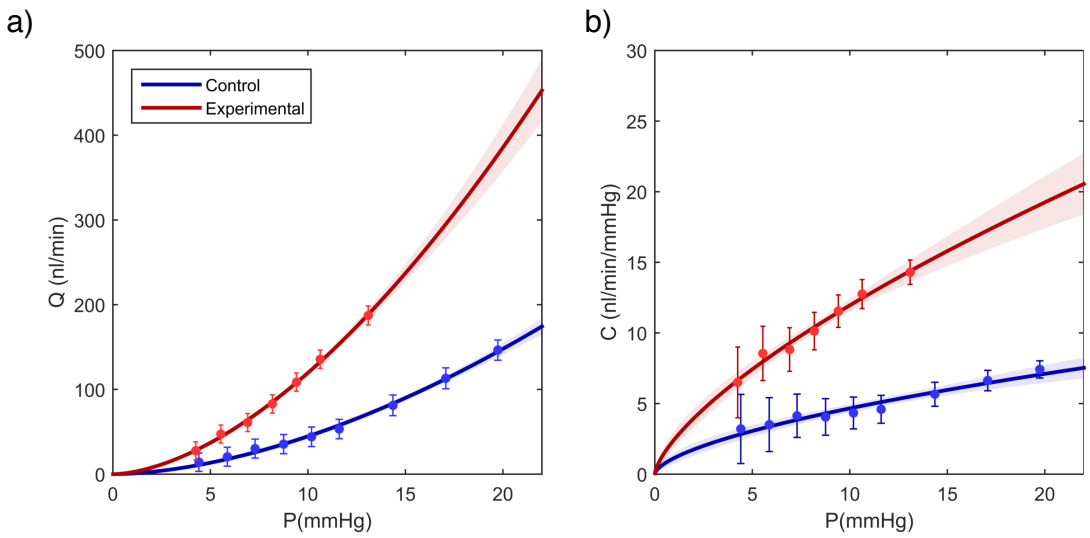


Figure 2.2: Q *vs.* P and C *vs.* P representative plot. a) Q *vs.* P representative plot of the averaged data from each pressure step applying a power law fitting and forcing a 0 intercept for a pair of eyes. Points are the measured data and error bars de 95% confidence intervals. Shaded regions are de 95% confidence bounds in the fitting. Blue data corresponds to the control eye perfused with DBG and red the contralateral eye perfused with 500 ng/ml $Vegf_{164}$a. b) C *vs.* P representative plot for the same data showed in panel a. Points are the measured data ($C = Q/P$) and error bars de 95% confidence intervals. Shaded regions are de 95% confidence bounds in the fitting.

thus a power law fitting forced to a 0-0 intercept is applied according to:

$$Q(P) = C_r \left(\frac{P}{P_r}\right)^{\beta} P \tag{2.1}$$

Where P_r is the reference pressure (8 mmHg) at which C_r is the facility for a given eye and β defines de non-linearity of the data. A representative Q *vs.* P plot can be seen in Figure.2.2a. That Q *vs.* P data are not linear implies that C changes at each pressure step (Figure.2.2b), hence C_r is defined at 8 mmHg. In order to apply this model, a minimum of 4 pressure steps are required.

We reported that facility is not a normally distributed variable but it is lognormally distributed[249]. Therefore, the statistical treatment and how the data is reported has to be done accordingly. To analyse the effect of a drug, only paired data was used. Briefly, we calculate the average difference between the treated eye and its contralateral control and report the change in facility as:

$$\% \; (\overline{D}^{*} \; ^{\times}/ \; ME_{\overline{D}^{*},95}(s^{*2}_{tre}))$$

where $\%$ is the percentage change calculated as $(\overline{D}^* - 1) \times 100$, $\overline{D}^*$ is the proportional change, $ME_{\overline{D}^*,95}$ is the margin of error given by the half-width of the 95% confidence interval on the estimate of $\overline{D}^*$ and s^{*2}_{tre} is the treatment variability represented as the range of the 95% of the treatment. Note that because we are not working with normally distributed data, $\overline{D}^*$ and the $ME_{\overline{D}^*,95}$ need to be reported as $^{\times}/$ instead of the $\pm$ used with normally distributed data.

Statistical significance was determined by a weighted t-test in MATLAB (Mathworks, US), where data points with higher uncertainties in the measurement contribute less to the weighted average. Full details are described in Sherwood *et al.* (2016)[249].

2.3 Results

2.3.1 Endogenous VEGF Signaling within the Conventional Outflow Pathway.

To determine whether VEGF is present endogenously within TM tissues, we immunolabeled $VEGF_{164}$ in the conventional outflow pathway of mice. Mice are a valuable model for aqueous humour outflow because, like primates, mice have a continuous SC and lamellated TM[206,254], and mice mimic the pharmacological response to several compounds that affect aqueous humour outflow facility in primates[42,191]. $VEGF_{164}$ was concentrated along the inner wall endothelium of SC, co-localizing with the vascular marker CD31/PECAM-1 expressed by SC endothelium[123] (Figure.2.3). $VEGF_{164}$ labeling was also present along the epithelium of the ciliary processes[101], corneal epithelium[224] and surrounding CD-31 positive vessels in the sclera. VEGF is therefore present endogenously within the TM and along the inner wall where it may initiate signal transduction via VEGF receptors that are expressed by SC endothelial cells.

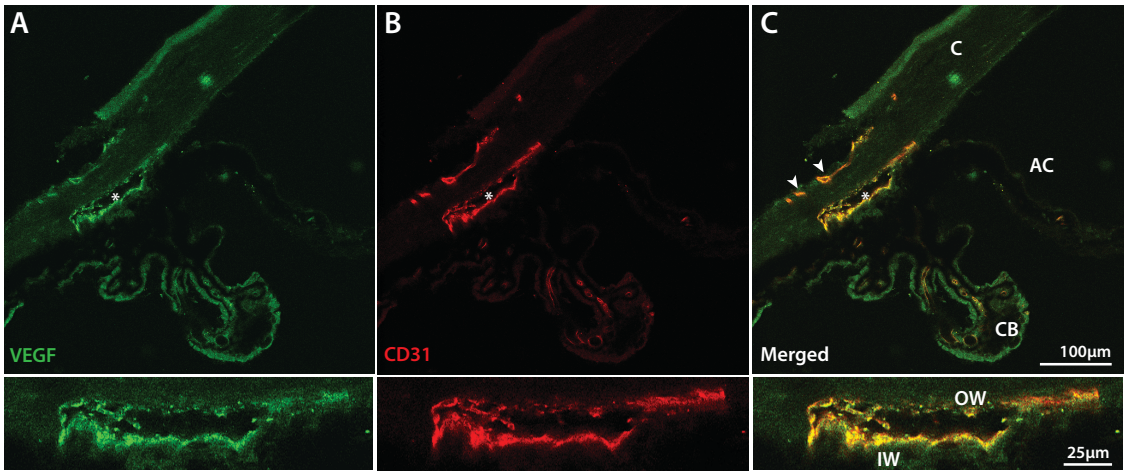


Figure 2.3: VEGF-A_{164} and CD31 staining in the mouse outflow pathway. Double immunostaining with antibodies raised against $Vegf_{164}a$ (green) and CD31 (red). a) VEGF is expressed mostly in the epithelium and was found in the ciliary body (CB), in the cornea (C) and very close to SC (*). b) CD31 was found in endothelial tissues: SC, capillaries in the CB and collector channels (arrows). AC: anterior chamber, IW: inner wall, OW: outer wall.

2.3.2 VEGF-A_{164}a Modulates Outflow Facility.

To determine whether VEGF influences aqueous humour outflow, we measured outflow facility in enucleated eyes from C57BL/6 mice (11-14 weeks) using the iPerfusion system[249]. Perfusion with $Vegf_{164}a$ at 500 ng/ml increased C by 87% (1.87 $^{\times}/$ 1.62 (2.82); p = 0.02; n = 8; Figure.2.4) relative to vehicle-treated contralateral eyes. A lower concentration of $Vegf_{164}a$ at 100 ng/ml tended to increase C, but did not achieve statistical significance (1.24 $^{\times}/$ 1.59 (2.11); p = 0.29; n = 6; Figure.2.4). At a higher concentration of 1 µg/ml, however, $Vegf_{164}a$ appeared to decrease C by 50% (0.5 $^{\times}/$ 2.73 (3.13); p = 0.11; n = 4; Figure.2.4). These data indicate that $Vegf_{164}a$ affects outflow facility in a dose-dependent and potentially biphasic manner, with a maximal effect on outflow facility at approximately 500 ng/ml.

2.3.3 Blockade of VEGFR-2 Decreases Outflow Facility.

To determine whether VEGF that is present endogenously within the TM influences outflow facility, we perfused enucleated mouse eyes with VEGFR antagonists. SC endothelium uniquely expresses all 3 VEGFR isoforms (VEGFR-1, -2, -3)[16,220,242], but VEGFR-2 is believed to mediate the effect of VEGF on vascular permeability[41,129,169]. In response to 3 µM SU5416, a moderately selective antagonist to VEGFR-2 with an IC_{50}

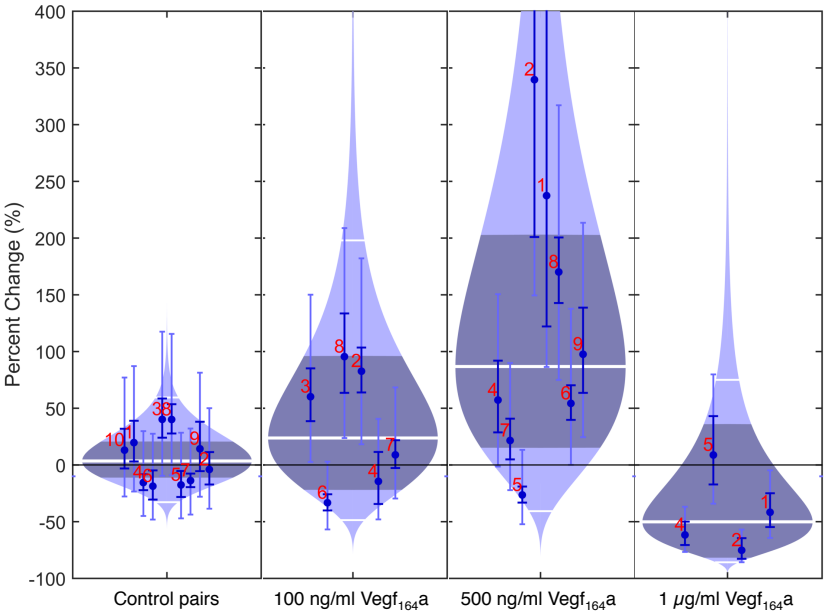


Figure 2.4: Effect of $Vegf_{164}a$ on outflow facility. Modified violin plots showing the percentage change of C between the control eye and its treated contralateral eye. Each data point corresponds to a pair of eyes, the white central line is the geometric mean change in C and the dark area around it is the margin of error around the mean. The blue coloured area shows the distribution of the data. The 1st panel shows pairs of eyes were both eyes were perfused with DBG (n = 10). The 2nd panel shows perfusions with 100 ng/ml VEGF164a (n = 6). The 3rd panel shows perfusions with 500 ng/ml $Vegf_{164}a$ (n = 8). The 4th panel shows perfusions with 1 µg/ml $Vegf_{164}a$ (n = 4). The numbers denote the pair ID.

of 1 µM[100,143,283], C decreased by 27% but did not achieve statistical significance (0.73 $^{\times}/$ 1.57 (1.00); p = 0.096; n = 4, Figure.2.5). However, a similar magnitude of effect was observed in response to 1 nM Ki8751, a highly selective antagonist to VEGFR-2 (IC_{50} = 0.9 nM)[171], which decreased C by 34% (0.66 $^{\times}/$ 1.50 (1.75); p = 0.044; n = 6, Figure.2.5). As an alternative approach to inhibit endogenous VEGF signaling, we perfused enucleated mouse eyes with $VEGF_{165}b$, an alternative splice isoform of VEGF-A that acts as a competitive inhibitor of VEGFR activity. $VEGF_{165}b$ lacks the neuropilin-binding domain required for VEGF receptor activation, while retaining its ligand-binding domain to VEGFR-1 and -2[217,226,310]. Similar to Ki8751, 500 ng/ml $VEGF_{165}b$ decreased C by 44% (0.56 $^{\times}/$ 1.65 (2.26); p = 0.029; n = 6, Figure.2.5) relative to vehicle-treated contralateral eyes. These data demonstrate that blockade of VEGFR-2 decreases outflow facility, presumably by inhibiting signaling from VEGF that is present endogenously within the TM.

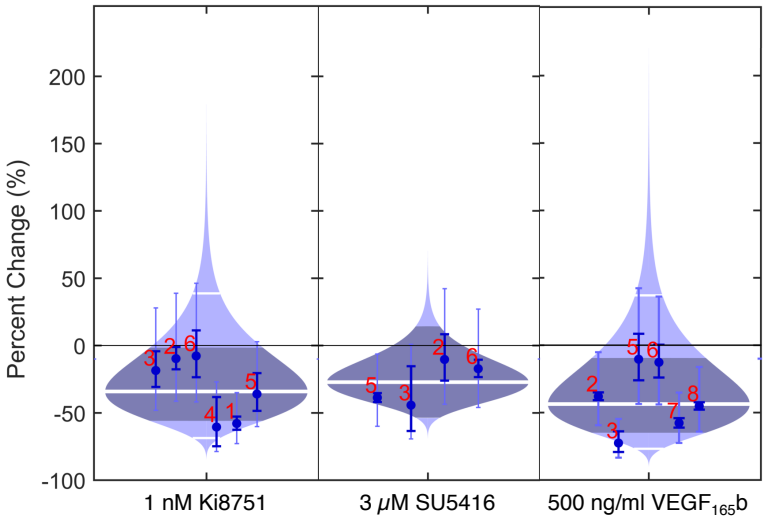


Figure 2.5: Effect of VEGFR inhibitors on outflow facility. Modified violin plots showing the percentage change of C between the control eye and its treated contralateral eye. Each data point corresponds to a pair of eyes, the white central line is the geometric mean change in C and the dark area around it is the margin of error around the mean. The blue coloured area shows the distribution of the data. The 1st panel shows perfusions with 1 nM Ki8751 (n = 6). The 2nd panel shows perfusions with 3 µM SU5416 (n = 4). The 3rd panel shows perfusions with 500 ng/ml $VEGF_{165}b$ (n = 6). The numbers denote the pair ID.

2.3.4 Vegf-D Increases Facility through VEGFR-2.

In addition to VEGFR-1 and -2, SC endothelial cells express VEGFR-3 that is found primarily in lymphatic endothelia[16,166]. Vegf-D is an endogenous ligand for VEGFR-2 and -3[2,3], and Vegf-D has been shown to reduce degradation of prostaglandins (PGs) by inhibiting 15-hydroxyprostaglandin dehydrogenase (PGDH)[158]. As PGs are known to regulate outflow[42,192], we examined whether Vegf-D and associated signaling via VEGFR-3 may be exploited as a therapeutic target to modulate outflow facility. Perfusion with 1 µg/ml Vegf-D increased C by 52% relative to vehicle-perfused contralateral eyes (1.52 $^{\times}/$ 1.27 (1.37); p = 0.004; n = 8), while 500 ng/ml Vegf-D had no detectible effect on C (0.92 $^{\times}/$ 1.59 (3.07); p = 0.70; n = 9; Figure.2.6). However, in the presence of a highly selective antagonist to VEGFR-2 (1 nM Ki8751), the facility increase induced by 1µg/ml Vegf-D was eliminated compared to the contralateral eye perfused with 1 nM Ki8751 alone (-17%, 0.83 $^{\times}/$ 1.55 (2.84); p = 0.35; n = 9, Figure.2.6). These data suggest that while Vegf-D may be used to increase facility, the effect is mediated almost entirely through VEGFR-2 such that agonism of VEGFR-3 is unlikely to significantly affect outflow facility, at least over acute time periods.

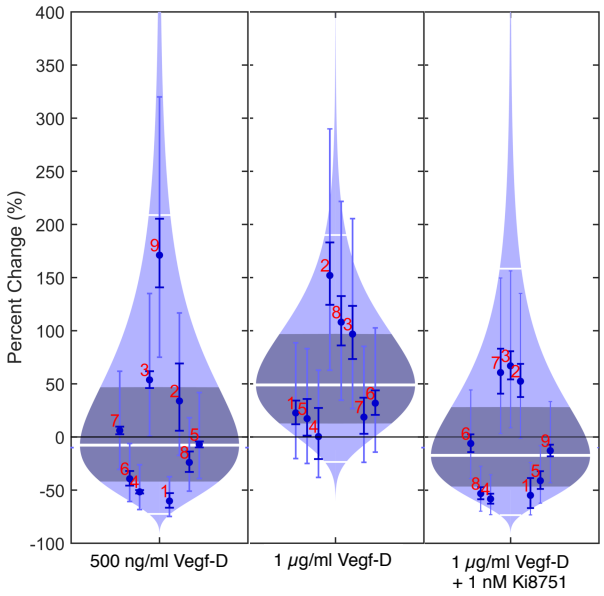


Figure 2.6: Effect of Vegf-D on outflow facility. Modified violin plots showing the percentage change of C between the control eye and its treated contralateral eye. Each data point corresponds to a pair of eyes, the white central line is the geometric mean change in C and the dark area around it is the margin of error around the mean. The blue coloured area shows the distribution of the data. The 1st panel shows perfusions with 500 ng/ml Vegf-D (n = 9). The 2nd panel shows perfusions with 1 µg/ml Vegf-D (n = 8). The 3rd panel shows perfusions with 1 µg/ml Vegf-D in the presence of 1 nM Ki8751 (n = 9). The numbers denote the pair ID.

2.3.5 The Facility-Increasing Effect of $Vegf_{164}a$ is mediated through both NO and Rac1.

The downstream effects of VEGF on vascular permeability are mediated via two separate pathways including nitric oxide synthase (eNOS) and Rac1 [105,121,134,185,197,205]. eNOS is expressed by SC cells and produces NO that increases outflow facility [60,83,127,260]. To determine whether the effect of VEGF on outflow facility is mediated through NO production, we perfused enucleated mouse eyes with 500 ng/ml $Vegf_{164}a$ in the presence of 10 µM L-NAME, a non-selective inhibitor of all NOS isoforms. In the presence of L-NAME, $Vegf_{164}a$ increased facility by approximately 36% but did not achieve statistical significance compared to contralateral eyes perfused with 10 µM L-NAME alone (1.36 $^{\times}/$ 1.42 (1.87); p = 0.08; n = 7; Figure.2.7). In comparison to the 87% increase reported above, L-NAME blunted the facility response to 500 ng/ml $Vegf_{164}a$. This suggests that VEGF-A partially mediates its effect on outflow facility through NO production, presumably via eNOS.

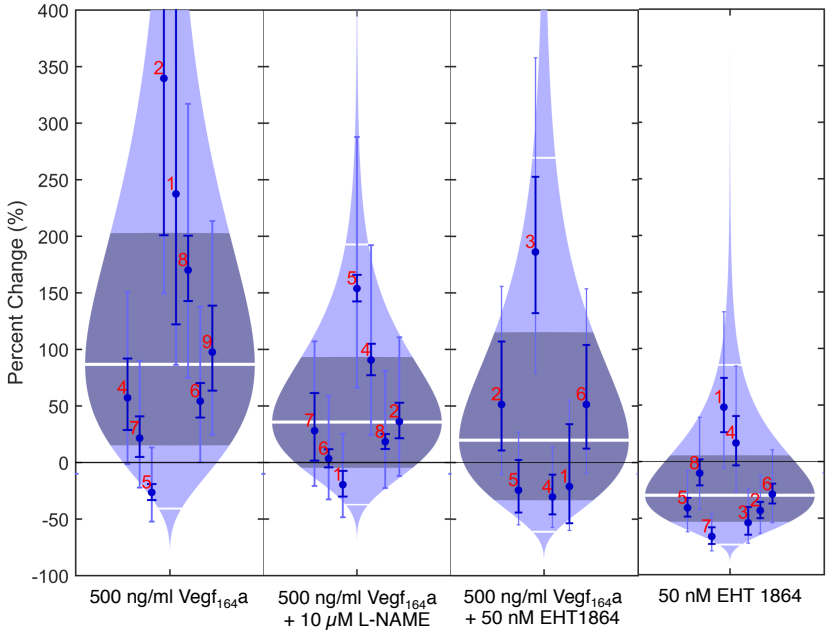


Figure 2.7: Effect of inhibiting eNOS and Rac1 on outflow facility. Modified violin plots showing the percentage change of C between the control eye and its treated contralateral eye. Each data point corresponds to a pair of eyes, the white central line is the geometric mean change in C and the dark area around it is the margin of error around the mean. The blue coloured area shows the distribution of the data. The 1st panel shows perfusions with 500 ng/ml $Vegf_{164}a$, same data as in Figure.2.4 (n = 8). The 2nd panel shows perfusions with 500 ng/ml $Vegf_{164}a$ in the presence of 10 µM L-NAME (n = 7). The 3rd panel shows perfusions with 500 ng/ml $Vegf_{164}a$ in the presence of 50 nM EHT1864 (n = 6). The 4th panel shows perfusions with 50 nM EHT1864 (n = 8). The numbers denote the pair ID.

To determine whether the effects of VEGF-A are partially mediated via Rac1, we perfused enucleated mouse eyes with or without 500 ng/ml $Vegf_{164}a$ in the presence of the selective Rac1 inhibitor EHT1864 (IC_{50} = 40nM)[76]. Rac1 controls the assembly of intercellular junctions that preserve the continuity of endothelial barriers and inhibition of Rac1 decreases the permeability of vascular endothelia, but the role of Rac1 on outflow facility has not been specifically investigated. Perfusion with 50 nM EHT1864 alone reduced C by approximately 30% relative to contralateral eyes perfused with vehicle, but the effect did not achieve statistical significance (0.70 $^{\times}/$ 1.50 (2.35); p = 0.07; n = 8; Figure.2.7). When eyes were perfused with 500 ng/ml $Vegf_{164}a$ in the presence of 50 nM EHT1864, the facility increase was blunted to 20% and was not statistically different from contralateral eyes perfused with EHT1864 alone (1.2 $^{\times}/$ 1.80 (2.68); p = 0.46; n = 6; Figure.2.7). These results suggest that the facility effect of $Vegf_{164}a$ is mediated through both NO and Rac1, as inhibition of either pathway abrogates the facility increase caused by $Vegf_{164}a$.

2.4 Discussion

In this study, we demonstrate in mice that VEGF modulates outflow facility in an isoform-specific and dose-dependent manner. These studies support a mechanism by which VEGF production within the TM acts as a physiological signal to modulate outflow facility, presumably by acting on the hydraulic conductivity of SC endothelium.

VEGF signaling is mediated through any of the three VEGFRs: VEGFR-1 is mostly expressed in the blood vasculature, VEGFR-3 is predominantly found in the lymphatic system and VEGFR-2 is expressed in both[99]. SC is unique because it expresses all 3 receptors[16,220,242], such that it exhibits both blood and lymphatic vascular properties[166,213,228]. Furthermore, VEGF has been detected in human AH[69,139,288,301]. Such data supports the idea that SC hydraulic conductance could be regulated in a similar manner than other microvasculature[23].

In line with other studies[24,32,86,217,226,310], differential VEGF-A isoforms have antagonistic effects; in this case, we showed that $Vegf_{164}a$ increased C whereas $VEGF_{165}b$ decreased it. Hence, differential splicing of VEGF-A may be a key factor for outflow facility regulation. In the same way, when VEGFR-2 was inhibited, a very similar reduction in C was measured compared to $VEGF_{165}b$. Thus $VEGF_{165}b$ may act as a competitive inhibitor and the signaling responsible for outflow regulation may be mediated through VEGFR-2. This agrees with the work from Sano *et al.* (2012)[242], who reported buphthalmia and IOP elevation in VEGFR-1 and VEGFR-2 knock down mice. Consequently, it seems that outflow resistance regulation changes in response to exogenous VEGF and VEGFR inhibition in a similar manner than endothelial hydraulic resistance does, which reinforces the idea that the inner wall of SC is crucial for outflow regulation.

The contribution of effectors downstream of VEGFRs to outflow regulation was also explored. We observed that when NOS is inhibited by L-NAME the efficacy of VEGF on outflow facility was reduced although not completely suppressed (from 90 to 30%), supporting findings in other systems[60,127,260]. However, the role of Rac1 is more controversial, since it seems to exert different effects depending on how it is activated. On one hand, Rac1 has been described as a downstream effector of VEGFR triggering sig-

naling cascades[88,105,121,134,185,197,205]. Several studies reported an increase in vascular permeability after Rac1 activation[51,197,294,295], which is necessary for VEGF mediated VE-Cadherin internalization[110] and fenestration induction[88]. On the other hand, if Rac1 gets activated through another source, for instance sphingosine-1-phosphate (S1P)[297], it seems to tighten cell-cell junctions[78,108,250]. In fact, S1P is known to decrease outflow facility in human[262] and mouse[42] eyes. In this study, we measured a reduction in C of 30% upon Rac1 inhibition (although significance was not achieved, $p = 0.08$), in contrast with the work of Pattabiraman and colleagues[214] who reported a decrease in transendothelial electrical resistance after Rac1 inhibition in a cell culture system. When $Vegf_{164}a$ was perfused with the Rac1 inhibitor EHT1864, the effect of VEGF was reduced from almost 90% to 20%. The fact that the effect of VEGF was blunt when blocking either NOS or Rac1 suggests that both pathways are important for AH drainage.

The fact that SC cells express VEGFR-3 makes it a very appealing therapeutic target for glaucoma because it would not disturb normal vascular function of the eye. Unfortunately, there are no endogenous selective ligands for VEGFR-3 and both VEGF-C and VEGF-D also bind VEGFR-2, hence, assessing the role of VEGFR-3 alone is challenging. In this study, VEGF-D was chosen as a ligand to test because Karnezis and colleagues reported that VEGF-D signaling inhibits PGDH, the enzyme responsible for PGs degradation[158] resulting in higher availability of PGs. This is interesting because some current treatments for glaucoma are based on PG analogues[192,306], therefore, they are known to reduce IOP. However, in this study, we could not attribute the effect seen when perfusing with Vegf-D to VEGFR-3. Even though Vegf-D significantly increased facility, its effect was suppressed when VEGFR-2 was inhibited. This observation may be due to the experimental time that is relatively short for an *ex vivo* perfusion (around 2 hours). Therefore, a different approach needs to be taken in order to exploit the possibility of using VEGFR-3 as a target to reduce ocular hypertension.

In conclusion, we have confirmed that VEGF signaling pathways are integrally involved in the regulation of the conventional aqueous outflow system. We have shown that VEGF-A differential isoforms and VEGFRs inhibitor provoke significant bidirectional changes in outflow facility. These changes in facility are consistent with previously described effects of VEGF in endothelial cell permeability mediated through VEGFR-2,

which reinforces the notion that permeability of SC is a key factor in conventional outflow regulation. Further work is needed to determine the specific morphological changes induced by VEGF on SC, for example, if VEGF effect is mediated through enhancing fenestration or disassembling cell-cell junctions or both and which biochemical pathways are involved. These results may help explain why some patients receiving chronic anti-VEGF therapy develop sustained high IOP that can result in vision loss from glaucoma[1,184,289]. What is more, our collaborators Dr. R Rand Allingham and Dr. Joanne C Wen (Department of Ophthalmology, Duke University) have data showing that patients receiving more than 20 anti-VEGF injections have lower outflow facility (personal communication, data not shown). This is clinically important since vision loss from glaucoma commonly causes loss of peripheral vision, compounding the loss of central vision that is characteristically caused by NVAMD and other retinal disorders that are treated in this manner. Therefore, monitoring IOP and treating it where necessary is central in order to preserve what vision may remain in these patients.

Chapter 3

The role of VEGF on outflow facility in mice with glucocorticoid-induced ocular hypertension

3.1 Introduction

Elevated intraocular pressure (IOP) is the principal risk factor for glaucoma. The only way to prevent the damage of the optic nerve characteristic of glaucoma and preserve vision is to lower IOP. The exact mechanisms that lead to an increased IOP are not fully understood, but it is generally agreed that elevated IOP is due to an increased aqueous humour (AH) outflow resistance (R)[117].

Many studies in recent years are using mice as a model to study AH dynamics. Mice are a better model than other non-human primate models because, like humans, they have a continuous Schlemm's canal (SC) with ciliary muscle tendons that connect to its inner wall and a laminated trabecular meshwork (TM)[168,206,254]. Furthermore, the AH dynamics is also comparable since they have similar IOP and AH turn-over rate[6]. They can be similarly used experimentally because they do not show "washout" effect[174] (increase in outflow facility due to perfusions) observed in all non-human species including monkeys and respond similarly to pharmacological treatment[42,191]. Moreover, they are easily accessible and can be genetically modified. However, even though different mice strains present different IOP[44], mice do not naturally experience ocular hypertension (OHT) associated with increased resistance in the outflow pathway tissues. Nevertheless, treating them with systemic glucocorticoids (GCs) (with dexamethasone (DEX), for instance), it is possible to mimic some of the features characteristic of primary open-angle glaucoma (POAG)[208].

The effects of GCs on outflow resistance have been extensively studied[65,208]. It has been reported that patients with POAG have higher blood levels of GCs than healthy individuals[187]. Furthermore, exogenous administration of GCs to treat inflammatory pathologies leads to increased AH outflow resistance and elevation of IOP in an important portion of patients without history of POAG and all of those suffering from glaucoma[208]. Moreover, morphological changes in the TM after DEX treatment have been shown in both humans[147] and mice[207]. Therefore, administration of GCs to animal models has been used to create a platform to study OHT associated to increased R[208].

The GC-induced mouse model for OHT was first described by Whitlock *et al.* in

2010[304] and further characterization was done by Overby *et al.*[211] and Zode *et al.*[319] in 2014. These studies showed that this model is characterised by: (1) IOP elevation, (2) reduction of conventional outflow facility (C), (3) increased MYOC gene expression, (4) presence of plaque-like sheath deposits in the TM and (5) more dense and continuos basement membrane underlying the inner wall of SC. These studies also showed that GC-induced OHT can be reversed pharmacologically.

The importance of having a good model of OHT relies on the fact that the final objective of glaucoma research is to find better drugs to reduce IOP and treat the disease more effectively. However, testing drug candidates in normotensive mice may not reflect the response in OHT. For example, compensatory mechanisms that may act to avoid ocular hypotension could alter the IOP response in normotensive individuals.

In the second chapter of this thesis (see Chapter.2) it has been described that vascular endothelial growth factor (VEGF) may be involved in outflow resistance regulation. In this chapter, we assessed the effect of VEGF in mice with GC-induced OHT. We examined 3 different forms of VEGF, shown to have different effects on outflow facility, in mice treated with 2 dosages of DEX.

3.2 Materials and Methods

3.2.1 Experimental design

DEX was delivered systemically by osmotic mini-pumps as described previously by Overby *et al.* 2014[211]: base line measurements of IOP and weight were carried out 24 hours before mini-pump implantation on the morning. The following day, mini-pumps containing DEX were implanted. During the four weeks duration of the treatment, IOP and weight were measured weekly. After this period of time mice were culled by cervical dislocation and the eyes enucleated for *ex vivo* perfusions. For each mouse, one eye was perfused with DBG (PBS including divalent cations and 5.5 mM glucose) and its contralateral with VEGF simultaneously. 3 forms of VEGF were tested: 500 ng/ml Vegf-A_{164}a, 500 ng/ml VEGF-A_{165}b and 1 µg/ml Vegf-D.

Two cohorts of male C57BL/6 mice (Charles River Laboratories, UK) of 13 to 15 weeks old (at the time of mini-pump implantation) were used, each one treated with a different dose of DEX. The first cohort had a control group of 5 mice treated with Dulbecco's Phosphate Buffered Saline (PBS, Gibco, Life Technologies, UK) and 15 mice treated with 0.1 mg/kg/day DEX. Of these 15 mice, 9 mice were used to perfuse Vegf-A_{164}a and 6 to perfuse VEGF-A_{165}b. The second cohort had 20 mice treated with 2 mg/kg/day and no control group. Of these mice, 2 were found dead before the end of the treatment, 1 was not included in the study because of malfunction of the mini-pump, 9 were used to perfuse with Vegf-A_{164}a and 7 were perfused with Vegf-D.

A very low concentration of DEX (0.1 mg/kg/day) was used for the first cohort because of a miss-communication with the DEX provider (Sigma Aldrich). Therefore, the experiments were repeated with a second cohort using the dose of DEX that is in accordance with the literature (2 mg/kg/day).

All procedures on living mice were done in compliance with the ARVO Statement for the Use of Animals in Ophthalmic and Vision Research under UK Home Office Project License 70/7306, which includes a humane endpoint stating that any animal losing more than 20% of its weight because of DEX treatment will be humane culled.

3.2.2 Animal husbandry and mini-pump implantation

Animals were brought into the animal facility one week prior surgery for an acclimatization period. 5 mice where housed per cage in individually ventilated cages, they had access to food and water *ad libitum* and were under 12 hours light cycle (7 am to 7 pm) at 21℃.

DEX (#D2915, Sigma Aldrich, UK) was dissolved in PBS (Gibco, Life Technologies, UK) at the required concentration, then, mini-pumps[1] (Alzet, model 1004; DURECT Corp., Cupertino, CA, USA) were weighted, filled with 100 µl of DEX and assembled inside a class two safety cabinet. Because within the cohort not all mice had exactly the

[1] Pumps deliver DEX at a constant flow rate of 0.11 µl/hr (Standard deviation = 0.01 µl/hr).

same weight, the concentration of DEX loaded in the pump needed to be different for each animal. Therefore, mice with ± 1 gr. were put together and the correct amount of DEX was delivered, within a group, the DEX dosage could change by 5%. DEX concentration loaded into the pump was calculated using Alzet's Drug Concentration Calculator[13].

Surgery was performed under general anesthesia induced by 5-minute exposure to 3% to 4% isoflurane (Isocare, Animalcare Ltd., UK) and 1 l/min oxygen in an anesthetic chamber. Then, the mouse was moved into a Bain coaxial circuit (Able Scientific, Perth, Australia) with 3% to 4% isoflurane and 1 l/min oxygen and placed facing downwards. At this point, the mouse was injected with 5 mg/kg enrofloxacin antimicrobial (Baytril; Bayer Healthcare, Leverkusen, Germany) subcutaneously and 0.05 mg/kg intramuscular buprenorphine (Vetergesic; Reckitt Benckiser Healthcare, Hull, UK). When the mouse did not react to toe pinch, the shoulder blade area was shaved and disinfected with chlorhexidine alcohol (Krusse, Langeskov, Denmark). A 1 cm long cut was performed in between the scapula and a subcutaneous pocket was created towards the ribs and lower limb using sterile blunt scissors. The mini-pump was placed in the pocket with the flow regulator facing away from the incision. The wound was closed using surgical tissue adhesive (Tissue Bond; 3M, St. Paul, MN, USA) and the mouse was then removed from the anesthesia supply to be placed in a 28℃ box to recover.

After surgery, mice were housed individually and healing of the wound was monitored daily to ensure that it did not get infected or inflamed. Because with the DEX treatment mice lose weight, every other day they were given access to a high-caloric dietary supplement (Complan; H. J. Heinz Co., Ltd., Middlesex, UK). If any mouse lost more than 20% of its weight, it was humanely culled and dropped from the study.

Once the mouse was culled, the pump was removed and the content was examined in order to confirm that DEX was delivered correctly. If a pump malfunctioned and did not deliver DEX completely, the mouse was not included in the analysis.

3.2.3 IOP measurement

IOP was measured using a commercial rebound tonometer (TonoLab; Icare, Finland). Measurements were done between 9 am and 12 pm in the right eye with the mouse under general anesthesia with isoflurane (3-4% + 1 l/min oxygen), mice were always assessed in the same order in order to be measured at the same time of the day every week. The animal was placed into the anesthetic chamber for exactly 3 minutes and then moved on a soft clay mold supported on an adjustable laboratory jack stand using a Bain coaxial circuit to maintain anesthesia. The TonoLab was held by a micro-manipulator supported by a ring stand with the tip positioned approximately 2 mm from the central cornea along the optical axis. IOP was defined following manufacturer's instructions: the TonoLab performs five rebound measurements and displays the IOP value on the screen, this process was repeated three times and the values obtained were averaged. IOP measurements were done the day before mini-pump implantation and every 7 days after surgery for 4 weeks.

3.2.4 *Ex vivo* mouse eye perfusion

After 4 weeks of DEX treatment, mice were culled by cervical dislocation and the eyes were enucleated within 5 minutes after death and stored in PBS at room temperature to await perfusion (around 15 minutes). Enucleated eyes were perfused using the iPerfusion system as described in Sherwood *et al.* (2016)[249][2]. Briefly, both eyes were perfused simultaneously using two perfusion systems working in parallel. Each eye was affixed on a platform using cyanoacrylate glue and submerge in PBS in a thermoregulated bath at 35℃. The eye was cannulated into the anterior chamber using a 33g beveled needle (NanoFil, #NF33BV-2, World Precision Instruments, US) and pressurised for 45 min at 8 mmHg using an adjustable hight reservoir. After the acclimatization period, 9 different pressure steps were applied (from 4.5 to 20 mmHg) by changing the hight of the reservoir while pressure inside the eye and flow rate into the eye were measured using a wet-wet differential pressure transducer (PX409, Omegadyne, US) and a flow

[2] More details already described in Section.2.2.4

sensor (SLG64-0075, Sensirion, Switzerland) respectively. All perfusates were filtered through a 0.22 µm filter (#28145-477, VWR international, UK) before use and backfilled from the needle. One eye (control) was perfused with DBG (PBS + 5.5 mM glucose) and its contralateral with the corresponding VEGF dissolved in DBG. VEGF forms used were: **Vegf-A$_{164}$a** (#V4512, Sigma Aldrich, UK), **VEGF-A$_{165}$b** (#ab104953, abcam, UK) and **Vegf-D** (#469-VD-025/CF, R&D Systems, UK).

To calculate C, the last 4 minutes of stable pressure and flow data of each pressure step were averaged, plotted and a power law fitting forced to a 0 intercept was applied. C_r was defined from the fitting according to Sherwood *et al.* (2016)[249] as:

$$Q(P) = C_r \left(\frac{P}{P_r}\right)^{\beta} P \tag{3.1}$$

Where Q is the flow rate, P is the pressure, C_r is the reference facility, P_r is the reference P (8mmHg) and β characterises the non-linearity of the flow-pressure relationship.

3.2.5 Statistical analysis

Significance in IOP and weight was determined by t-test, a paired t-test was used when comparing these variables for the same group of mice before and after treatment and un-paired when comparing control *vs.* treated groups.

The effect of the drugs perfused was determined by the averaged percentage difference between the treated eye and its contralateral control using paired analysis. For the first cohort of mice, the difference in C between the DEX and the PBS treated was determined calculating the percentage change of the average facility of each group using unpaired analysis. Significant changes in C were determined by a weighted t-test according to Sherwood *et al.* (2016)[249].

The C for a population is calculated as the weighted geometric mean of C_r. C, as

lognormally distributed variable is reported as,

$$\overline{C}^{*} \times / \ ME_{\overline{C}^{*},95}(s^{*2}_{pop})$$

where $\overline{C}^{*}$ is the average C, $ME_{\overline{C}^{*},95}$ the margin of error given by the half-width of the 95% confidence interval on the estimate of $\overline{C}^{*}$ and s^{*2}_{pop} is an estimate of the range that would encompass 95% of the facility values within the population.

The comparison of two populations is reported as,

$$\% \ (\overline{D}^{*} \times / \ ME_{\overline{D}^{*},95}(s^{*2}_{tre}))$$

where $\%$ is the percentage change $((\overline{D}^{*}-1)^{\times}100)$, $\overline{D}^{*}$ is the proportional change, $ME_{\overline{D}^{*},95}$ is the margin of error given by the half-width of the 95% confidence interval on the estimate of $\overline{C}^{*}$ and s^{*2}_{tre} the range of the 95% of the treatment.

3.3 Results

3.3.1 Mice treated with 0.1 mg/kg/day DEX

Previous studies of GC-induced OHT used systemic DEX concentrations of about 3-4 mg/kg/day[211,304]. In this study, a much lower concentration of 0.1 mg/kg/day was used for the first set of experiments (n = 15) and a small control group (n = 5) were treated with PBS alone. IOP and weight changes were measured weekly and the effect of $Vegf_{164}a$ and $VEGF_{165}b$ on outflow facility was assessed after 4 weeks of DEX treatment.

IOP and weight evolution during DEX treatment

IOP was measured by rebound tonometry the day before implantation of the mini-pump and once a week after surgery, always at the same time of the day to avoid changes due to circadian cycles[72,182].

There was no significant difference between the average IOP for the control and

the treated group before surgery (Wk 0), being 10.9 $\pm$ 0.2 mmHg (mean $\pm$ SD, n = 5) and 11.0 $\pm$ 0.8 mmHg (n = 15) respectively (p = 0.6).

At the end of the treatment (Wk4), IOP did not significantly change for the control group, it was 10.1 $\pm$ 1.1 mmHg (p = 0.2), whereas, the treated group had an average IOP of 13.3 $\pm$ 0.9 mmHg, as can be seen in Figure.3.1. Therefore, after 4 weeks there was a significant difference of 2.3 mmHg between IOP before and after the treatment (p = 3 x 10^{-5}). The difference between the control and the treated group was 3.2 mmHg (p = 7 x 10^{-6}). The difference in the standard deviation between the measurement at Wk0 and all the following weeks is because after mini-pump implantation, IOP was measured inside a hood and the vibrations create noise in the measurement.

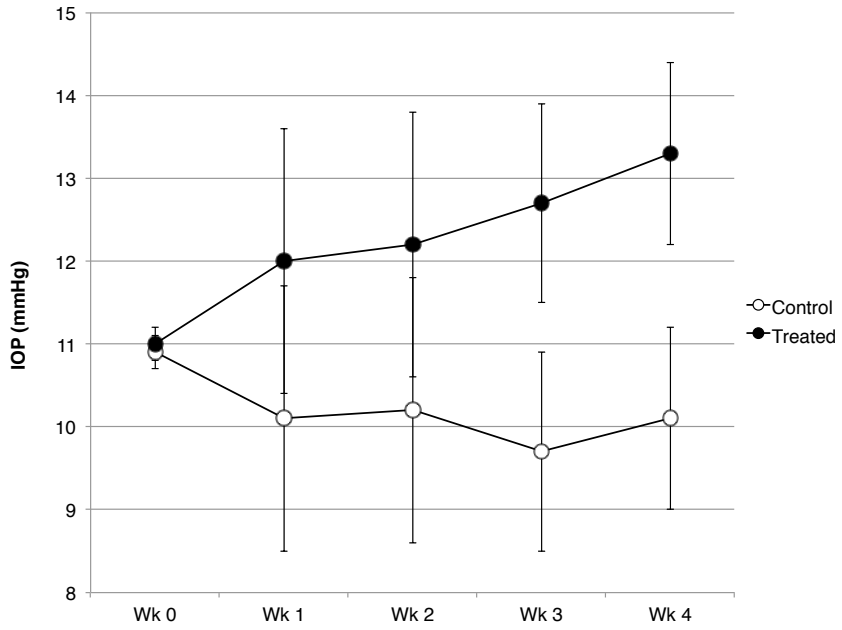


Figure 3.1: IOP evolution during 0.1 mg/kg/day DEX treatment. Each data point is the averaged IOP for the same group of mice measured weekly during DEX treatment, filled dots correspond to the treated group (n = 15) and open dots to the control group (n = 5). Wk 0 corresponds to the base line measurement done the day before mini-pump implantation. Error bars show SD. Wk: week

Apart from IOP, the weight of the mice was also monitored weekly. Due to the DEX treatment mice loose weight and for that reason they were given access to a high-caloric dietary supplement. If any mice lost more than 20% of its body mass it was humanely culled. In this particular case, none of the mice had to be dropped from the study.

Before surgery (Wk0), there was no difference in weight between the control and the treated group, 28.7 $\pm$ 1.5 gr and 29.1 $\pm$ 1.5 gr respectively (p = 0.6). At the end of the

treatment (Wk4), the control group had an average weight of 31.2 $\pm$ 1.7 gr (+2.1 gr, p = 0.003) and the treated 27.2 $\pm$ 1.6 gr. (-1.5 gr, p = 0.001). As can be seen from Figure.3.2, treated mice lost most of the weight during the first 2 weeks of the treatment.

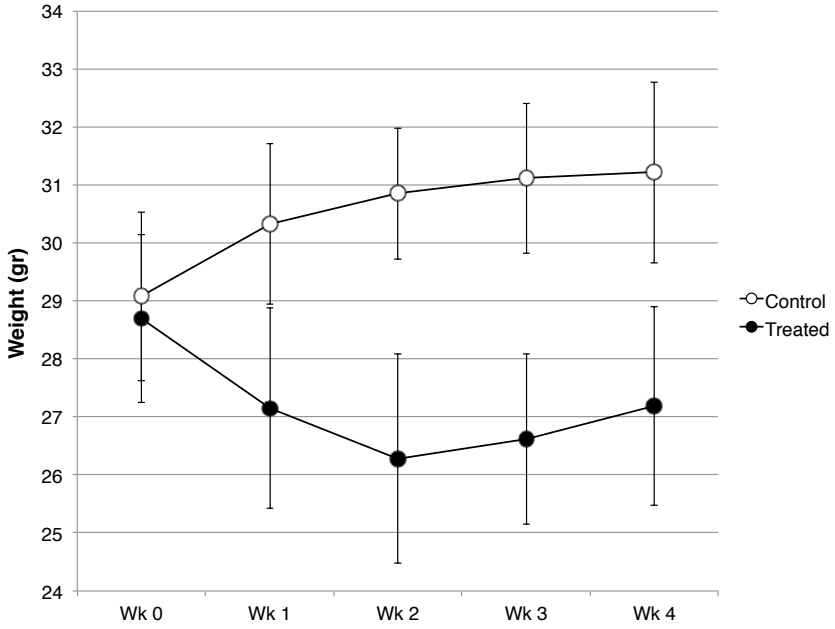


Figure 3.2: Weight evolution during 0.1 mg/kg/day DEX treatment. Each data point is the averaged weight for the same group of mice measured weekly during DEX treatment, filled dots correspond to the treated group (n = 15) and open dots to the control group (n = 5). Wk 0 correspond to the base line measurement done the day before mini-pump implantation. Error bars show SD. Wk: week

Differences in facility between control and treated mice

C was measured for all eyes using the iPerfusion system[249]. For mice treated with DEX, both eyes were perfused, one with DBG and the other one with the drug of interest. For the control group, only one eye was perfused with DBG. All eyes perfused with DBG were used to compare C between mice treated with DEX and those treated with PBS. The average C for the control group was 6.77 $^{\times}/$ 1.62 (2.68) nl/min/mmHg (n=5) and it was 5.48 $^{\times}/$ 1.48 (1.0) nl/min/mmHg (n=13) for the treated one, representing no change in facility (0.96 $^{\times}/$ 1.7 (2.68); p = 0.86) after 4 weeks treatment with 0.1 mg/kg/day of systemic DEX (Figure.3.3). Even though a significant change in IOP was detected, it did not seem to correlate with a change in C, very likely due to the small sample size of the control group. If we focus on the treated group, all data points seem to accumulate at the lower part of the plot.

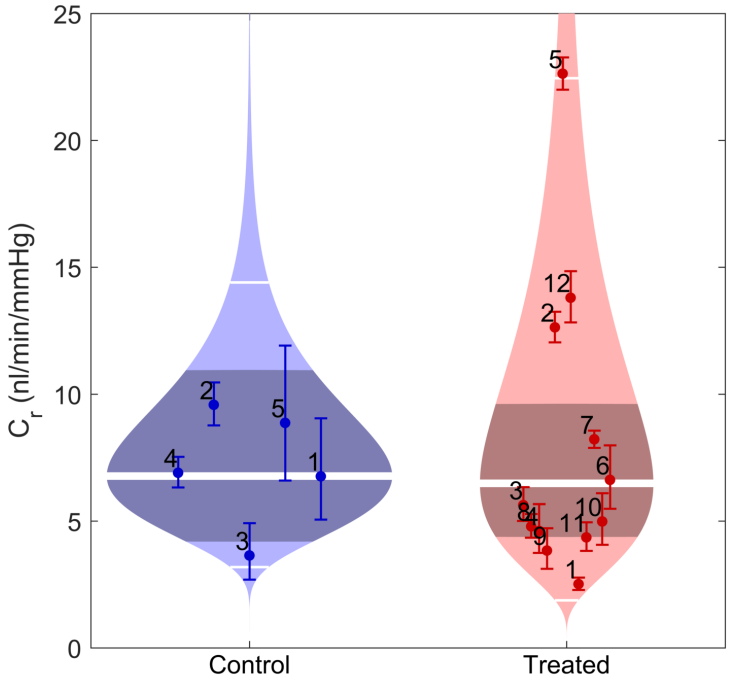


Figure 3.3: Facility values of eyes from controls and DEX treated mice. Each data point shows the reference facility, with the error bars showing 95% confidence intervals in the measurament. Shaded regions show the sample distributions fit to a lognormal distribution, with the geometric mean and two-sigma levels shown by the light horizontal lines. Dark central bands show 95% confidence intervals on the mean values. Numbers denote the eye ID.

Perfusions with $Vegf_{164}a$ and $VEGF_{165}b$

Eyes from mice treated with DEX were used for *ex vivo* perfusions. For a given mouse, both eyes were perfused: one with DBG (control) and the other one with VEGF (500 mg/ml $Vegf_{164}a$ or 500 mg/ml $VEGF_{165}b$ in DBG). These compounds are two different isoforms from VEGF-A with opposite effects on outflow facility, as it has been reported in Chapter.2. $Vegf_{164}a$ is an active form that binds VEGFR-1 and -2 leading to a more permeable endothelium[99], whereas $VEGF_{165}b$ binds the receptors with the same affinity but does not successfully activate it, thus it acts as a competitor inhibitor[310].

In Chapter.2 we reported that $Vegf_{164}a$ increased C by almost 90%. In an attempt to assess the suitability of VEGF to lower IOP in hypertensive mice, eyes from DEX treated mice were perfused with 500 mg/ml $Vegf_{164}a$, the same concentration used in the study mentioned before. Surprisingly we measured that $Vegf_{164}a$ had no statistical significant effect on these mice, although a reduction of 32% (0.68 $^{\times}/$ 1.62 (1.9), n = 5, p = 0.09, Figure.3.4) in C was detected.

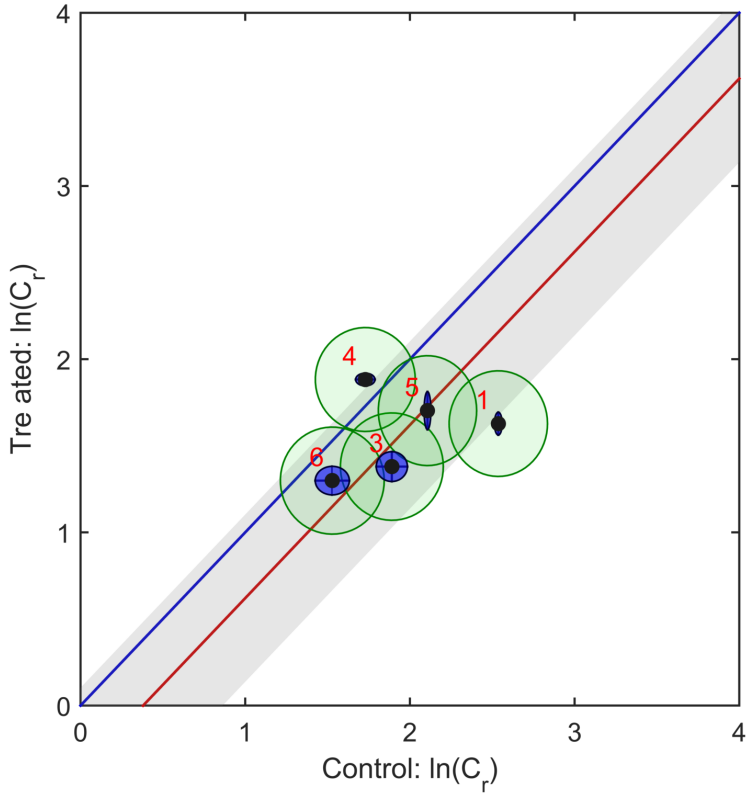


Figure 3.4: Eyes from 0.1 mg/kg/day DEX treated mice perfused with 500 mg/ml $Vegf_{164}a$. Each data point represents one pair of eyes, with the log-facility of the control eye in the X-axis and the treated in the Y-axis. Filled ellipses indicate 95% confidence intervals in the measurement and outer ellipses indicate additional uncertainty between contralateral eyes[249]. Red line shows average difference, with its confidence intervals in grey. Numbers denote the pair ID.

500 mg/ml $VEGF_{165}b$ was perfused as well, and, it resulted in an increase in C of 104% (2.04 $^{\times}$/ 1.81 (2.11), n = 4, $p = 0.03$, Figure.3.5) in comparison to the 44% reduction reported previously in naïve mice (Figure.3.5). Similar to $Vegf_{164}a$, we measured the opposite effect to what it was observed previously in naïve mice.

3.3.2 Mice treated with 2 mg/kg/day DEX

A second cohort of mice was treated with a higher concentration of DEX. In this occasion 2 mg/kg/day was delivered, similar to what was used in other studies[211,304]. The experimental design was exactly the same as described for the lower concentration but in this occasion there was no control group since the concentration used was known to be effective based on previous studies[207].

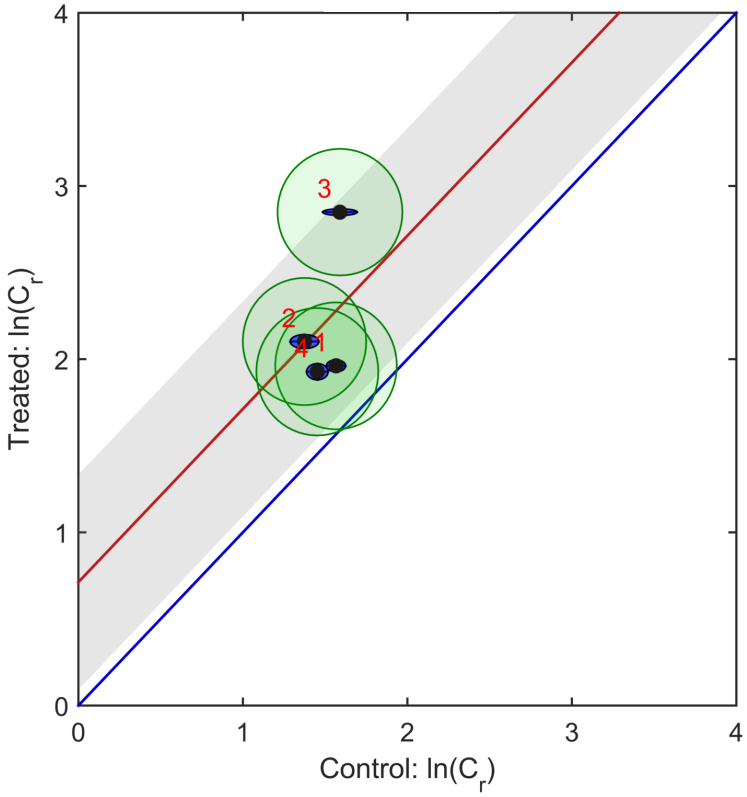


Figure 3.5: Eyes from 0.1 mg/kg/day DEX treated mice perfused with 500 mg/ml $VEGF_{165}b$. Each data point represents one pair of eyes, with the log-facility of the control eye in the X-axis and the treated in the Y-axis. Filled ellipses indicate 95% confidence intervals in the measurement and outer ellipses indicate additional uncertainty between contralateral eyes[249]. Red line shows average difference, with its confidence intervals in grey.

IOP and weight evolution during DEX treatment

IOP was measured the day before the mini-pump was implanted and once a week during the treatment, in the same way as the previous cohort of mice. Due to the larger sample size, perfusions required more than a week, for that reason, IOP was measured again at week 5 on the remaining mice (n = 7) to ensure that IOP did not drop after cessation of treatment at week 4.

Before the treatment (Wk0), the average IOP was 12.3 $\pm$ 2.5 mmHg (n = 20). Four weeks after treatment the average IOP was 14.7 $\pm$ 3.0 mmHg (n = 18) a significant increment of 2.4 mmHg (p = 0.01) in respect to the IOP before the mini-pump implantation. A week later, the 7 remaining mice had the same average IOP of 14.9 $\pm$ 2.5 mmHg than the previous week (p = 0.87). As can be seen in Figure.3.6, in this occasion, there was a peak in IOP at week 1, this may be due to adjustment to the high dose of DEX after

surgery, after that, IOP dropped to the base line value and continued increasing until the end of the treatment.

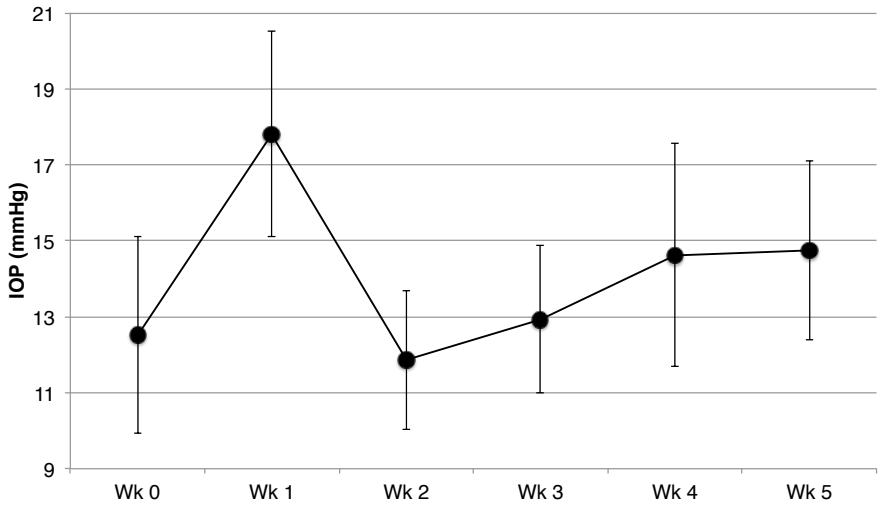


Figure 3.6: IOP evolution during 2 mg/kg/day DEX treatment. Each data point is the averaged IOP from all mice measured weekly during DEX treatment. Wk 0 correspond to the base line measurement done the day before mini-pump implantation (n = 20). Wk 5 represents the mice (n = 7) that could not be perfused during wk 4. Error bars show SD. Wk: week.

Regarding the weight, the average weight before implanting the mini-pumps was 27.4 $\pm$ 1.7 gr (n = 20), at week 4 it was 24.9 $\pm$ 2.2 gr (-2.5 gr, n = 18, p = 0.0005) and the last group at week 5 gained some weight, 26.5 $\pm$ 2.6 gr (n = 7) (Figure.3.7), probably because mini-pumps delivered all DEX by week 4 and mice were recovering from the treatment.

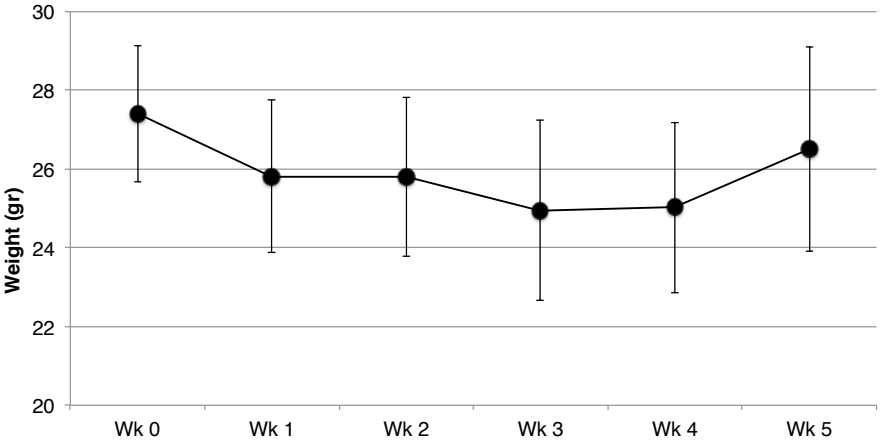


Figure 3.7: Weight evolution during 2 mg/kg/day DEX treatment. Each data point is the averaged weight from all mice measured weekly during DEX treatment. Wk 0 correspond to the base line measurement done the day before mini-pump implantation (n = 20). Wk 5 represents the mice (n = 7) that could not be perfused during Wk 4. Error bars show SD. Wk: week.

Due to the higher dosage of DEX, 2 mice were dropped from the study because they were found dead. They were not humanly culled because they did not lose 20% of their weight but when investigating the possible causes we found out that those mice lose 10% of their body weight within a single week. Consequently, in the future, we will include this terminating point in the protocol. A third mouse was dropped from the study because when the pump was removed from the mouse after the treatment, it still contained the 100µl of DEX it was filled with.

Perfusions with $Vegf_{164}a$ and Vegf-D

Eyes from mice treated with 2 mg/kg/day od DEX were perfused with 500 mg/ml $Vegf_{164}a$. Similarly to the low dose of DEX, $Vegf_{164}a$ did not change C, for the high dose C decreased by 5% (0.95 $^{\times}/$ 1.49 (1.27), n = 4, p = 0.70, Figure.3.8).

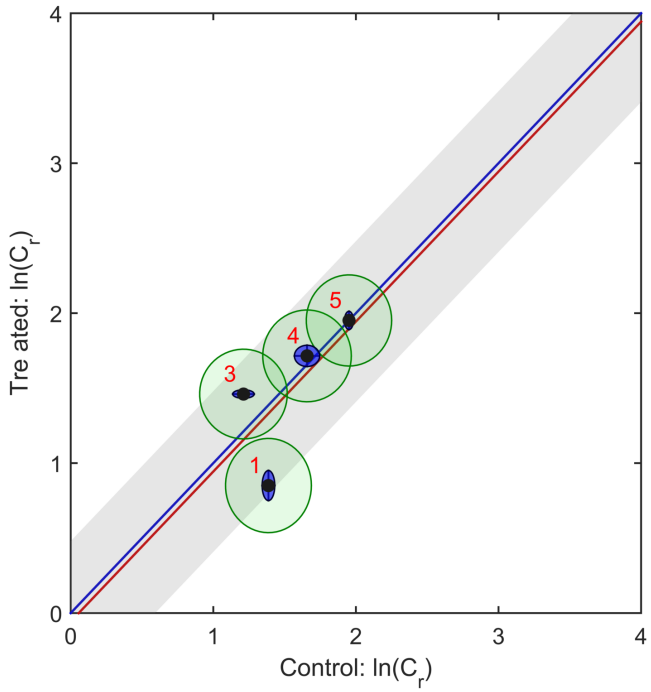


Figure 3.8: Eyes from 2 mg/kg/day DEX treated mice perfused with 500 mg/ml $Vegf_{164}a$. Each data point represents one pair of eyes, with the log-facility of the control eye in the X-axis and the treated in the Y-axis. Filled ellipses indicate 95% confidence intervals in the measurement and outer ellipses indicate additional uncertainty between contralateral eyes[249]. Red line shows average difference, with its confidence intervals in grey.

The effect of 1 µg/ml Vegf-D was also tested. Vegf-D is a ligand for VEGFR-2 and -3. It is known that SC has the unique characteristic to express all three VEGFRs[16,220],

thus, it should be responsive to compounds associated to lymphatic vasculature as it is Vegf-D. In Chapter.2 it was shown that 1 µg/ml Vegf-D was able to increase C, although it is very likely to be mediated by VEGFR-2.

When eyes from DEX-treated mice were perfused with Vegf-D a non significant effect of -14% (0.86 $^{\times}/$ 1.42 (1.62), n = 6, p = 0.32, Figure.3.9) in C was measured. This is, again, opposite of what we reported for naïve mice, where we measure an increase in C of 49%.

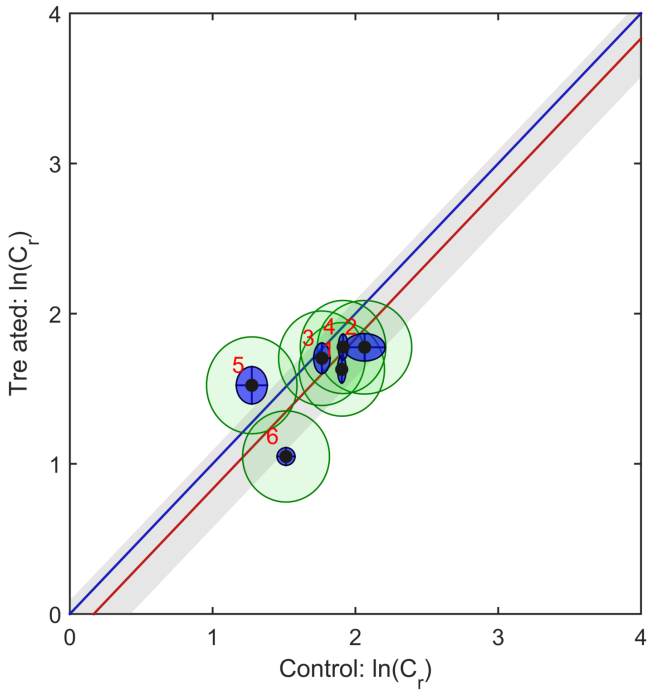


Figure 3.9: Eyes from 2 mg/kg/day DEX mice perfused with 1 µg/ml Vegf-D. Each data point represents one pair of eyes, with the log-facility of the control eye in the X-axis and the treated in the Y-axis. Filled ellipses indicate 95% confidence intervals in the measurement and outer ellipses indicate additional uncertainty between contralateral eyes[249]. Red line shows average difference, with its confidence intervals in grey.

3.3.3 IOP and R correlation

According to the modified Goldmann's equation (Equation.3.2) and assuming that C *ex vivo* represents C *in vivo*, a linear relationship between IOP and outflow resistance

($R = 1/C$) is predicted (Equation.3.5):

$$Q_{in} = C \times (IOP - EVP) + Q_u \tag{3.2}$$

$$Q_c = Q_{in} - Q_u \tag{3.3}$$

$$IOP = \frac{Q_c}{C} + EVP \tag{3.4}$$

$$IOP = Q_c \times R + EVP \tag{3.5}$$

Where Q_{in} is the production rate of AH, EVP is the episcleral venous pressure, Q_u is the outflow rate through the unconventional outflow pathway, Q_c is the outflow rate through the conventional outflow pathway and R the outflow resistance. Measuring C *ex vivo*, one can assume that there is no inflow (Q_{in} = 0) and EVP = 0 mmHg since it is open to the atmosphere.

Figure.3.10a shows all eyes used in this study with IOP (at Wk4) and R data available. A regression liniar fitting has been applied to all data to find the IOP *vs.* R correlation. It can be seen that there is a positive correlation but the fitting is not significant (r^2 = 0.014). Figure.3.10b presents the fitting for each individual cohort, interestingly, the control group shows a positive correlation (r^2 = 0.72), but, the 2 cohorts treated with DEX do not. Perhaps, this is a consequence of the very different accuracy of the two techniques used to measure these parameters, while the iPerfusion system gives a very accurate and precise measurement of R with a very good resolution, the TonoLab can only display measurements with a resolution of 1 mmHg and the effects of anesthesia on IOP are still not well defined.

Nevertheless, if IOP and R values are analysed in terms of population, by averaging each variable from the 3 groups available (control, 0.1 mg/kg/day DEX and 2 mg/kg/day DEX) it can be seen from Table.3.1 that the control group had the lowest IOP and R whereas mice treated with 2 mg/kg/day had the highest IOP and R and mice treated with 0.1 mg/kg/day laid in between. This approach is more consistent with the modified Goldmann's equation (Equation.3.5).

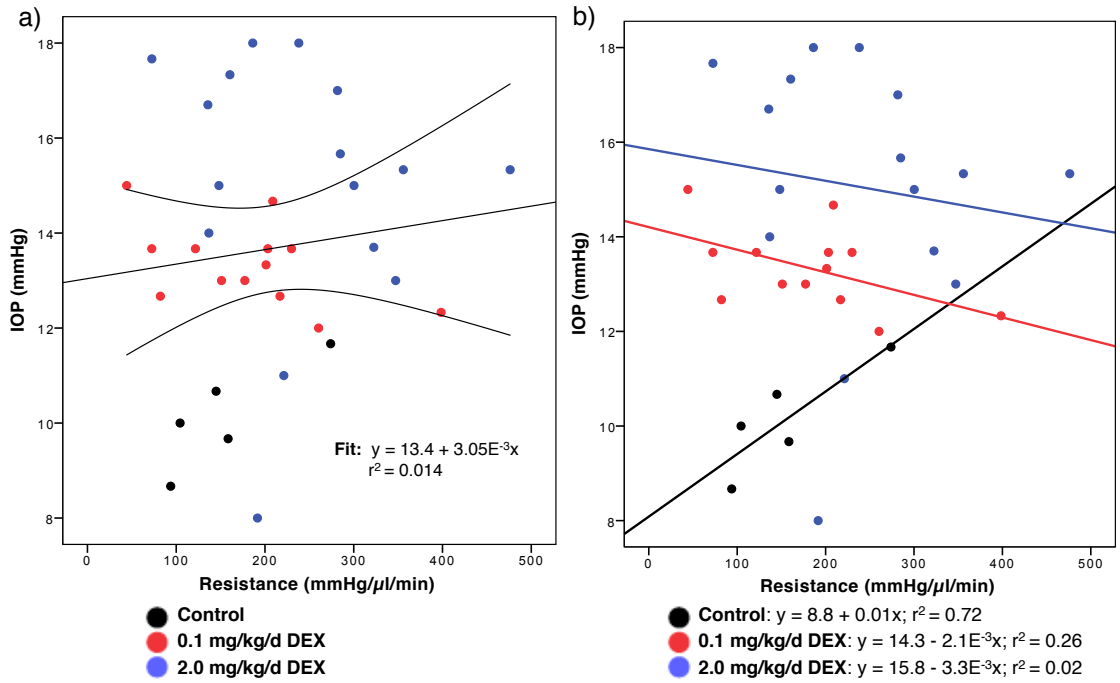


Figure 3.10: IOP and outflow resistance correlation. a) shows a linear fitting with 95% confidence intervals applied to all three groups of mice. b) shows a linear fitting applied to each group of mice individually. Black dots: control; red dots: 0.1 mg/kg/day DEX; blue dots: 2 mg/kg/day DEX.

Table 3.1: Averaged IOP, R and C values for 3 different groups of mice: control, 0.1 mg/kg/d DEX and 2.0 mg/kg/d DEX.

		IOP (mmHg)		Resistance (mmHg/µl/min)		Facility (nl/min/mmHg)	
	n	Average	SD	Average	SD	Average	SD
Control	5	10.13	1.12	147.68	71.72	6.77	2.78
0.1 mg/kg/d DEX	13	13.00	0.86	154.22	53.42	6.48	2.88
2.0 mg/kg/d DEX	16	15.05	2.71	210.97	104.82	4.74	1.96

3.4 Discussion

In the present study mice were systemically treated with two different doses of DEX (0.1 and 2.0 mg/kg/day) for four weeks to induce OHT[211,304]. These mice were used to study the potential efficacy of VEGF as an agent to lower IOP based upon previous results in naïve mice (Chapter.2).

The first interesting finding was regarding the OHT model itself. Even though a very low concentration of DEX was used for the first cohort of mice, virtually the same increase in IOP was measured, the lowest dose of DEX increased IOP by 2.3 mmHg whereas the highest did it by 2.4 mmHg (p = 0.91). Mice treated with the lower dose exhibited lesser weight loss when compared with the higher dose (-1.5 gr *vs.* -2.5 gr) and all animals survived the treatment, whereas 2 died with the higher dose. Moreover, eyes

from mice treated with both concentrations were not responsive to perfused $Vegf_{164}a$, indicating that a low dose of DEX is enough to affect the VEGF signaling pathway.

Despite the increment in IOP, we did not measure a significant reduction in C for the mice treated with the lowest concentration of DEX. The fact that no significance was achieved between the control group and the group treated with 0.1 mg/kg/day DEX can be attributed to the small sample size in the control group. As reported by Sherwood *et al.* (2016)[249] the range in C values in C57BL/6 mice is very wide, hence, a much bigger sample size is required to detect difference in C between two populations of mice (un-paired data). Despite the promising results using a lower concentration of DEX, further characterization is necessary in order to confirm a significant reduction in C and investigate changes in the outflow pathway comparable with those described for higher concentrations of DEX[208].

Another point of discussion is the relationship IOP *vs.* R. It can be predicted from the modified Goldmann's equation (Equation.3.5) that there is a linear relationship between these two variables. However, when individual IOP values are plotted against R calculated from the measured C ($R = 1/C$), this relationship is, most of the time, not observed (Figure.3.10). We can speculate that this is due to, on one hand, that these parameters are not measured at the exact same time and it is known that IOP and R are dynamic parameters and can fluctuate during the day[72,182]. On the other hand, the precision and resolution of the techniques used to measure them are very different, the tonolab has a resolution of 1 mmHg whereas the iPerfusion system can measure flow rate and pressure with a resolution of $\pm$4 nl/min and $\pm$0.024 mmHg respectively[249] . For these reasons, we analysed the IOP *vs.* R correlation in terms of population, looking at the average values within each group. This way, there is a more clear link between the two parameters.

The effect of exogenous VEGF on outflow facility in eyes from DEX treated mice was surprising. Data from naïve mice (Chapter.2) showed that $Vegf_{164}a$ and Vegf-D increased C while $VEGF_{165}b$ decreased it and these effects are very likely mediated by VEGFR-2. However, the opposite response was measured in this study. $Vegf_{164}a$ and Vegf-D tended to reduce C, although it was not significant, and $VEGF_{165}b$ significantly

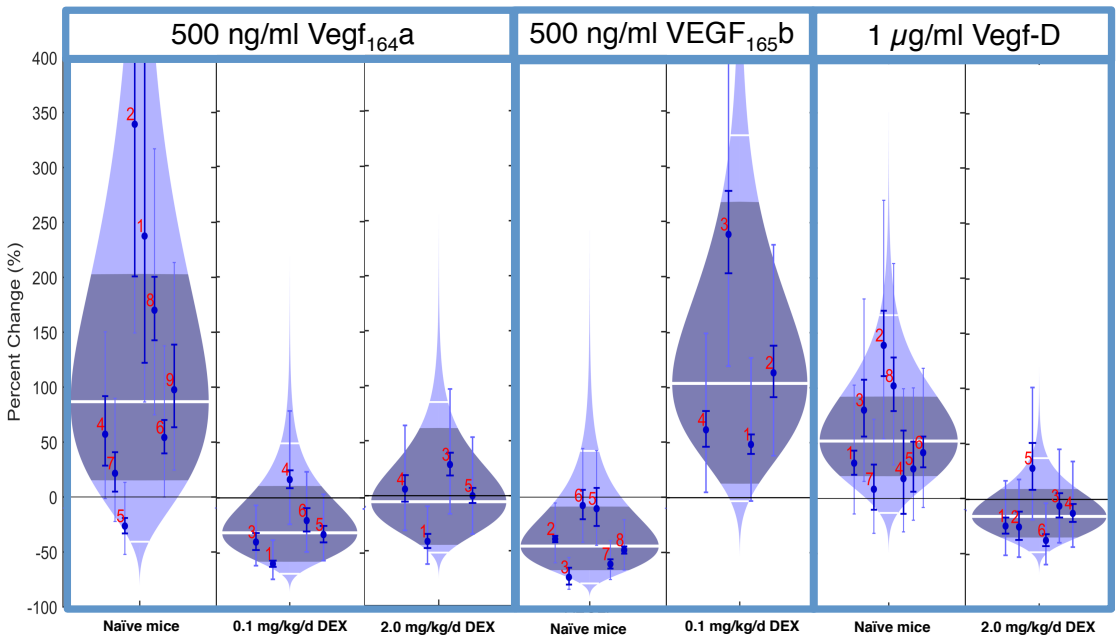


Figure 3.11: Effect of all forms of VEGF on eyes from DEX treated mice compared to naïve mice. Each data point corresponds to a the percentage change between the control and the treated eye from a single mouse, with the dark error bars showing 95% confidence intervals and light error bars the indicate additional uncertainty due to variability in the treatment. Shaded regions show the sample distributions, with the geometric mean and two-sigma levels shown by the light horizontal lines. Dark central bands show 95% confidence intervals on the mean values.

increased C by 104% (Figure.3.11). More research is needed to understand why this phenomenon occurs, but, it could be that the expression of VEGFR in the SC is somehow impaired, as has been reported to happen with other growth factor receptors (such as fibroblast growth factor receptor, epidermal growth factor receptor and hepatocyte growth factor receptor) expressed by TM cells after DEX treatment[65]. Similar studies determined that, after DEX treatment, TM cells showed an inhibition in migration, proliferation and retraction, functions usually attributed to VEGF as well. A recent study[212] showed that rat embryos treated with DEX had a reduced expression of VEGF, VEGFR-1 and VEGFR-2 mRNA. It could be, then, that DEX treated eyes are not responsive to VEGF due to the impaired expression of VEGFRs. However, to our knowledge, there is no information available about the effect of DEX in VEGFR expression in SC cells. Moreover, more research is needed as well in order to understand why $VEGF_{165}b$, which is known to not activate VEGFRs increases C in this context. An additional factor that could interfere with VEGF-induced increase in C in DEX-treated mice is that some studies showed that DEX inhibits nitric oxide (NO) production by endothelial cells[176,271,314], therefore, if one of the key VEGF effectors is suppressed, its effect is blunt, as shown in naïve mice in

Chapter.2 and in previous studies[26].

It could be inferred, then, that when the levels of GCs in the organism is elevated, as detected in glaucoma patients[187] or when GCs are administrated exogenously, cells in the outflow pathway stop responding to endogenous VEGF, contributing to a less permeable SC, thus increasing outflow resistance and IOP. However, more information is needed about the changes in VEGF and VEGFR expression by TM and SC cells in response to DEX as well as histological changes in the outflow pathway. Moreover, it would also be interesting to test whether SC cells from glaucomatous eyes respond differently to exogenous VEGF in order to confirm that a dysfunction in the VEGF signaling is contributing to elevated IOP, which would reaffirm the GC-induced OHT mouse model as an appropriate model to study outflow resistance and IOP as a glaucoma model.

Chapter 4

Influence of plasmalemmal vesicle-associated protein on conventional outflow facility in mice

4.1 Introduction

Maintenance of intraocular pressure (IOP) within physiological levels is essential for the correct functioning of the eye. IOP is controlled by the resistance to aqueous humour (AH) drainage (outflow). An increase in outflow resistance leads to elevated IOP, which is the principal risk factor for glaucoma. It is not fully understood where this resistance is generated but previous studies have reported to be in close vicinity of the inner wall of Schlemm's canal (SC)[148,210].

Schlemm's canal (SC) is an endothelial lining located in the iridocorneal angle of the eye, adjacent to the trabecular meshwork (TM). AH flows through SC and from there into the collector channels; this is commonly referred to as the conventional outflow pathway. As AH flows through this pathway, it must cross the continuous endothelium of SC, presumably through micron-sized pores that pass through the endothelium. These pores can pass either between neighboring SC cells (B-pores), or can pass transcellularly through individual cells (I-pores). Pores are suspected to be important for outflow regulation because, as previous studies have indicated, the density of pores decreases in glaucomatous eyes, which have increased outflow resistance, but it is unclear what controls pore formation, why pores are decreased in glaucoma or how the extra resistance is generated[84,259,287].

Other endothelial linings form similar pores, although these are typically smaller than pores in SC and are known as fenestrae, which provide a high conductivity pathway for fluid flow across the endothelium. Fenestrated endothelia are found in the liver[125], kidney[263] and even in the choriocapilaries in the eye[126]. Fenestrae are about 65 nm in diameter, which is much smaller than the SC pores, and are often bridged by a diaphragm structure. Interestingly, along the inner wall, structures known as "mini-pores" have been described that are about the same size and also contain a diaphragm. It was originally proposed by Anders Bill in 1975[38] that these mini-pores may be precursors to the larger micron-sized pores which may form due to tension produced by AH flowing through[141,275]. As it has been shown, tension triggers pore formation in SC cells in culture[46].

A key characteristic of fenestrae is the presence of diaphragms, a peculiar structure that crosses the aperture in a cartwheel like manner that is similar in all fenestrated endothelia[31], except for endothelial cells of the kidney glomerulus and liver sinusoids[267]. These diaphragms are known to be made of plasmalemmal vesicle-associated protein (PLVAP also known as PV-1 and MECA-32), an endothelial-specific single-span membrane glycoprotein of 60 KDa[265]. PLVAP form homodimers *in vivo* with a short intracellular tail and a long extracellular domain displayed in an octagonal symmetry of radial fibrils from the rim to a central knob[264,266]. This protein is necessary and sufficient for fenestra formation[266] and high expression of PLVAP correlates with higher permeability[308]. When PLVAP is knocked down, fenestrae density decreases and become disorganised, the characteristic arrangement in sieve plates with equidistant spacing is lost[142].

The similarity between fenestrae and mini-pores in SC motivated the study of the influence of PLVAP on SC hydraulic conductivity. For that, we used a transgenic mouse line developed by Herrnberger *et al.* (2012)[124], which are PLVAP deficient. Heterozygous mice have a reduced expression of PLVAP and knock out mice have no diaphragms present compared to their wild-type littermates. Furthermore, fenestration is significantly reduced in endothelial linings such as the choriocapillaries[126] and sinusoids of the liver[125]. For these reasons, we hypothesised that SC cells from PLVAP deficient mice would experience impaired I-pore formation resulting in a reduced outflow facility (C).

It is known that cytoskeletal disrupting drugs increase both fenestration[49,50,142,268] and outflow facility[85,94,180,223,229,282]. However, their mechanism of action is not fully understood, therefore, PLVAP depleted mice provides a good model to understand how these drugs effect outflow resistance. For this reason, eyes from both groups of mice were perfused with latrunculin B (Lat-B). Latrunculins are a family of actin disrupting drugs that had already been described to induce fenestration through cytoskeleton reorganization[49,142]. Moreover, there are also studies reporting an increment in C in porcine[85], monkeys[223] and human eyes[94] perfused with Lat-B. However, to our knowledge, there is no information about mice although a similar effect was expected. Because PLVAP deficient mice are less able to form fenestrae, we hypothesised that they would be less

sensitive to Lat-B.

4.2 Materials and Methods

4.2.1 Experimental Design

The present study investigated the influence of the protein PLVAP on conventional outflow facility in mice that were a kind gift of Professor Ernst Tamm (University of Regensburg). To achieve this objective, transgenic mice deficient in this protein (heterozygous, *Plvap*$^{+/-}$) and their wild-type (*Plvap*$^{+/+}$) littermates were used. Unfortunately, the negative homozygous genotype (*Plvap*$^{-/-}$) was lethal on the genetic background used (C57BL/6N) and knock out mice were not available for the study. Rebound tonometry and the iPerfusion system were used to measure IOP and C respectivebly eyes in order to find differences between both genotypes. Moreover, the effect of 1µM Lat-B on outflow facility was tested to understand the mechanism of pore formation. All perfused eyes were immersion fixed in Karnovsky's fixative to be used for electron microscopy and count the number of pores in the inner wall of SC.

4.2.2 Animal Husbandry

Mice used in this study were imported from University of Regensburg, where they were developed[124], and bred in-house at Imperial College London. Heterozygote mice were used as breeders, pups were weaned at 1 month old and housed in ventilated cages with a maximum of 5 mice per cage. Mice were provided with food and water *ad libitum* and kept at 21℃ with 12 hour light-dark cycles. Mice with a C57BL/6N genetic background of either gender between 8 and 14 weeks old were used.

Genotyping was performed on ear tissue samples obtained at weaning. Tissue lysis and DNA extraction were performed according to the manufacturer's instructions (Express Extract kit, Kapa-Biosystems, US). Extracted DNA was used directly for PCR analysis using a hot-start mix (KAPA2G Robust HotStartReadyMix; Kapa- Biosystems,

US). A 3 primer PCR was employed to detect wild-type or heterozygous alleles[124], 29 cycles were performed with an annealing temperature of 59℃. Sense primer for wild-type: AGAGCCTTCTCTGCCAAGTG, sense primer for knock-out: TCTCATGCTGGACTTCTTCG and antisense primer: GGCTAGCCTGAGCTACAGAGG, predicted product size of 672bp for wild-type, 672bp and 552bp for heterozygous. PCR products were resolved by gel electrophoresis (1% agarose) in the presence of DNA gel stain (SYBR Safe; Invitrogen, US). Bands were visualised on an imaging station (Biospectrum 500; UVP, US). A representative electrophoresis gel can be seen in Appendix II (7.2.5).

All experiments were conducted in compliance with the ARVO Statement for the Use of Animals in Ophthalmic and Vision Research under UK Home Office Project License approval for research at Imperial College London.

4.2.3 IOP measurements.

IOP was measured on the right eye of the mouse, always between 9 am and 12 pm to avoid changes due to circadian cycles. IOP was measured under general anesthesia with isoflurane (Isocare; Animalcare Ltd., UK) using a commercial rebound tonometer (TonoLab; Icare, Finland).

To induce anesthesia, the mouse was placed into an anesthetic chamber delivering 3-4% isoflurane + 1 l/min oxygen for exactly 3 minutes to account for anesthetic effects. Then, it was moved to a soft clay mould supported on an adjustable laboratory jack stand, the snout of the mouse was placed at the end of a Bain coaxial circuit to maintain anesthesia. Immediately, IOP was measured with the TonoLab held by a micro-manipulator supported by a ring stand to ensure stability. The tip of the TonoLab was positioned along the optical axis approximately 2 mm away from the cornea and IOP measured by 5 rebound events. This procedure was repeated 3 times and the arithmetic mean of these values define the IOP of the mouse, following manufacture's instructions. Afterwards, the mouse was placed in a 28℃ chamber to recover from anesthesia before returning to the cage.

4.2.4 *Ex vivo* Mouse Eye Perfusion

C was measured *ex vivo* on enucleated eyes using the iPerfusion system as described by Sherwood *et al.* (2016)[249]. Briefly, mice were culled by cervical dislocation, the eyes enucleated within 5 minutes and stored in Dulbecco's Phosphate Buffered Saline (PBS; Gibco, Life Technologies, UK) at room temperature until perfused, generally within 20 minutes. Both eyes of a mouse were perfused simultaneously using two perfusion systems at the same time to avoid post-mortem changes.

Briefly, eyes were fixed on a support placed in a thermoregulated bath (35℃) using cyanoacrylate glue and submerged in PBS. The eye was then, cannulated into the anterior chamber with a 33g beveled needle (NanoFil, #NF33BV-2, World Precision Instruments, US) and pressurised at 8 mmHg for 45 minutes using an inline reservoir. After this time, the reservoir was brought down to 4.5 mmHg to start applying 9 discrete pressure steps up to 21 mmHg. For each step, pressure (P) and flow rate (Q) inside the eye were measured using a wet-wet differential pressure transducer (PX409, Omegadyne, US) and a flow sensor (SLG64-0075, Sensirion, Switzerland) respectively.

The perfusate used was PBS including divalent cations and 5.5 mM glucose (referred to as "DBG") filtered through a 0.22 µm filter (#28145-477, VWR international, UK). Lat-B (#428020; Calbiochem, Merck Millipore, UK) was purchased as powder and dissolved in DMSO to a stock concentration of 12.6 mM, aliquoted and store at -20 ℃. For perfusions, the experimental eye was perfused with the stock solution of Lat-B dissolved in DBG to a concentration of 1 µM and the contralateral control was perfused with DBG + 0.008% DMSO to account for any effect that the drug vehicle could have.

After perfusion, eyes were fixed in Karnovsky's fixative which consisted of the following: a stock solution (2.8% paraformaldehyde, 0.1 M cacodylate-Na-salt buffer ($C_2H_6AsO_2$ Na $3H_2O$)) was made and kept at 4℃. Fixative solution was prepared fresh immediately before fixation with 90% stock solution and 10% of 25% glutaraldehyde. Eyes were immersed in the solution and fixed overnight at 4℃. The next day, eyes were washed for 20 minutes, 3 times in 0.1 M cacodylate buffer and stored in the same buffer solution at 4℃.

C was determined as stated by Sherwood *et al.* (2016)[249]. Briefly, the last 4 minutes of stable Q and P were averaged for each perfusion step and used to generate a Q *vs.* P plot. A power law fitting was applied and forced to a 0-0 intercept, then, C was defined as the quotient of Q over P at the reference P of 8 mmHg from the fitting.

The effect of Lat-B on outflow facility was calculated as the average percentage change in C between the control and the contralateral treated eye, hence, all experiments used contralateral paired eyes. Unpaired eyes (due to an experimental failure in one eye) were rejected.

4.2.5 Statistical Analysis

Two types of C analysis were carried out, unpaired analysis for genotype comparison and paired analysis for Lat-B effect assessment. Paired analysis required that both eyes of the mouse were perfused to compare the control and treated contralateral eye. For the unpaired analysis, only one eye per mouse was necessary and the average C for each genotype was compared. Hence, data from control eyes from Lat-B perfusions were also used compare genotypes. Weighted t-tests[249] were used to analyse significance in C both for paired and un-paired data.

C measurements for a group of mice are a log-normally distributed, for this reason, they are reported as,

$$\overline{C}^{*} \times / \; ME_{\overline{C}^{*},95}(s^{*2}_{pop})$$

where $\overline{C}^{*}$ is the average C, $ME_{\overline{C}^{*},95}$ the margin of error given by the half-width of the 95% confidence interval on the estimate of $\overline{C}^{*}$ and s^{*2}_{pop} is an estimate of the range that would encompass 95% of the facility values within the population.

The comparison of two populations is reported as,

$$\% \; (\overline{D}^{*} \times / \; ME_{\overline{D}^{*},95}(s^{*2}_{tre}))$$

where $\%$ is the percentage change ($(\overline{D}^{*}-1)^{\times}100$), $\overline{D}^{*}$ is the proportional change, $ME_{\overline{D}^{*},95}$ is the margin of error given by the half-width of the 95% confidence interval on the estim-

ate of $\overline{C}^*$ and s^{*2}_{tre} the range of the 95% of the treatment.

A two-tailed un-paired t-test (SPSS; IBM, Armonk, U.S.) was used to determine statistical significance in IOP. IOP is reported as average $\pm$ standard deviation (SD).

4.3 Results

4.3.1 Effect of PLVAP depletion on outflow facility and IOP in mice

We hypothesis that mice lacking PLVAP would have impaired pore formation and reduced C. To investigate that, eyes from *Plvap*$^{+/-}$ and *Plvap*$^{+/+}$ mice were perfused using the iPerfusion system to measure C *ex vivo*.

One eye from each mouse was perfused with DBG in order to calculate C for each genotype. The average C for *Plvap*$^{+/+}$ mice was 8.47 $^{\times}/$ 1.29 (2.98) nl/min/mmHg (n = 21) while *Plvap*$^{+/-}$ mice had a C of 5.61 $^{\times}/$ 1.20 (2.03) nl/min/mmHg (n = 17). This represents a significant reduction in C of 34% (0.66 $^{\times}/$ 1.35 (1.00), p = 0.009) when PLVAP expression is diminished (Figure.4.1).

IOP was also measured for both groups of mice but no difference was detected, *Plvap*$^{+/+}$ mice had an average IOP of 12.3 $\pm$ 1.7 mmHg (n = 12) and *Plvap*$^{+/-}$ mice had an IOP of 12.2 $\pm$ 2.1 mmHg (n = 11) (p = 0.85) (See Table.4.1 and Figure.4.2). With a reduction in C one should expect an increment in IOP in accordance to the modified Goldmann's equation (Equation.3.2) described in Chapter.3. However, this was not observed. It could be possible that AH production is impaired in these mice since capillaries in the ciliary processes are fenestrated[279]

Table 4.1: IOP and C measurements on *Plvap*$^{+/+}$ and *Plvap*$^{+/-}$ mice. SD: standard deviation, SEM: standard error of the mean.

Genotype	n	IOP (mmHg)	SD	SEM	*p*-value	C (nl/min/mmHg)	*p*-value
Plvap$^{+/+}$	12	12.3	1.7	0.50		8.47 $^{\times}/$ 1.29	
Plvap$^{+/-}$	11	12.2	2.1	0.65	0.85	5.61 $^{\times}/$ 1.20	0.009

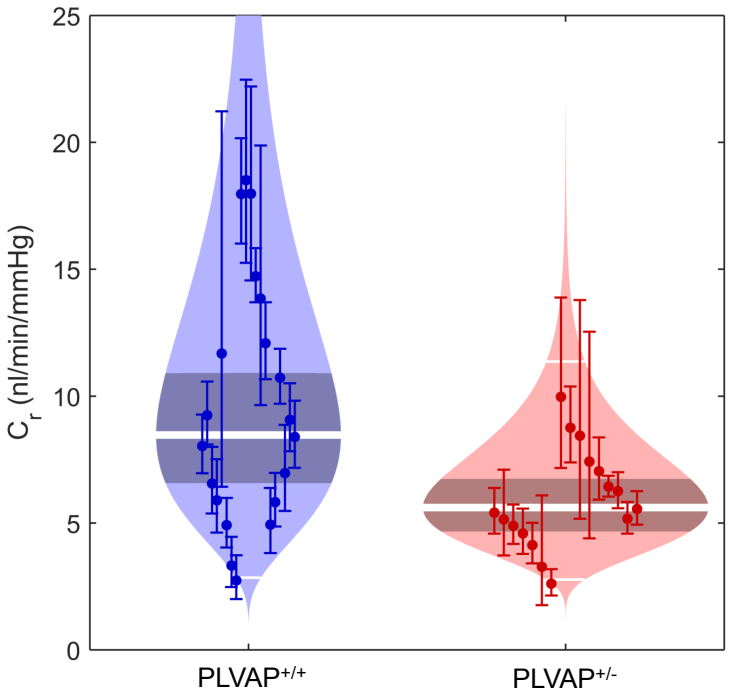


Figure 4.1: Facility values for *Plvap*$^{+/+}$ and *Plvap*$^{+/-}$ mice represented in a modified violin plot. Each data point corresponds to the measured C for a single eye perfused with DBG and the error bars are the 95% confidence interval for that particular measurement. The white central line is the geometric mean, the dark area around it is the error of the mean and two-sigma levels are shown by the light horizontal lines. The coloured area is the distribution of the data. **Left plot:** Facility measurements from *Plvap*$^{+/+}$ mice (n = 21). **Right plot:** Facility measurements from *Plvap*$^{+/-}$ (n = 17).

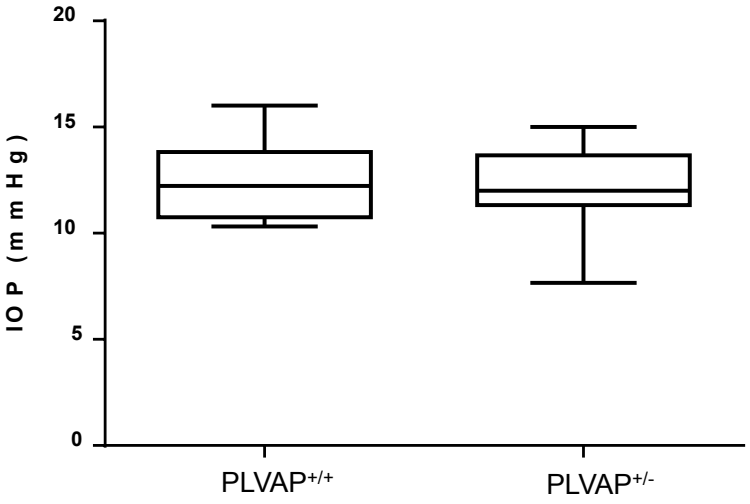


Figure 4.2: IOP values for *Plvap*$^{+/+}$ and *Plvap*$^{+/-}$ mice represented in a box plot. **Left plot:** IOP measurements from *Plvap*$^{+/+}$ mice (n = 12). **Right plot:** IOP measurements from *Plvap*$^{+/-}$ (n = 11). The central line in the box represents the average IOP and the whiskers the 95% confidence interval.

4.3.2 Effect of PLVAP-depletion on the outflow facility response to Latrunculin in mice

In order to test the mechanisms that lead to PLVAP-mediated pore formation, eyes from *Plvap*$^{+/-}$ and *Plvap*$^{+/+}$ mice were perfused with 1 µM Lat-B. Lat-B is known to induce pore formation through disassembly of actin filaments and to increase C in other animal models[85,94,223]. We speculate that mice with impaired pore formation should respond less to Lat-B.

Plvap$^{+/+}$ mice perfused with Lat-B showed a 29% increment in C (1.30 $^{\times}/$ 1.30 (1.39), n = 7, p = 0.05) and *Plvap*$^{+/-}$ mice experienced a 64% increment (1.64 $^{\times}/$ 2.02 (3.53), n = 6, p = 0.13) as shown in Figure.4.3a. Therefore, despite the fact that *Plvap*$^{+/-}$ have less hydraulic conductance reflective of possible less pores, when the cytoskeleton is disassembled C can be enhanced. However, due to the high variability in the response to 1 µM Lat-B, significance was not reached.

Interestingly, if only eyes treated with Lat-B from both genotypes are compared, we found out that there was no difference and both genotypes reached the same average facility (Figure.4.3b). The average C of eyes perfused with 1 µM Lat-B from *Plvap*$^{+/+}$ mice was 9.03 $^{\times}/$ 1.60 (3.05) nl/min/mmHg (n = 8) and it was 8.52 $^{\times}/$ 1.76 (3.39) (n = 7) for *Plvap*$^{+/-}$ mice, corresponding to a 6% difference (1.06 $^{\times}/$ 1.93 (1.00), p = 0.85).

4.3.3 Pore imaging in the inner wall of SC of PLVAP depleted mice

Figure.4.4 shows an example of one of the samples that are being imaged where putative pores can be seen. Pore counting on these samples will give an insight of the importance of pores in outflow resistance regulation and the involvement of PLVAP on pore formation. Moreover, discerning between I- and B-pores on eyes perfused with Lat-B may give valuable information about the role of the cytoskeleton in pore formation.

Because of the experimental design for pore counting, it is not known if this image belongs to a *Plvap*$^{+/+}$ or a *Plvap*$^{+/-}$ mouse.

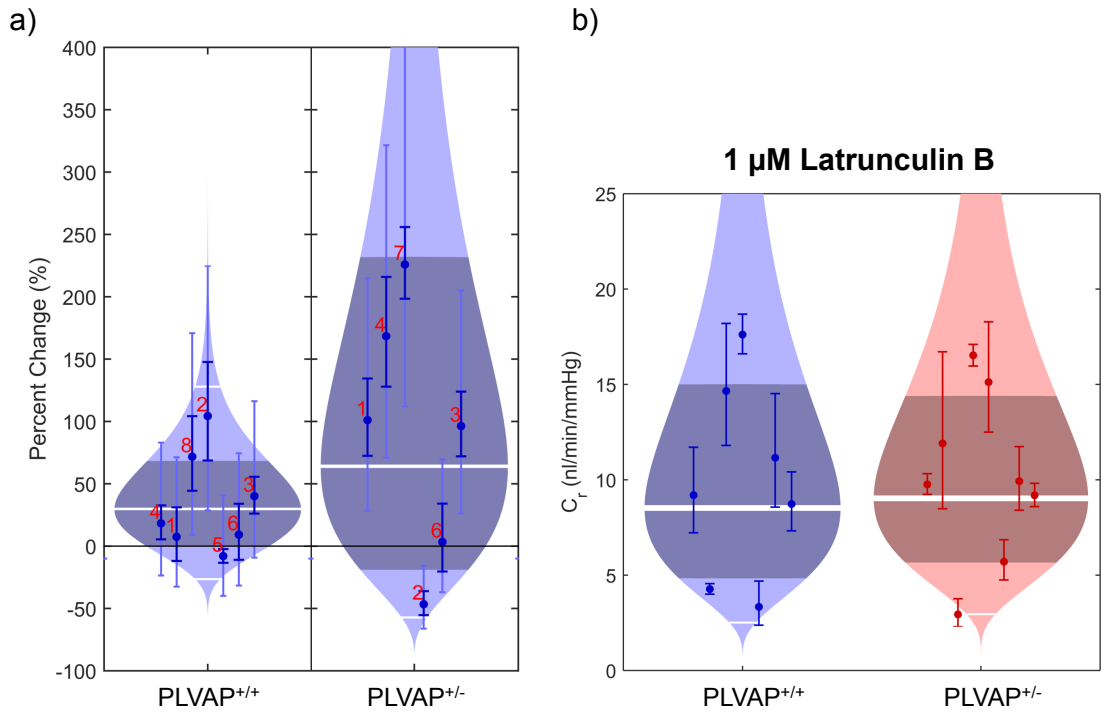


Figure 4.3: a) Effect of Lat-B on facility on *Plvap*$^{+/+}$ and *Plvap*$^{+/-}$ mice. Modified violin plots showing the percentage change of C between the control eye and its treated contralateral. Each data point corresponds to a pair of eyes (numbers are the pair ID) showing the percentage change and the 95% confidence for that particular measurement. The white central line is the geometric mean of the C change, the dark area around it is the error of the mean and two-sigma levels are shown by the light horizontal lines. The blue coloured area is the distribution of the data. **Left plot:** Eyes from *Plvap*$^{+/+}$ mice perfused with 1 µM Lat-B (n = 7). **Right plot:** Eyes from *Plvap*$^{+/-}$ mice perfused with 1 µM Lat-B (n = 6). **b) Facility values for eyes from *Plvap*$^{+/+}$ and *Plvap*$^{+/-}$ mice perfused with 1 µM Lat-B** represented in a modified violin plot. Each data point corresponds to the measured C for a single eye perfused with 1 µM Lat-B and the error bars are the 95% confidence interval for that particular measurement. The white central line is the geometric mean, the dark area around it is the error of the mean and two-sigma levels are shown by the light horizontal lines. The coloured area is the distribution of the data. **Left plot:** Facility measurements from *Plvap*$^{+/+}$ mice (n = 8). **Right plot:** Facility measurements from *Plvap*$^{+/-}$ (n = 7).

4.4 Discussion

We have shown in this project that AH outflow facility is reduced in PLVAP depleted mice. PLVAP is necessary for fenestra formation, which is thought to be the initial structure that triggers larger pore formation in SC. Hence, we hypothesised that PLVAP depleted mice have reduced outflow facility associated with impaired pore forming ability. We measured a 34% reduction in C when comparing *Plvap*$^{+/+}$ and *Plvap*$^{+/-}$ mice.

PLVAP expression and permeability of endothelia are linked, high PLVAP expression correlates with higher permeability[308]. Inhibition of PLVAP leads to a reduced fenestration and thus less openings are available for fluid and solutes to cross an other-

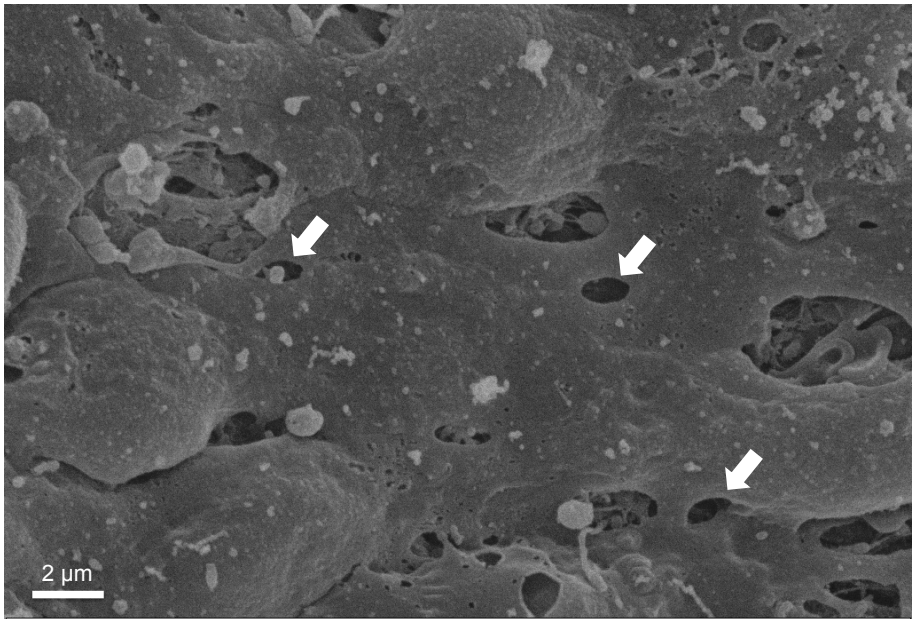


Figure 4.4: Scanning electron micrograph of the inner wall of SC from a mouse eye (10k x magnification). White arrows show putative pores. Image reproduced with permission from Dr. Herrnberger (University of Regensburg).

wise continuous endothelium. In the outflow pathway, PLVAP is exclusively expressed in SC[126], therefore, PLVAP depleted mice should have a less permeable SC but a normal TM. The fact that we measured a reduction in C on *Plvap*$^{+/-}$ mice compared to wild-types corroborates the importance of the inner wall of SC on outflow resistance generation. Moreover, these results are also in agreement with previous studies showing that glaucomatous eyes have less pores and elevated outflow resistance, which results in elevated IOP characteristic of glaucoma.

In *Plvap*$^{+/-}$ mice, however, we did not detect an increase in IOP, both genotypes had an IOP of just over 12 mmHg. No change in IOP could be explained by the fact that AH formation is also dependent on fenestrations, capillaries within the ciliary processes are highly fenestrated[279]. Ford *et al.* (2012)[101] showed IOP reduction when these fenestrae were inhibited, which served as a indirect assessment of AH inflow reduction. Hence, in *Plvap*$^{+/-}$ mice both inflow and outflow are expected to be impaired. Since IOP is defined by the balance of inflow and outflow if both parameters are reduced to the same extend IOP is expected to remain stable.

To test a possible mechanism responsible for outflow resistance modulation through PLVAP, the effect of Lat-B was assessed in both genotypes. Latrunculins are actin disrupt-

ing agents that depolymerises F-actin filaments by sequestering G-actin monomers[257] that are able to induce fenestration very rapidly (10 - 20 minutes)[49,142]. Moreover, other studies have reported that Lat-B increases outflow facility in porcine[85], monkeys[223] and human eyes[94]. For these reasons, it was expected that *Plvap*$^{+/-}$ mice would be less sensitive to Lat-B since PLVAP is essential for fenestra formation[142,266]. Similarly to other species, eyes from *Plvap*$^{+/+}$ mice experienced almost 30% increase in C in response to Lat-B. While we measure a 64% increase in facility on eyes from *Plvap*$^{+/-}$ mice, the wide range in the effect measured for each pair did not allow to reach significance. Nevertheless, the interesting fact was that differences between both genotypes disappeared after perfusions with Lat-B. This is an indication that extra resistance in PLVAP depleted mice may have a cellular origin, since it can be overcome by agents affecting cell physiology.

The fact that we saw a bigger percentage increase in C on *Plvap*$^{+/-}$ mice perfused with Lat-B than wild-types could be due to an increase in B-pores instead of I-pores. Actually, Ethier *et al.* (2006)[94] did a similar study on human eyes and they found out that Lat-B increases the number of paracellular pores but did not have an effect on intracellular pores. It may be that the deficiency in I-pores due to lack of PLVAP is compensated by an increment of B-pores. To confirm that, work is underway to get SEM images of the inner wall of SC to quantify pores and correlate them with C values. Theses results, will give an insight to the importance of each pore type in outflow resistance regulation.

Chapter 5

Targeting tight junctions in the inner wall of Schlemm's canal endothelium to modulate outflow facility

5.1 Introduction

Glaucoma is a degenerative optic neuropathy generally associated with ocular hypertension. Sustained elevated intraocular pressure (IOP) can damage the optic nerve leading to irreversible blindness. Currently, the only way to stop the progression of the disease is to lower IOP[281]. It is known that IOP is partly determined by the resistance to aqueous humour (AH) drainage and that abnormally high conventional outflow resistance is responsible for elevated IOP[148]. However, current treatments do not target the main source of resistance but aim to either lower AH production or enhance alternative outflow routes, making these treatments less efficient[70].

It is not entirely clear where the bulk of outflow resistance is generated, but studies suggest that it is located in the vicinity of the juxtacanalicular connective tissue (JCT) of the trabecular meshwork (TM), the inner wall of Schlemm's canal (SC) and its basement membrane[148,210]. We hypothesise that the inner wall of SC plays an important role in regulating outflow resistance. SC cells form a continuous endothelium containing tight junctions with intracellular pores (I-pores) and paracellular pores (or border pores, B-pores) of about 1 µm in size. These pores are thought to be the route that AH follows to cross the inner wall endothelium. In fact, Braakman *et al.* (2015)[47] showed that human eyes perfused with fluorescent tracers present higher density of pores in regions of higher tracer intensity, hence, pore density correlates with active drainage regions. Interestingly, this study also reported that B-pores may be the dominant pathway.

Endothelial cells form a tight and semipermeable endothelium, in order for this to happen, cells need to be in contact and linked together. The principal junctional complexes are adherent junctions (or *zonula adherens*) and tight junctions (TJs or *zonula occludens*). These junctions control a variety of functions necessary to maintain vascular homeostasis, the most important ones include leukocyte extravasation, intracellular signal transduction and permeability to fluids and solutes[29,30]. TJs are those areas where the membrane of adjacent cells are in tight contact[96], this can occur between two (bicellular TJs, bTJs) or three cells (tricellular TJs, tTJs). There are two types of proteins associated to TJs: **membrane proteins** and **intracellular proteins**. The first type might be involved in cellular adhesion while the second are responsible for communica-

tion between the membrane and the cytoskeleton. Membrane proteins associated with TJs include occludins, claudins and tricellulin, while intracellular are classified between membrane-associated guanylate kinases (MAGUK, ZO family) and non-MAGUK[29,106]. For this project, we are going to focus on a membrane protein (tricellulin) and an intracellular protein (ZO-1).

Tricellulin (also known as MARVELD2) is highly expressed in tTJs. It is a tetraspan transmembrane protein with two extracellular loops and the C-terminus contains the domain responsible for ZO-1 binding. Interference RNA studies on epithelial cell cultures have shown that the inhibition of tricellulin leads to not only unstable tTJs but also bTJs[140]. To our knowledge, previous studies have not studied the role of tricellulin in SC endothelium and how it may affect the regulation of AH outflow.

ZO-1 was the first TJ related protein to be discovered[269]. It is located beneath the cellular membrane where there is a TJ and it acts as a scaffold to recruit other proteins with structural and signal transduction functions as well as actin filaments of the cytoskeleton[106]. ZO-1 has previously been shown to be expressed in the SC endothelium as well as its implication in hydraulic resistance generation[291]. Moreover, it is also known that SC cells can be distinguished from TM cells because SC mostly express the isoform ZO-1α^+ together with smaller quantities of ZO-1α^-, while TM express only ZO-1α^-[12,291]. The difference between these isoforms resides on whether the protein includes or not the 80 amino acids α domain. It has been found that, ZO-1α^- isoform is expressed alone in tissues that do not form TJ, like glomerular podocytes[20] and the TM.

We hypothesise that the disassembly of tight junctions would lead to an increase of outflow facility, thus reducing IOP. In this project, we inhibited simultaneously ZO-1 and tricellulin in the outflow pathway through small interfering RNA (siRNA) techniques[196]. siRNA was injected into the anterior chamber of mouse eyes and reached the outflow pathway following normal AH drainage. 48 hours after treatment, *ex vivo* outflow facility (C) and IOP were assessed.

5.2 Materials and Methods

5.2.1 Experimental Design

The results presented in this chapter are part of a big project that is still ongoing in collaboration with Professor Humphries (Trinity College Dublin), Dr. Elke Lütjen-Drecoll (University of Erlangen-Nürnberg), Dr. Tom Read and Professor Ross Ethier (Georgia Institute of Technology). The main objective of the project is to study the role of TJ on outflow facility and IOP regulation. Professor Humphries's group showed that ZO-1 and tricellulin are expressed in the outflow pathway of mouse eyes and that the siRNAs used are able to reduce protein expression 48 hours after treatment in human SC cells and in the outflow pathway of African green monkeys (personal communication, data not shown). Our role has been to assess the effect of ZO-1 and tricellulin inhibition on outflow facility and IOP. Currently, transmission electron microscopy (TEM) and scanning electron microscopy (SEM) are being used to detect histological changes in the outflow pathway in mouse eyes treated with ZO-1 and tricellulin siRNA.

We injected 1 µg ZO-1 siRNA and 1 µg of tricellulin siRNA (targeting siRNA, t-siRNA) into the anterior chamber of one eye and 2 µg of non-targeting scrambled siRNA (nt-siRNA) into the anterior chamber of its contralateral eye as a control (vol injected: 1.5 µl/eye). 48h after injection, the effect of protein inhibition was assessed. The effect on outflow facility (C) was measured using the iPerfusion system on enucleated mouse eyes and IOP was measured using two techniques: rebound tonometry and by cannulation using an adaptation of the iPerfusion system. A summary of the groups of mice used and the experiments done with each group can be found in Table.5.1. Work involving the use of the iPerfusion system *in vivo* (group 3) were carried out at Trinity College Dublin in Professor Humphries's laboratory, which I visited for 3 weeks. At Trinity College Dublin, they have 2 iPerfusion systems which are exactly the same as the ones we have at Imperial College London.

Table 5.1: Groups of mice used in this chapter, defining which experiments were done, the anesthetic regimen used and the institution where the experiments were carried out.

	Experiments	Anesthesia	Institution
Group 1	*Ex vivo* outflow facility	–	Imperial Collge London
Group 2	Tonometric IOP	66.6 mg ketamine + 0.66 mg Domitor®	Imperial College London
Group 3	Cannulation IOP	100 mg/kg ketamine + 16 mg/kg xylazine	Trinity College Dublin
	TEM	–	University of Erlangen-Nürnberg
Group 4	Tonometric IOP	3% Isoflurane + 1 l/min oxygen	Imperial College London
	Tracers *ex vivo* perfusions	–	Imperial College London
	TEM	–	University of Erlangen-Nürnberg

5.2.2 Animal Husbandry

Animals where brought into the animal facility one week prior to start the experiments for acclimatization. Mice were housed in individually ventilated cages with 5 mice per cage. They were provided with food and water *ad libitum* and were under 12 hours light/dark circles (7 am to 7 pm) at 21 ℃. Male C57BL/6 mice (Charles River Laboratories, UK) of 10 to 12 weeks old were used.

All animals were treated in compliance with the ARVO statement for the Use of Animals in Ophthalmologic and Vision Research under UK Home Office Project License 70/7306 or Irish Medicine Board Project license AE191361P017.

5.2.3 Pulled Glass micro needles

Custom made glass micro needles were used for intracameral injections and *in vivo* perfusions. Needles were made out of borosilicate glass capillaries (#B100-50-10, Sutter instruments, US) with an inner diameter of 0.5 mm and outer diameter of 1 mm. Capillaries were pulled using a laser-based micropipette puller (P2000, Sutter instruments, US) with the following settings: HEAT= 400, FIL= 004, VEL= 050, DEL= 225, PUL= 150. Pulled capillaries were then broken to a needle tip diameter of around 100 µm by pushing the needle tip against another needle oriented perpendicularly with the point of contact at the desired tip diameter.

For intracameral injections, non-beveled needles were used. However, for *in vivo* perfusions, needles were beveled to approximately 150 µm using a MicroBeveler Sys-

tem (SYS-48000, World Precision Instruments, US) with a 3 µm Alumina lapping disc (#48015-30, World Precision Instruments, US) under a stereoscope microscope.

Each needle was observed down an inverted microscope to control for the tip diameter. Prior to use, needles were autoclaved and stored in 70% ethanol.

5.2.4 Intracameral Injections

siRNAs were dissolved in sterile DBG (RNAase free PBS including divalent cations and 5.5 mM glucose (#PHR1000, Sigma-Aldrich, UK)) under a class II safety cabinet. For t-siRNA, each siRNA (ZO-1 and tricellulin) was at a concentration of 0.66 mg/ml. While scramble siRNA was at 1.33 mg/ml for nt-siRNa. Solutions were stored at -20℃. During injections, siRNA was kept on ice.

The siRNAs used were kindly provided by Professor Humphries. Sequence were as follows. ZO-1 sense sequence: 5'-CAUUCGCCUUCAUACAAUAtt-3'. ZO-1 antisense sequence: 5'-UAUUGUAUGAAGGCGAAUGat-3'. Tricellulin sense sequence: 5'-ACGAGAGAAUUUCAAGAAUtt-3'. Tricellulin antisense sequence: 5'-AUUC UUGAAAUU CUCUCGUtt-3' (Ambion®, Thermo Scientific, US).

Injections were carried out under general anesthesia. For outflow facility studies (Group 1) and IOP measurements by rebound tonometry in Group 2 and cannulation (Group 3), mice were anesthetised with 66.6 mg/kg ketamine (Fort Dodge Animal Heatht, Fort Dodge, US) and 0.66 mg/kg Medetomidine hydrochloride (Domitor®, Orion Pharma, UK) injected intraperitoneally (IP). When assessing IOP by rebound tonometry in Group 4, injections were done under general anesthesia with isoflurane (Isocare, Animalcare Ltd., UK), 3% isoflurane + 1 l/min oxygen.

For either anesthetic regiment, once the mouse lost consciousness, it was injected with 5 mg/kg enrofloxacin antimicrobial (Baytril; Bayer Healthcare, Germany) subcutaneously. Topical pupil dilation drops (phenylephrine hydrochloride (2.5% w/v) and tropicamide (1% w/v), Bausch & Lomb, UK) and hydration gel (Vidisic, 0.2 % w/w Eye Gel, Bausch & Lomb, UK) were subsequently applied to both eyes. Eyes were kept moist to avoid formation of cataracts[55] and corneal damage[170], especially when using

ketamine/Domitor® because the mouse was anesthetised for longer periods.

Once the mouse was fully anesthetised and no longer reacted to toe pinch, it was mounted on a stereotaxic head holder (Model 923-B, Kopf Instruments, US) to minimise head movement during injections. Mice rested on a flask filled with warm water at 32℃. The mouse was placed under a stereoscopic microscope on a flex arm stand with the eye oriented upwards. The hydration gel was removed and the eye was cannulated via the anterior chamber with a glass micro needle to remove a small amount of AH ($\approx$ 1 µl) by capillarity. The puncture was done parallel to the iris and slightly above the limbus. A glass needle connected to a 10 µl glass syringe (Gastight 1700 Series Syringes, Hamilton Company, US) was used to inject siRNA. The syringe was filled with sterile RNase free PBS and 1.5 µl siRNA was backfilled from the needle, we left an air bubble between both solutions to visualise the volume injected. The syringe was hold in place using a micro manipulator. The same hole made for the previous puncture was used to insert the second needle and slowly deliver 1.5 µl of either t-siRNAs or nt-siRNA. Before removing the needle, a drop of antibiotic (1% w/w Fucithalmic, LEO Pharma, Denmark) was added on the eye, the viscous ointment seemed to minimised reflux from the eye. Immediately, the head of the mouse was turned and the second eye was injected following the same procedure. Whether t-siRNA or nt-siRNA was injected in the left or right eye was randomised in the cohort used for outflow facility experiments. However, t-siRNA was always injected in the right eye when measuring tonometric IOP to minimise the possibility of error since multiple measurements were necessary.

To accelerate recovery from ketamine/Domitor® anesthesia, 1.5 mg/kg of atipamezole hydrochloride (Antisedant®, Orion Pharma, UK) was injected by IP route. Mice were left in a 28℃ thermoregulated box to recover with special care that eyes were moist. Mice were housed in their cage again when they were fully recovered from anesthesia.

5.2.5 *Ex vivo* mouse eye Perfusions

48 hours after injecting siRNAs, mouse eyes were perfused *ex vivo* to measure outflow facility using the iPerfusion system (Group1). Mice were culled by cervical dislocation and the eyes were enucleated within 5 minutes *post mortem* and stored in PBS at

room temperature to await perfusion, generally no more than 20 minutes.

Both eyes were perfused simultaneously using two independent perfusion systems as described previously[249]. Briefly, each eye was affixed to a support using a small amount of cyanoacrylate glue and submerged in a PBS bath regulated to 35℃. The eye was cannulated via the anterior chamber with a stainless steel 33-gauge beveled needle (NanoFil, #NF33BV-2, World Precision Instruments, US) under a stereomicroscope using a micromanipulator. The iPerfusion system comprises an automated pressure reservoir, a thermal flow sensor (SLG64-0075, Sensirion, Switzerland) and a wet-wet pressure transducer (PX409, Omegadyne, US) in order to apply a desired pressure, measure flow rate into the eye and measure IOP respectively. The perfusate was DBG filtered through a 0.22 µm filter (#28145-477, VWR international, UK).

Following cannulation, eyes were perfused for 30 minutes at 8 mmHg to allow the eye to acclimatise to the environment. Subsequently, 9 discrete pressure steps were applied from 4.5 to 21 mmHg, while flow and pressure were recorded, the last four minutes of stable data were averaged. A non-linear model was fit to flow-pressure data to account for the pressure dependence of outflow facility in mouse eyes, and the reference facility at 8 mmHg (approximately physiological pressure drop across the outflow pathway) was analysed further. The data analysis methodology described by Sherwood *et al.* (2016)[249] was applied in order to analyse the treatment effect, whilst accounting for measurement uncertainties and statistical significance was evaluated using the paired weighted t-test described therein.

5.2.6 IOP measurements

Rebound tonometry under ketamine/Domitor® anesthesia

IOP measurements were done by rebound tonometry (TonoLab, Icare, Finland) under general anesthesia with 66.6 mg ketamine + 0.66 mg Domitor®. Measurements were done on both eyes between 9:30 am and 12:30 pm. Whether left or right eye was measured first was alternated. The first measurement was always taken 4 minutes after injection of anesthetic and the second one 5 minutes after injection, at these time points,

mice were immobile but not deeply anesthetised yet.

First measurement was done prior to siRNA injection and the second one 48 hours after injection (Group2). Both measurements were carried out as follows: mice were placed on a soft clay mold supported on an adjustable laboratory jack stand. The TonoLab was held by a micro-manipulator supported by a ring stand with the tip positioned approximately 2 mm from the central cornea along the optical axis. 3 IOP readings were performed to each eye and the average is what we define as IOP for a given eye.

To determine the effect of the siRNA, we calculated the difference in IOP before and after injection. Statistical significance was assessed by the non-parametric Wilcoxon signed-rank test using SPSS (IBM, Armonk, New York, USA).

IOP measurements by cannulation using the iPerfusion system *in vivo*

In vivo perfusions where carried out in order to detect difference in IOP between t-siRNA treated eyes and their contralateral control injected with nt-siRNA (Group3). The iPerfusion system and the perfusion regimen were adapted for this purpose. The general protocol implies 2 tonometric IOP measurements (IOP1 and IOP2), the cannulation of the eye followed by an IOP decay until IOP stabilises (IOP3), a perfusion for a series of pressure steps and a final IOP decay (IOP4). Therefore, 4 IOP measurements at different time points are obtained for each eye.

To carry out *in vivo* work with the iPerfusion system, two systems were used to perfuse both eyes simultaneously. In this case, only one microscope was used and the mouse was placed below it with the head held by a head holder. The mouse rested on a metallic platform that was kept at 32°C. Two micro-manipulators held beveled micro glass needles filled with DBG. Needles were connected to the iPerfusion system as described for *ex vivo* perfusions.

In vivo perfusions were done under general anesthesia with 100 mg/kg ketamine + 7.5 mg/kg xylazine (Xylacare, Animalcare Ltd., UK) injected IP. Special care was taken to keep the eyes constantly moist by applying Vidisic or PBS drops as required. Two tonometric IOP measurements were done to both eyes before the perfusion using the

method described previously (5.2.6) but 10 readings were taken instead of 3. The first measurement was done about 5 minutes after injection (IOP1), when the mouse was already still but not under deep anesthesia yet, and the seconds one, about 20 minutes after anesthesia administration (IOP2), when the mouse was unconscious (it did not react to toe pinch). The average IOP between both eyes for the last measurement was the pressure used to cannulate the eyes.

Immediately after the second tonometric measurement, the mouse was mounted on the head holder, the mouse was facing down and the body length perpendicular to the user. An IP catheter was placed to administrate a bolus 50 µl of anesthetic every 15 minutes to maintain deep anesthesia during the whole procedure.

Before cannulation, P = 0 mmHg was defined by placing the needle in the tear film, then, eyes were cannulated at the second tonometric IOP with the needle along the optical axes and perpendicular to the center of the cornea holding the eye with a modified spoon-shaped curette. Special care was taken to avoid hitting the lens during cannulation and to keep the eye constantly moist with Vidisic. For at least 30 minutes or until IOP was stable (not changing by more than 0.2 mmHg/min), an IOP decay was measured by closing the system to the reservoir, so there was no external pressure applied. Then, IOP3 was defined as the average IOP for the last minute measured. Next, the eye was perfused for a cycle of 6 pressure steps of 2.5 mmHg starting at IOP3. Similarly to the *ex vivo* perfusions, Q and P were measured and the length of the pressure step was defined by stability, in this case, by stable pressure ($\Delta P \leq 0.02$ mmHg/min). When the steps were over, another IOP decay was measured from a pressure equal to IOP3 - 2 mmHg. IOP4 was defined as the average P data for the last minute of stable P ($\Delta P \leq 0.01$ mmHg/min). A representative pressure trace can be seen in Figure.5.1.

After the perfusion, mice were culled by cervical dislocation and the eyes enucleated and fixed in Karnovsky's fixative which consisted of the following: a stock solution (2.8% paraformaldehyde, 0.1 M cacodylate-Na-salt buffer ($C_2H_6AsO_2$ Na $3H_2O$)) was made and kept at 4℃. Fixative solution was prepared fresh immediately before fixation with 90% stock solution and 10% of 25% glutaraldehyde. Eyes were fixed overnight at 4℃. The next day, eyes were washed 3 times for 20 minutes in 0.1 M cacodylate buffer

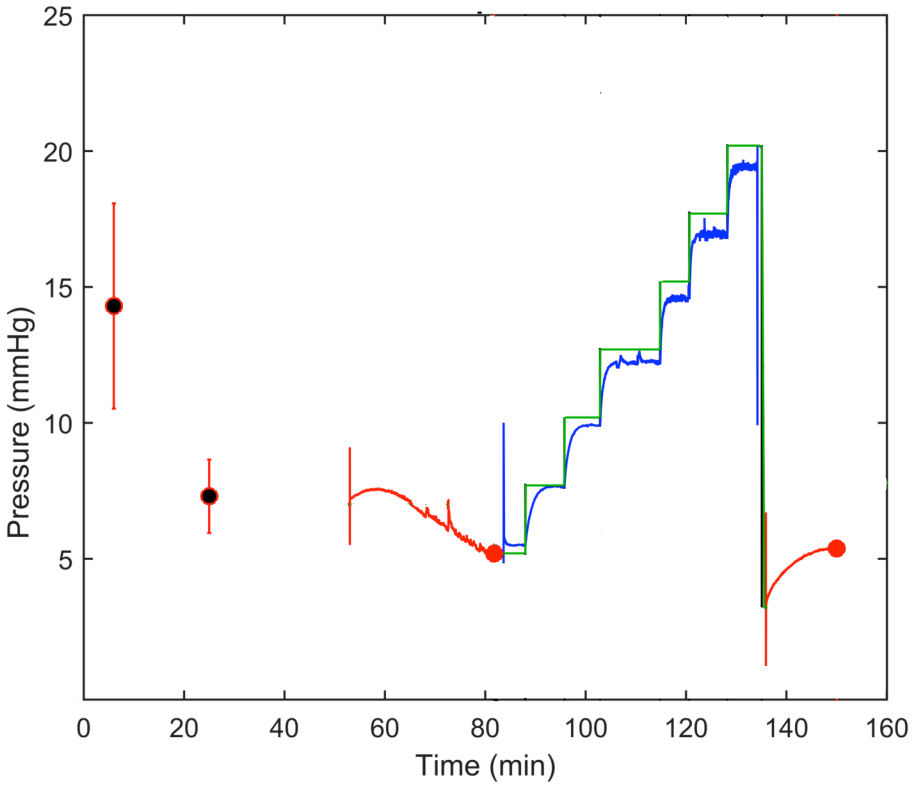


Figure 5.1: Representative pressure trace to measure sIOP. Two tonometric measurements (IOP1, IOP2) were performed before the beginning of the perfusion (black filled dots). Eyes were cannulated at IOP2 and a pressure decay was measured for 30 minutes (red line) followed by a series of pressure steps (blue line) and a last pressure decay. Red filled dots are the IOP3 and IOP4 and the green line represents the applied pressure. Time 0 is when the mouse was injected with the anesthetic.

and stored in the same buffer solution at 4℃.

Rebound tonometry under Isoflurane anesthesia

IOP measurements were done by rebound tonometry under general anesthesia with isoflurane (3% + 1 l/min oxygen). Measurements were done on both eyes always between 5 and 7 pm to minimise changes due to circadian cycles. The measurements were done in the afternoon at the moment where IOP is naturally higher while lights in the room were still on so it was not necessary to work in the dark[72,182]. First measurement was done prior to siRNA injection and the second one 48 hours after injection (Group 4).

Several studies report that IOP decays under general anesthesia[56,79,144], for that reason, IOP values must be compared at an equivalent time point relative to the onset

of anesthesia (data regarding IOP decay under anesthesia in naïve mice can be seen in Chapter.6). In order to account for the IOP decay and improve the accuracy of the IOP measurements, the following protocol was developed: For each animal, anesthesia was induced by placing the animal into an anesthetic chamber delivering isoflurane for exactly 2 minutes. Immediately, the mouse was mounted on a stereotaxic head holder connected to the isoflurane machine. First IOP measurement was done exactly 3 minutes after the flow of isoflurane commenced. The contralateral eye was measured 1 minute later, and this was repeated three times yielding three IOP measurements, two minutes apart for each eye. In order to optimise accuracy, 5 IOP readings were acquired at each time point, these readings needed 30-40 seconds to be completed.

To our experience, the TonoLab has a minimum measurable pressure of 7 mmHg, although according to the TonoLab's "Users's and Maintenance manual" the measurement range is 1-99 mmHg. Hence, it was necessary to use a non-parametric approach to the analysis. Initially, the median of the 5 IOP readings at each time point was calculated. Subsequently, a straight line was fitted to the three data time-points and interpolated to estimate the IOP 5 minutes after onset of anesthesia. Although this approach may show bias towards overestimating IOP when the measured values go below 7 mmHg over the measurement period, this is conservative with regards to investigating the hypothesised IOP lowering effect of the siRNA treatment. The non-parametric Wilcoxon signed-rank test (using MatLab) was used to investigate whether the IOP changed between pre- and post-injection measurements in each eye.

After the IOP measurement, mice were allowed to recover and, about 1 hour later, they were culled by cervical dislocation and eyes were enucleated. Eyes from 8 mice were stored in PBS to be perfused with fluorescent tracers to generate tracers maps that are used to localise where to take TEM images. The rest were directly immersed in ITO's fixative. ITO's fixative was freshly made of 4.6% of saturated picric acid, 25% of 10% paraformaldehyde (PFA), 50% of 0.2 M Sodium Cacodylate (pH 7.3), 10% of 25% glutaraldehyde and 10.4% double-distilled water.

5.2.7 Fluorescent tracers patterns

Eyes treated with both t-siRNA and nt-siRNA (Group 4) were perfused at a constant pressure of 8 mmHg for 1 hour using the iPerfusion system, special care was taken to cannulate the eye at the same point where the injections were performed. These eyes were perfused with 0.1% (v/v) of 20 nm fluorescent nano-particles (FluoSpheres® Carboxylate-Modified Microspheres, red fluorescent (580/605), #F-8786, Thermo Scientific, US) in DBG. After the perfusion, eyes were immersion fixed in 4% PFA overnight at 4℃, then, they were stored in in PBS at 4℃ until imaged.

Eyes were dissected under a dissection microscope for flat mount imaging for tracers patters as follows: the posterior part including the lens was removed preserving the iris untouched. The anterior segment was then cut into a ”clover leaf” shape differentiating the four quadrants. The cannulation site was taken as a reference point to orientate the eye, since right eyes were cannulated in the inferior quadrant and left eyes in the superior quadrant. In order to track the eye orientation the sclera was marked, 2 triangular cuts were done in the superior quadrant and 1 in the temporal. Once dissected, each eye was placed on a glass slide and flat mount with PBS for *en face* visualization.

Fluorescent and bright field images were taken using a confocal microscope (Leica SP5) using a a 10x/0.4 NA dry objective. Images were taken as a z-stack with planes of 60 µm hight. Moreover, a ”Tile Scan” mode was used to generate an image of the entire eye. All eye were imaged under the same confocal settings to allow comparisons between eyes. After imaging, anterior segments were fixed in ITO's fixative.

5.3 Results

5.3.1 *Ex vivo* mouse eye Perfusions

To assess the effect of ZO-1 and tricellulin down regulation on outflow facility, siRNA-injected eyes were perfused using the iPerfusion system. All eyes injected with t-siRNA showed an increase in facility when compared to their contralateral controls in-

jected with nt-siRNA. For the 6 pairs of eyes perfused, a 82% increase in facility (1.82 $^{\times}/$ 1.35 (1.40)[1], n = 6, p = 0.004, Figure.5.2) was measured.

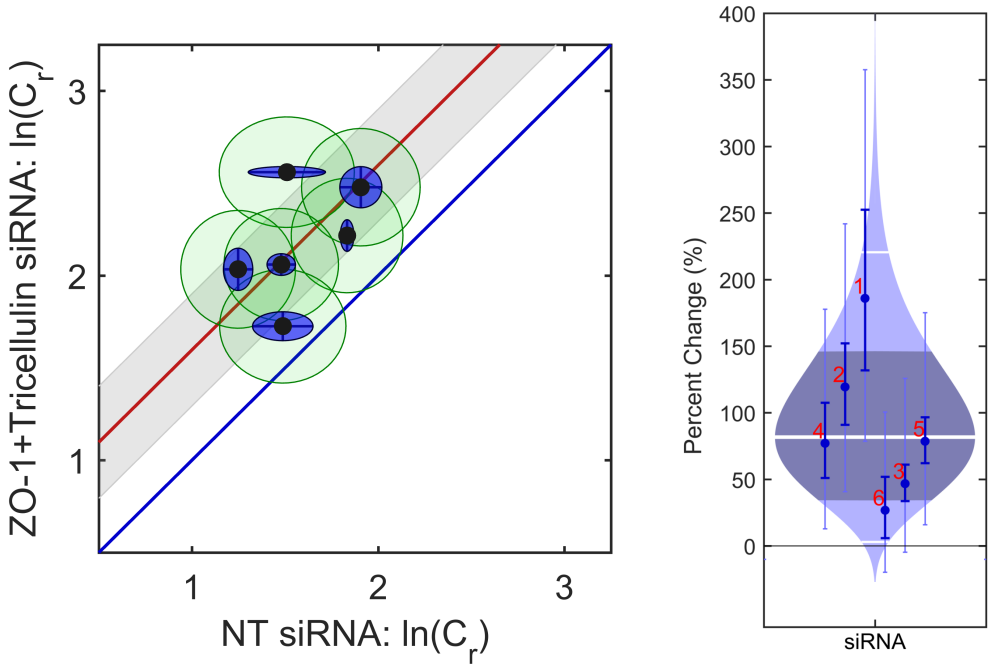


Figure 5.2: Effect of ZO-1 and Tricellulin down regulation on outflow facility of enucleated mouse eyes. Left plot: Each data point represents one pair of eyes, with the log-facility of the control eye in the X-axis and the treated in the Y-axis. Filled ellipses indicate 95% confidence intervals in the measurement and outer ellipses indicate additional uncertainty between contralateral eyes[249]. The red line shows the average difference, with its confidence intervals in grey. **Right plot:** Percentage change in facility represent in a modified violin plots showing the percentage change of C between the control eye and its treated contralateral. Each data point corresponds to a pair of eyes showing the percentage change and the 95% confidence for that particular measurement. The white central line is the geometric mean, the dark area around it is the 95% confidence interval around the mean and two-sigma levels are shown by the light horizontal lines. The blue colored area is the distribution of the data. n = 6 pairs.

5.3.2 IOP measurements

Rebound tonometry under ketamine/Domitor® anesthesia

A first attempt to detect differences in IOP between after ZO-1 and tricellulin siRNA injection was carried out using rebound tonometry under general anesthesia with ketamine/Domitor®. IOP measurements were taken immediately before siRNA injection

[1]Results reported as: $\%\ (\overline{D}^{*}\ ^{\times}/\ ME_{\overline{D}^{*},95}(s^{*2}_{tre}))$, where $\%$ is the percentage change $((\overline{D}^{*}-1)\times 100)$, $\overline{D}^{*}$ is the proportional change, $ME_{\overline{D}^{*},95}$ is the margin of error given by the half-width of the 95% confidence interval on the estimate of $\overline{C}^{*}$ and s^{*2}_{tre} the range of the 95% of the treatment.

and 48 hours after. Eyes injected with nt-siRNA showed a reduction of 2.6 mmHg in IOP while those injected with t-sRNA experienced a reduction of 3.4 mmHg. Even though the treated eye showed a greater reduction than the control, there was no significant difference between the control and the treated group (p = 0.94, n = 8, Figure.5.3).

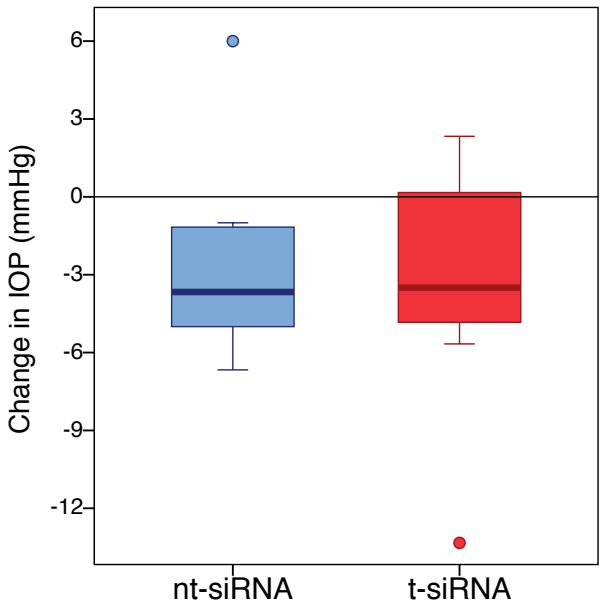


Figure 5.3: Effect of ZO-1 and Tricellulin down regulation on IOP measured by rebound tonometry under ketamine/xylazine anesthesia. Box plot showing change in IOP between before and after nt-siRNA and ZO-1 + Tricellulin t-siRNA. Central band is median, boxes show interquartile range and error bars show 5th and 95th percentiles.

IOP measurements by cannulation using the iPerfusion system *in vivo*

A different approach was used to detect differences in IOP in eyes injected with t-siRNA: sIOP measurements were carried out using the iPerfusion system[249]. According to the protocol, two tonometric measurements (IOP1 and IOP2) were done to define the pressure used to cannulate the eye. With the iPerfusion system, two spontaneous IOP measurements were obtained (IOP3 and IOP4).

It is known that anesthetics affect IOP[56,79,144]. To account for this effect, several IOP measurements were taken (Table.5.2). First measurement (IOP1) was a tonometric reading taken 5 minutes after the anesthetic was injected, at this point, mice were not under deep anesthesia but they were immobile, hence, there was no need to restrain and stress the mouse. The average IOP1 for control eyes was 12.9 $\pm$ 3.5 mmHg (mean $\pm$

SD, n = 12) while it was 13.0 $\pm$ 2.9 mmHg (n = 12) for the treated. A second tonometric reading (IOP2) was done around 20 minutes after anesthesia, when mice were under deep anesthesia already. The average IOP2 for control eyes was 9.8 $\pm$ 2.1 mmHg (n = 10) and for treated ones it was 9.1 $\pm$ 1.3 mmHg (n = 10). None of these readings report a significant reduction in IOP for the eyes injected with t-siRNA. The sample size is different for both time points because for some mice it was not possible to obtain the second measurements since the TonoLab displayed an error constantly (E03).

Using the iPerfusion system, 2 more IOP measurements were taken. Average IOP3 was 6.5 $\pm$ 3.9 mmHg (n = 8) and 6.0 $\pm$ 2.0 mmHg (n = 10) for control and treated eyes respectively. IOP4 was measured after a cycle of pressure steps. For IOP4, the average IOP measured was 4.0 $\pm$ 1.8 mmHg (n = 6) for the control group and 4.8 $\pm$ 2.0 mmHg (n = 7) for the treated ones.

Table 5.2: Averaged IOP (mmHg) measurements for eyes injected with t-siRNA or nt-siRNA. IOP1 and IOP2 were tonometric measurements done 5 minutes and 20 minutes after injection of anesthetic respectively. IOP3 and IOP4 correspond to the measurements done with the iPerfusion system.

	Tonometric IOP						**Cannulation IOP**					
	IOP1			**IOP2**			**IOP3**			**IOP4**		
	Average	SD	n	Average	SD	n	Average	SD	n	Average	SD	n
t-siRNA	13.0	2.9	12	9.1	1.3	10	6.0	2.0	10	4.8	2.0	7
nt-siRNA	12.9	3.5	12	9.8	2.1	10	6.5	3.9	8	4.0	1.8	6

Rebound tonometry under Isoflurane anesthesia

In order to account for the lowering effect that anesthesia has on IOP, a new protocol was designed to measure tonometric IOP and assess the effect of ZO-1 and tricellulin inhibition. As described, for each eye, multiple readings were done at different time points and IOP was determined as the interpolation at 5 minutes from a linear regression. It can be seen from Figure.5.4 how for almost all cases IOP was reduced over the period of time measured. It can also be seen that, even though the data is noisy, t-siRNA injected eyes showed lower IOP after the treatment while eyes injected with nt-siRNA did not experience as much reduction.

For eyes injected with nt-siRNA, IOP was not significantly affected, with a reduc-

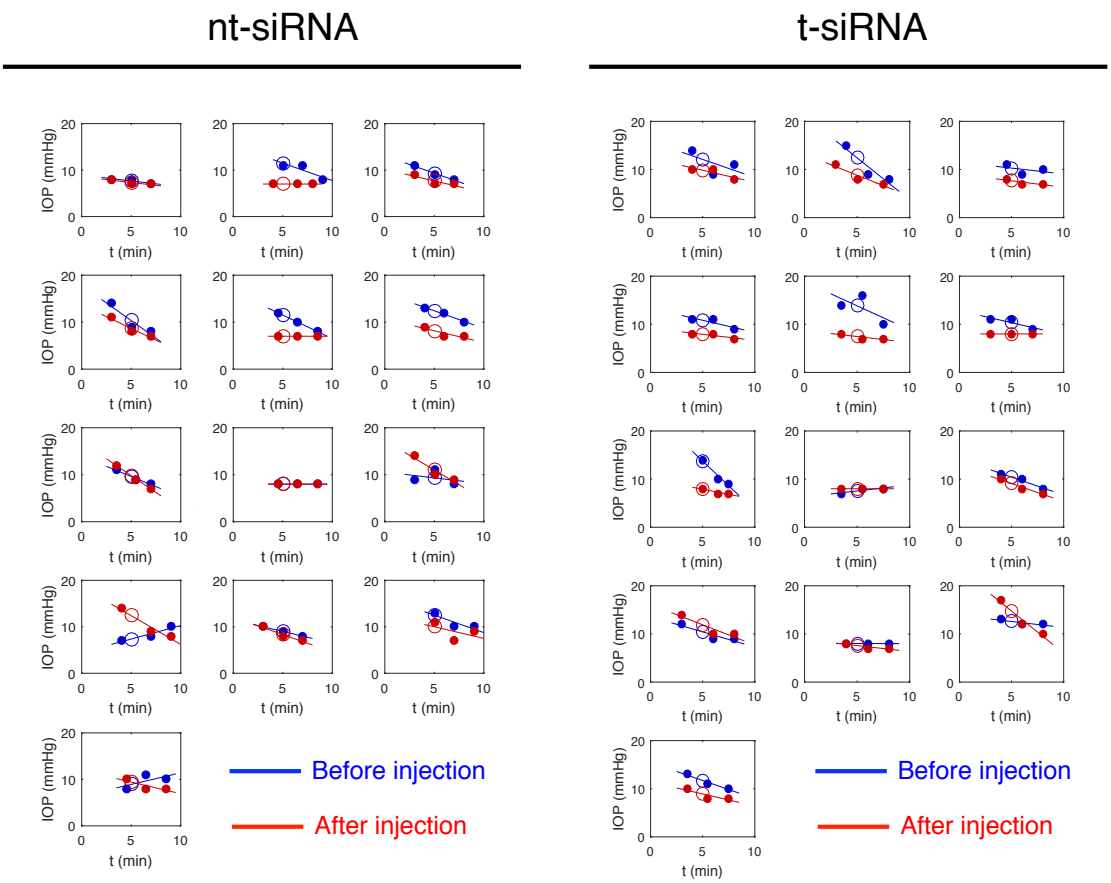


Figure 5.4: IOP decays under isoflurane anesthesia. For each eye (individual plot), IOP was measured at 3 time points (filled dots), a linear regression was applied and IOP was defined as the interpolation at 5 minutes (open circles). Data in blue correspond to the measurement done before siRNA injection and data in red are the measurements performed 48 hours after injection. Time 0 represents when the isoflurane flow started. **Left panel:** eyes injected with nt-siRNA (n = 13). **Right panel:** eyes injected with t-siRNA (n =13).

tion in IOP of 0.7 $\pm$ 1.7 mmHg (median $\pm$ median absolute deviation (MAD), n =13, p = 0.151). In eyes injected with targeting siRNA, a reduction of 2.3 $\pm$ 1.9 mmHg (median $\pm$ MAD, n = 13, p = 0.013; Figure.5.5) was observed.

5.3.3 Fluorescent tracers patterns

In order to confirm that the increase in facility and decrease in IOP is due to the formation of more para-cellular spaces, siRNA-treated eyes will be imaged by TEM. The current imaging technique selects random regions of SC endothelium to be imaged. However, because of segmental outflow[59] it is difficult to find active areas of flow in both the control and treated eye. To overcome this problem, some of the eyes (n = 8) from Group 4 were perfused for 1 hour at a constant pressure of 8 mmHg with fluorescent

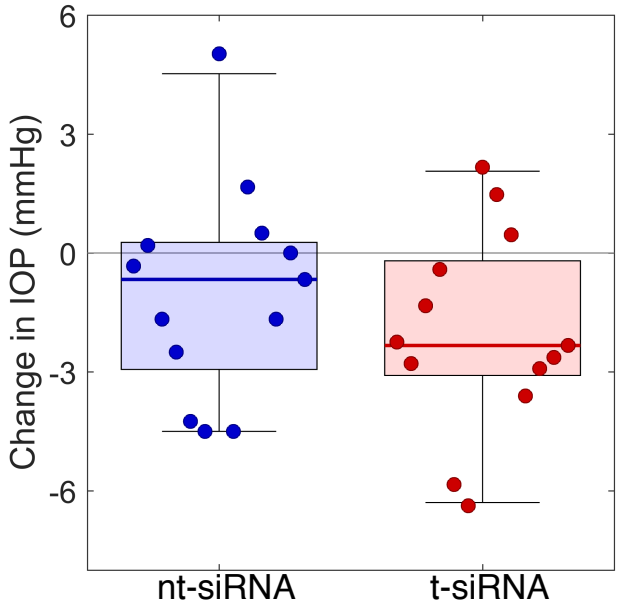


Figure 5.5: Effect of ZO-1 and Tricellulin down regulation on IOP measure by rebound tonometry under isoflurane anesthesia. Box plot showing change in IOP in nt-siRNA and t-siRNA. Individual data points indicate separate eyes. Central band is median, boxes show interquartile range and error bars show 5th and 95th percentiles.

nano-particles to map tracers patterns, which were imaged with confocal microscopy. These maps will be used to localise the areas in the outflow pathway that have higher and low fluorescent intensity to compare the histological sections of similar conditions.

During perfusion, the nano-particles flow towards the outflow pathway to decorate the preferential drainage routes in the TM, Figure.5.6 shows an example of a pair of eyes. It can be seen how the tracer distribution is not uniform. We assume that areas with higher fluorescent intensity are active areas of flow since the nanoparticles are drained there. Signal quantification analysis is necessary to determine whether the siRNA treatment changes flow patterns. Due to the small size of the nanoparticles particles (20 nm), they can cross the SC and drain to the post trabecular pathway, as can be seen in the nasal quadrant of the right eye (Figure.5.6).

These tracers maps will be used to chose high flow *vs.* low flow regions of the outflow pathways for ultrastructural analysis with TEM. Choosing randomly where to image could bring a situation where a low flow area is compared to a high flow area providing misleading and false results. By comparing the ultrastructure of the active regions of TM/SC we will be able to determine whether the ZO-1 + tricellulin siRNA affects the TJs

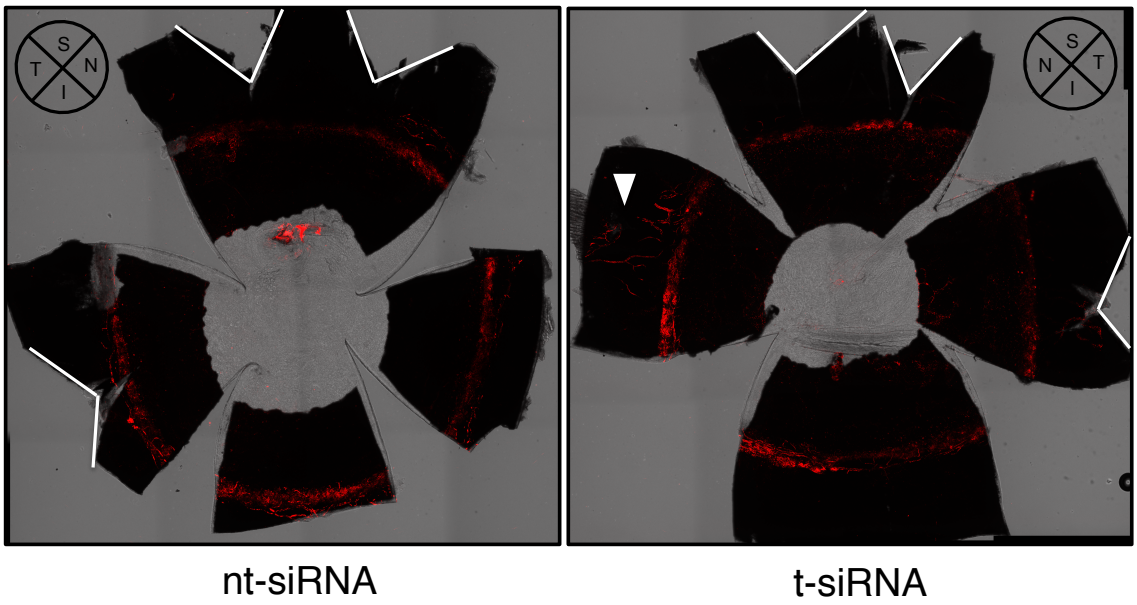


Figure 5.6: Fluorescent tracers patterns. Representative pair of eyes injected with siRNA and perfused with 20 nm fluorescent nano-particles at a constant pressure of 8 mmHg. The eye in the left panel was injected with nt-siRNA while the right one was injected with t-siRNA. Fluorescent signal represents areas of active outflow. Arrow head shows post-trabecular pathway. White lines show marks in the sclera to orientate the eye. S: superior, N: nasal, I: inferior, T: temporal.

as hypothesised.

5.4 Discussion

Targeting the resistance sites of the AH outflow pathway is, in principle, the best approach to reduce IOP as increased resistance is the cause of the ocular hypertension[148]. However, the majority of current glaucoma treatments aim to reduce AH production or enhance alternative outflow routes[70]. Here, we propose a method to enhance hydraulic conductivity of SC, which leads to a reduction in IOP, based on disassembly of TJs.

Endothelial cells of the inner wall of SC are known to form TJs. Nevertheless, gaps between cells are found along the SC endothelium, these are known as B-pores and they are thought to form by disassembly of TJs. Moreover, the presence of B-pores seems to correlate with active areas of flow[47], thus, the endothelium may regulate cell junctions to allow flow to pass through. Therefore, inhibiting proteins necessary for the formation of TJs should lead to more openings in the inner wall of SC that should result in

an increase in outflow facility. TJs require the expression of membrane proteins that bind cells together (like tricellulin) as well as intracellular proteins (like ZO-1) that allow communication between the membrane and the cytoskeleton[30]. In this project ZO-1 siRNA and tricellulin siRNA[196] were injected into mouse eyes in order to assess changes in outflow facility and IOP. A combination of both siRNAs (1 µg each) was injected into the anterior chamber of one eye while 2 µg of scramble siRNA were injected in the contralateral eye. The effects of these siRNAs were measured 48 hours after injection based on the *in vitro* protein inhibition data provided by our colleagues at Trinity College Dublin (personal communication, data not shown).

After 48 hours of treatment with siRNA we measured an increase in outflow facility ($\approx$ 80%) with all eyes responding to the treatment. The fact that the drug was injected into the eye prior to the perfusion instead of through the perfusate reduces the variability in the response to the treatment because the siRNA had 48 hours to reach the outflow pathway. However, with the injections performed, it is not possible to know the exact amount of siRNA delivered because we could not know the reflux escaping the eye through the puncture once the needle was removed, this, and the natural variability in C between mice can influence the range of effects observed.

With such an increase in facility a reduction in IOP was expected. Different approaches were considered to measure IOP: rebound tonometry and cannulation using the iPerfusion system. The main challenge we faced was that IOP is affected by anesthesia, which interferes with the measurements if not taken into account. Over the course of this project, we have tried to overcome this problem since reliable and accurate IOP measurements are crucial to our field. Assessment of IOP under anesthesia in non-treated naïve mice is describe in more detail in Chapter.6.

In a first attempt we used rebound tonometry under ketamine/Domitor® anesthesia measuring at a single time point. Nevertheless, we were cautious and measurements were taken at the same time after injection of anesthesia. However, we did not see any change in IOP on eyes treated with t-siRNA. We were assessing the effect of ZO-1 and tricellulin siRNA on normotensive mice and we did not expect a major change in IOP, hence, we thought that the effects of anesthesia and the variability in measurements

from the TonoLab could be masking the IOP reduction. Therefore, we performed the measurements again cannulating the eyes and using the iPerfusion system to measure IOP.

The recently developed iPerfusion system[249] can be adapted for *in vivo* work apart from the *ex vivo* perfusions extensibly used in this thesis. One of the applications is the possibility to cannulate the eye with a glass micro-needle and measure IOP directly with the pressure transducer when no-pressure from the reservoir is applied. The main technical changes from the *ex vivo* perfusions are that the mouse needs to be under general anesthesia and that the orientation of the eyes is very different and cannulations are more difficult when both eyes are tested simultaneously. A combination of ketamine and xylazine was used and despite the fact that mice were weighted and the corresponding dose was given, it was very difficult to achieve the same depth of anesthesia. Measuring IOP with the iPerfusion system is an invasive and long procedure and the animal needs deep anesthesia throughout the experimental time frame, it implies that mice need around 30 minutes before they can be cannulated plus about 2 hours perfusion. During this time, it would be desirable that the animal is at the same anesthetic state, which is very complicated to achieve with injectable anesthesia without either loosing the anesthetic effects or over-dosing the mouse. Therefore, it seems possible to measure IOP using the iPerfusion but the methodology needs further improvements, thus the results obtained need to be taken into consideration cautiously.

Finally, we developed a multi-time protocol to measure IOP by rebound tonometry under general anesthesia with isoflurane to account for the lowering effect that anesthesia has on IOP. Using this approach, we measured a significant reduction in IOP in eyes injected with t-siRNA despite some limitations in the methodology. The first important limitation is that the TonoLab does not seem to be able to measure IOPs below 7 mmHg and the device is not well characterised for such low pressures, as can be seen from the calibration curve performed with our device[44]. Therefore, every time 7 mmHg was measured we may be overestimating the value. This is especially a problem when using normal-tension mice because we expected low values more frequently, which leads to the second limitation. In this study we tried to lower IOP on mice that had normal IOP, hence, final IOP would be at non-physiological levels. This is a potential problem since

the eye may have compensatory mechanisms to avoid ocular hypotension. It would be advice, then, that IOP lowering drugs are tested on hypertensive mice. Nevertheless, the fact that we measured a reduction in IOP despite these limitations is very encouraging for future considerations to used this approach as a therapy for ocular hypertension.

To conclude, the treatment of mouse eyes with ZO-1 and tricellulin siRNA resulted in an increase in outflow facility and a reduction in IOP. The changes observed lead to think that the siRNA is affecting the outflow pathway. From the *in vitro* data provided by our collaborators at Trinity College Dublin we assume that the siRNA are knocking down the expression of ZO-1 and tricellulin, which would lead to the disassembly of TJs and formation of intra-cellular spaces. However, we still do not have protein inhibition data in mice injected with siRNA. This data is being acquired at Trinity College Dublin using laser capture micro dissection to isolate SC from treated mouse eyes.

Chapter 6

Effects of anesthesia on intraocular pressure in mice

6.1 Introduction

Reduction of intraocular pressure (IOP) is the ultimate goal on glaucoma therapies, thus being able to accurately measure IOP is fundamental to assess the potential of IOP lowering drugs. IOP measuring techniques used for animal models can be non-invasive or invasive. For **non-invasive methods**, like rebound tonometry, measurements may be performed on conscious animals. This implies training of the animal so it remains still, otherwise, restraint can cause distress and alter physiological parameters that can affect IOP[109]. An alternative, is to sedate or anesthetise the animal but this may affect IOP as well. **Invasive methods** require cannulation of the anterior chamber by a micro-needle or the implantation of a telemetric device[77], in this case, anesthesia is definitely needed. Even though several studies reported that anesthesia reduces IOP[54,56,58,66,73,79,119,144,145,195,302], most of the studies measuring IOP on animal models do not report details on the anesthetic regimen. It is important to report whether the IOP measurement was carried out before or after the onset of anesthesia, wether all IOP readings were acquired at the same time point after the induction of anesthesia or whether the control or experimental eye was measured first. Therefore, it is necessary to characterise the effect of the anesthetic regimen used to understand how anesthesia may affect IOP since it would influence the design of experiments. This chapter contains an initial assessment on the effects of anesthesia on IOP.

There are two types of anesthetics that vary depending on the administration route: inhaled and injectable. For **inhaled anesthetics**, the agent is mixed with air and delivered via a nose cone. The effect of the anesthetic remains as long as the animal is inhaling the drug. **Injectable anesthetics** are liquid drugs injected intraperitoneally (IP), intravenous (IV) or intramuscularly (IM), they can be re-administrated when necessary following the same administration route to prolong their effect. Both types of anesthetics have advantages and disadvantages. Inhaled agents are safer for long-term procedures because the depth of anesthesia is more constant and controllable, and provide fast induction, onset and recovery. Moreover, because inhaled anesthetics are metabolised in the lungs, they do not damage the liver nor the kidneys. However, inhaled anesthetics are not recommended when studying the lungs, they induce respiratory and myocardial

depression, vasodilation and hypotension. Furthermore, administration of additional analgesics is recommended and vaporizers and inhaling equipment can be expensive. On the other hand, injectable anesthetics are simple to administrate, they do not required extra equipment, they are suitable for short and deep anesthesia and there is a big range of drugs or combination of drugs available. However, the slow metabolism of injected drugs implies that, once injected, the drug can not be cleared from the organism although some compounds have reversing agents to eliminate its effect (e. g. α-2 adrenergic receptor agonists can be reversed with atipamezole hydrochloride (Antisedan®)). Side effects of injectable drugs depend on the type used[109].

In this study, we measured IOP over a period of time in mice under general anesthesia to study IOP decays. 3 anesthetic regimens were assessed: isoflurane (inhaled) and ketamine/xylazine and ketamine/medetomidine hydrochloride (Domitor®) combinations (injectable). **Isoflurane** is a non-flammable liquid that is administrated via a vaporizer, inhalation results in deep general anesthesia. The exact mechanisms of action of isoflurane are not fully understood but it seems to act on the cell membrane of neurons resulting on impaired neuronal transmission and to enhance the release of GABA, an inhibitory neurotransmitter[200]. The use of analgesics are recommended in combination with isoflurane[109]. **Ketamine** is a dissociative drug, it activates the central nervous system and stimulates the sympathetic system, which produces analgesia, amnesia, catalepsy and immobilization[109,222]. It is usually used in combination with other drugs to complement and enhance its effect[296], these drugs can be, for example, xylazine or Domitor®. Both **xylazine** and **Domitor®** are α-2 adrenergic receptor agonists that result in analgesia, sedation, hypnosis and muscle relaxation. Domitor® is a synthetic compound and it is 10 times more potent than xylazine and has higher affinity for α- 2 receptors[109]. Interestingly, the α-2 adrenergic receptor agonist Brimonidine (Alphagan®) is used as a glaucoma therapy in the form of eye drops[286].

In this chapter the effect of isoflurane was assessed by rebound tonometry and the effect of both Ketamine/Xylazine and Ketamine/Domitor® combos was assessed by cannulation using the iPerfusion system. The preliminary results shown here were used to design the experiments previously shown in Chapter.5.

6.2 Materials and Methods

6.2.1 Experimental design

Initial assessment of the effect that anesthetics have on IOP were carried out in order to develop a better protocol for measuring IOP taking into account the IOP decay due to the anesthetics. These experiments were performed before the IOP measurements described in the previous Chapter.5. The effect of isoflurane was tested by rebound tonometry and the effect of ketamine/xylazine and ketamine/Domitor® were tested using the iPerfusion system. IOP decays were generated by measuring IOP at different time points after induction of anesthesia.

The IOP measurements using the iPerfusion system were done at Trinity College Dublin in Professor Humphries laboratory, which I visited for 3 weeks.

6.2.2 Animal Husbandry

Animals where brought into the animal facility one week before the experiments for acclimatization. Mice were housed in individually ventilated cages with 5 mice per cage. They were provided with food and water *ad libitum* and were under 12 hours light/dark circles (7 am to 7 pm) at 21℃. Male C57BL/6 mice (Charles River Laboratories, UK) of 10 to 12 weeks old were used.

All animals were treated in compliance with the ARVO statement for the Use of Animals in Ophthalmologic and Vision Research under UK Home Office Project License 70/7306 or Irish Medicined Board Project license AE191361P017.

6.2.3 Tonometric IOP measurement

The effect of isoflurane on IOP was tested using a commercial rebound tonometer (TonoLab; Icare, Finland). The mouse was anesthetised by placing it into the induction

chamber with a constant flow of 3% (≈ 2.6 MAC[1]) isoflurane (Isocare; Animalcare Ltd., UK) + 1 l/min oxygen for exactly 2 minutes. Then, the mouse was mounted on an stereotaxic head holder (Model 923-B, Kopf Instruments, US) connected to the isoflurane machine. The TonoLab was held by a micro-manipulator supported by a ring stand with the tip positioned approximately 2 mm from the central cornea along the optical axis. IOP measurements were done in the right eye while the left eye was kept moist by adding an hydration gel (Vidisic, 0.2 % w/w Eye Gel, Bausch & Lomb, UK), PBS was added in between readings on the right eye to prevent dehydration.

IOP was determined according to the manufacturer's instructions. Briefly, the TonoLab performs 5 rebound events and displays the IOP on the screen, corresponding to a reading. 5 IOP readings were taken and averaged per time point. For each mouse, IOP was measured every 3 or 5 minutes for 30 minutes, hence t = 0 was defined as the moment that isoflurane flow started. Measurements were done on the right eye with the mouse and TonoLab still for the probe to hit the cornea at the same exact point.

Mice were placed in a 28℃ thermoregulated box to recover from anesthesia before putting them back to their cage.

6.2.4 IOP measurements using the iPerfusion system

The effect of injectable anesthetics (ketamine/Domitor® and ketamine/xylazine) was assessed using the iPerfusion system[249] following a protocol based on the one described in Section.5.2.6. Briefly, mice were anesthetised with either 66.6 mg/kg ketamine (Fort Dodge Animal Heatht, Fort Dodge, US) and 0.66 mg/kg Domitor® (Orion Pharma, UK) or 100 mg/kg ketamine + 7.5 mg/kg xylazine (Xylacare, Animalcare Ltd., UK) injected intraperitoneally (IP), the moment of injection was defined as t = 0. Ketamine/xylazine anesthesia was maintained by injecting 50 µl every 15 minutes via an IP catheter, for ketamine/Domitor® it was not necessary to re-dose. Eyes were kept moist by applying Vidisic.

[1] Minimum alveolar concentration is the concentration of gas in the lungs necessary to prevent movement in response to pain in 50% of individuals.

At about 5 minutes time, when the mouse was immobile but not under deep anesthesia, a tonometric IOP reading (IOP1) was performed as described previously (but taking 10 readings instead of 5 in order to get more accurate data). A second tonometric reading (IOP2) was done when the mouse was completely anesthetised ($\approx$ 20 minutes). With the iPerfusion system arranged for *in vivo* work (described in section.5.2.6), the eye was cannulated at IOP2 by adjusting the height of the reservoir. Immediately, the system was closed to the reservoir to directly measure IOP with the pressure transducer without any external pressure applied. An IOP decay was recorded until pressure was stable (ΔP $\leq$ 0.02 mmHg/min).

After the procedure, mice were culled by cervical dislocation.

6.3 Results

6.3.1 Effect of isoflurane anesthesia on IOP

IOP was measured in 3 mice under general anesthesia with isoflurane by rebound tonometry. For mouse 1, IOP was measured every 5 minutes and for mice 2 and 3 every 3 minutes. 5 IOP readings were done at each time point and they were averaged to define IOP at a given time, all readings can be found in Table.6.1.

The TonoLab does not seem to display IOP values below 7 mmHg. With our device, we have never seen a value below 7 mmHg. Moreover, as can be seen with Mouse 3, after a series of readings at 7 mmHg the device displays and error (E03) and it was not possible to get any other IOP measurement afterwards. The manufacturers define E03 as ”Probe speed was too low: The measurement was made from too far away or the tonometer was tilted upwards too much”, in this particular experiment, both the mouse and the TonoLab were firmly held throughout the experiment, hence it was unlikely that the TonoLab moved. Although we also tried changing the probe, no more IOP readings could be acquired.

As shown in Figure.6.1, all mice experienced a sudden drop in IOP after a few minutes of anesthesia. The rate of IOP decay was different for each mouse. We meas-

Table 6.1: Individual tonometric IOP readings for IOP decay under isoflurane anesthesia. E03 is the error displayed by the TonoLab.

		IOP Readings (mmHg)						
Mouse	**Time (min)**	**1**	**2**	**3**	**4**	**5**	**Average (mmHg)**	**SD**
1	5	13	15	15	14	13	14.0	1.00
	10	14	16	14	14	13	14.2	1.10
	15	8	8	8	8	7	7.8	0.45
	20	11	11	10	9	9	10.0	1.00
	25	8	7	7	7	7	7.2	0.45
	3	8	7	7	8	7	7.4	0.55
2	3	16	17	18	16	16	16.6	0.89
	6	15	16	17	16	16	16.0	0.71
	9	10	12	11	7	8	9.6	2.07
	12	8	9	10	7	7	8.2	1.30
	15	7	7	7	7	7	7.0	0.00
	18	8	10	9	7	7	8.2	1.30
	21	8	8	7	8	8	7.8	0.45
	24	7	8	8	7	9	7.8	0.84
	27	7	8	9	8	7	7.8	0.84
	30	7	7	8	7	7	7.2	0.45
3	3	11	12	14	11	12	11.4	0.55
	6	7	8	8	8	8	8.0	0.71
	9	7	10	10	9	7	8.0	1.41
	12	7	7	7	7	7	7.0	0.00
	15	7	7	7	E03	E03	7.0	0.00

ured fairly stable IOP for up to 10 minutes in Mouse 1, 6 minutes for Mouse 2 and 3 minutes for Mouse 3. Them IOP dropped in all mice and IOP seemed to remain more or less constant afterwards. However, these low values need to be taken cautiously because the device is not well characterised at its lower detection limit.

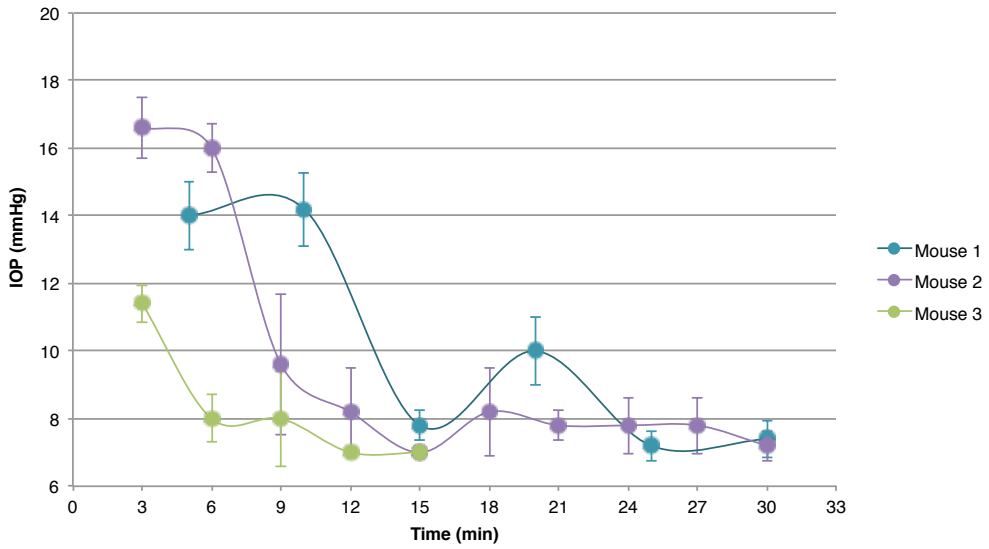


Figure 6.1: IOP decay under isoflurane anesthesia. Tonometric IOP measurements as a function of time under general anesthesia with isoflurane. 5 readings were performed at each time point (dots). Each curve corresponds to a mouse and error bars are standard deviations (SD). Time = 0 corresponds to the moment where the isoflurane flow started.

6.3.2 Effect of ketamine/Domitor® anesthesia on IOP

4 mice anesthetised with a mix of ketamine and Domitor® were assessed for time dependent IOP changes (Figure.6.2). Two tonometric measurements were taken before cannulation and IOP seemed to decrease by the second measurement, IOP decreased from an average of IOP1 = 14.4 $\pm$ 2.6 mmHg (n = 4) to IOP2 = 9.9 $\pm$ 2.0 mmHg (n = 4) (p = 0.06, paired t-test). Once the mouse was completely anesthetised, eyes were cannulated and the IOP decay recorded. All mice anesthetised with ketamine and Domitor® ended up to an IOP $\leq$ 0 mmHg.

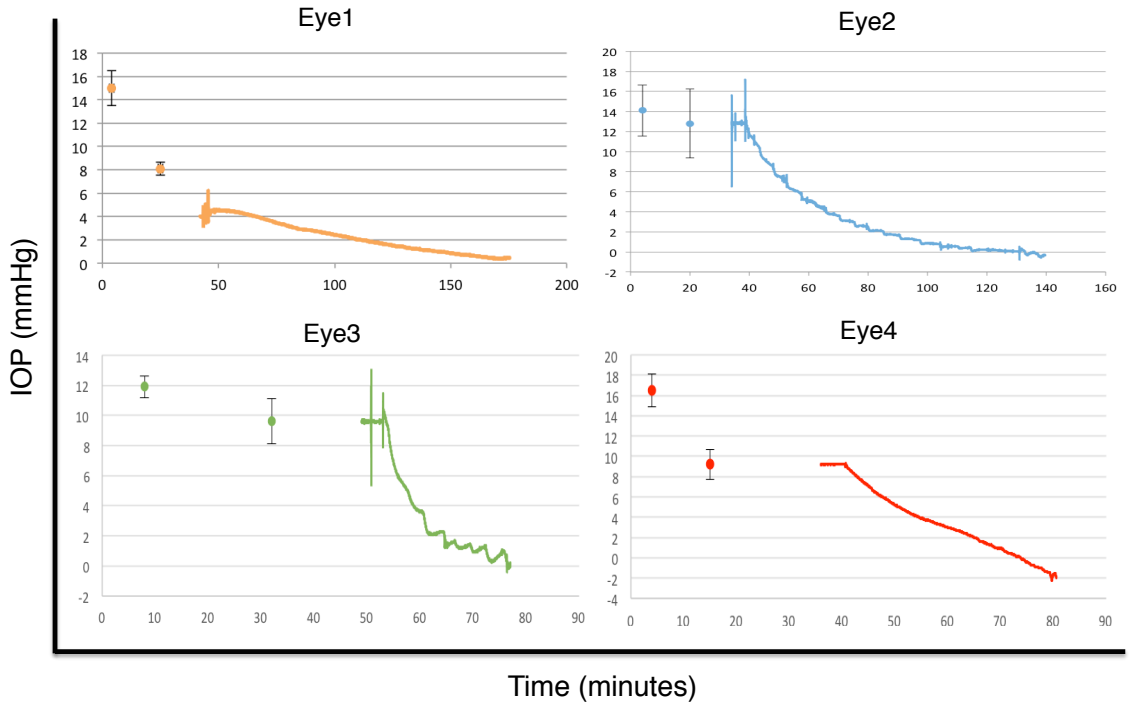


Figure 6.2: IOP decay under ketamine/Domitor® anesthesia. IOP measurements as a function of time of anesthesia. Dots represent the tonometric readings performed before cannulation and the curves are the IOP measured with the iPerfusion system. Time states the time after injection of anesthetics. Error bars represent SD.

6.3.3 Effect of ketamine/xylazine anesthesia on IOP

The effects of a combination of ketamine and xylazine on IOP was also tested (Figure.6.3). In this case, the average IOP for the first tonometric measurement was 14.7 $\pm$ 2.5 mmHg (n = 5) and it fell to 9.7 $\pm$ 1.2 mmHg (n = 3) for the second measurement (p = 0.02, unpaired t-test). As can be seen from the individual measurements in Figure.6.3, for

eye1 and eye3 it was not possible to acquire the second tonometric IOP measurement, most likely because IOP was below the lower detection limit for the TonoLab. Using ketamine/xylazine as anesthetic we measured different effects on IOP. For eye2 and eye3, IOP dropped to 0 mmHg similarly to the ketamine/Domitor® anesthesia, whereas eye1, eye4 and eye5 suffered a reduction in IOP but remained within positive values of 7.5, 6.0 and 9.5 mmHg respectively, traces can be seen in Figure.6.3. It was unexpected that, for eye1, which it was not possible to measure the second tonometric IOP, we measured an IOP of 8.0 mmHg by cannulation.

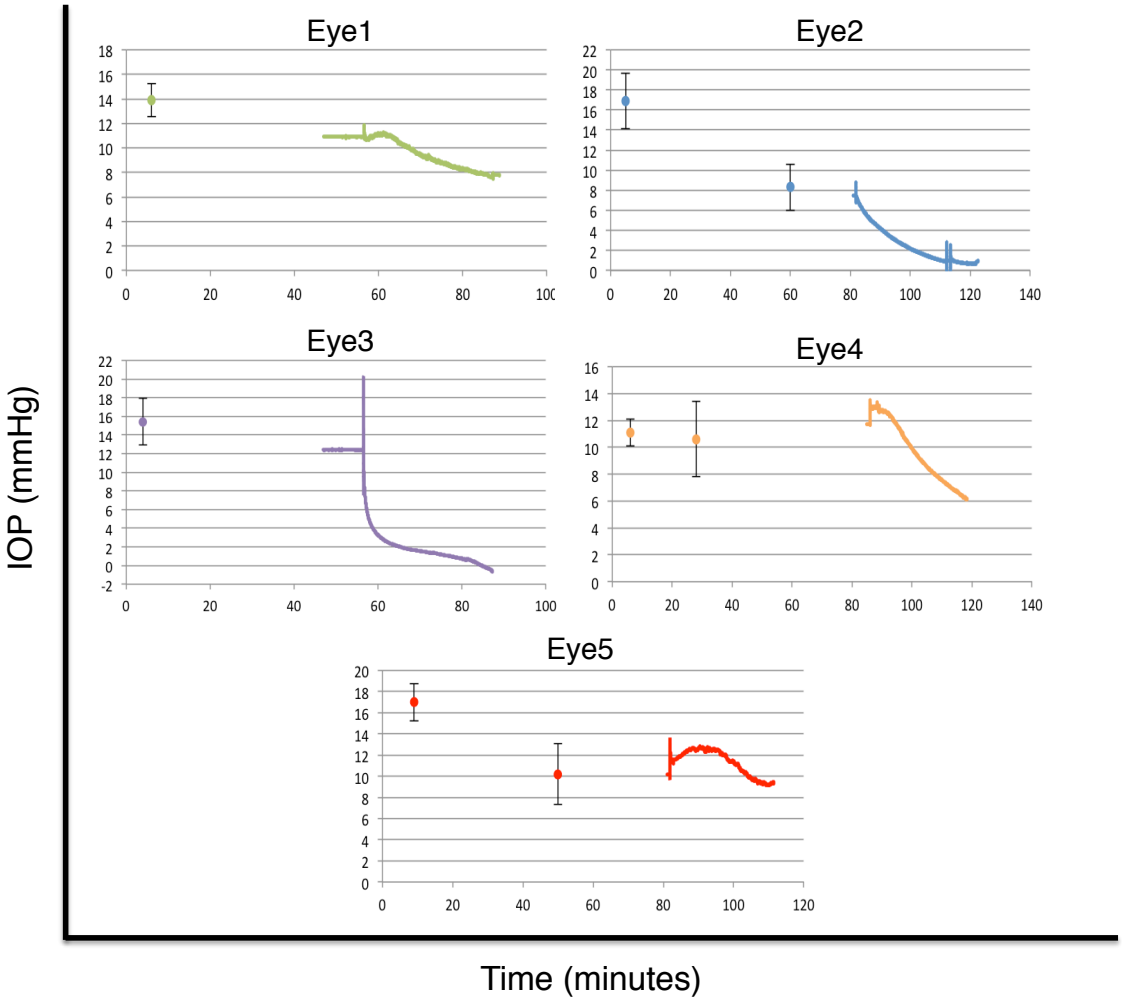


Figure 6.3: IOP decay under ketamine/xylazine anesthesia. IOP measurements as a function of time of anesthesia. Dots represent the tonometric readings performed before cannulation and the curves are the IOP measured with the iPerfusion system. Time states the time after injection of anesthetics. Error bars represent SD.

6.4 Discussion

IOP measurements are essential for glaucoma research. However, when using animal models where it is necessary to sedate or anesthetise the animal, the effect that anesthetics can have on IOP needs to be taken into account. In order to characterise the IOP response to anesthetics, IOP decays were generated for mice under isoflurane, ketamine/Domitor® and ketamine/xylazine anesthesia. Consistently with the literature[54,56,58,66,73,79,119,144,145,195,302], we measured a drop in IOP for all anesthetics.

Isoflurane anesthesia was assessed by rebound tonometry over a period of 30 minutes. Isoflurane provides fast and constant depth anesthesia without the need to re-administrate since it is delivered constantly through the mouse snout. For this case, 2 out of the 3 mice tested showed constant IOP for the first few minutes of anesthesia (6 - 10 minutes) followed by a sudden drop, for the third mouse, the drop occurred much faster. Later, IOP seemed to stabilise. However, the TonoLab used do not seem to display IOP measurements bellow 7 mmHg and, for low values, the device is not very well characterised, as can be seen from the calibration performed in Boussommier-Calleja *et al.* (2013)[44]. Therefore, the stable pressure observed after 15 minutes of anesthesia should be considered carefully. Nevertheless, when values were extremely low (like in mouse 3), the TonoLab could not work and displayed and error (E03) even though the prove was changed twice. Surprisingly, the technical information available in the TonoLab's "Users's and Maintenance manual" states that the measurement range is 1-99 mmHg. Consequently, it would be advised to assess the effect of isoflurane on IOP using the iPerfusion system.

Mice anesthetised with ketamine/Domitor® were deeply anesthetised for the entire duration of the experiments without the need of re-dose. However, this group of mice suffered the acutest IOP drop. Tonometric readings were within measurable values but when eyes were cannulated, all of them fell down to an IOP $\leq$ 0 mmHg when stable P was reached. This phenomenon is most likely due to Domitor®. Medetomidine hydrochloride, the active ingredient in Domitor®, is a very potent synthetic α-2 adrenoreceptor agonist[109], these compounds are used as glaucoma treatments[286] because of their IOP lowering effects due to reduction of AH formation[61,111,186] and increase in uveo-

scleral outflow facility after long-time exposure[286]. For that reason, it was decided to use ketamine/xylazine instead. Xylazine is also a α-2 adrenoreceptor agonist although it is not as potent as Domitor®.

Mice anesthetised with ketamine/xylazine exhibited less stable anesthesia and it was necessary to re-administrate. How often and how much anesthetic is necessary to administrate in order to maintain deep anesthesia is not trivial, if not enough anesthetic is given the animal can start recovering from anesthesia in the middle of the procedure, which it is a problem not only for the welfare of the mouse but also because it can interfere with the results. On the other hand, if too much anesthetic is given, the mouse can die of anesthetic over-dose. For the dose of ketamine/xylazine used, we injected 50 µl every 15 minutes and seemed enough to maintain anesthesia despite the fact that 3 mice died[2] when the end of the experiment was approaching and for some mice (eye2 and eye5) it took more than the standard 20 minutes for the mouse the be deeply anesthetised. Hence, all mice did not respond exactly in the same way to the same dose of ketamine/xylazine. Regarding the IOP measurements, similarly to the mice anesthetised with ketamine/Domitor®, there was a reduction in IOP between the 2 tonometric readings. However, the IOP decay recorded with the iPerfusion system was different, although 2 out of 5 mice also reached an IOP of 0 mmHg. For the other 3 mice, IOP remained stable for a few minutes (around 10 minutes) and then declined at much lower slope than the previous cases until it reached stability ($\Delta P \leq 0.02$ mmHg/min). At this point, we consider that IOP was not changing significantly although it was still dropping, it would be interesting to assess longer times.

The differences between mice in the ketamine/xylazine group could rely on slight difference in the the dosage. Anesthesia was delivered using a 1 ml syringe when the volume injected was around 300 µl, depending on the weight of the mouse. With such small animals, a few µl error in the administration results in a big change in the dose injected. If the effects are dose-dependent, it could explain why some mice had more severe changes in IOP than others and it could also explain why there was a difference between the group anesthetised with ketamine/xylazine and the group anesthetised with

[2]These mice belonged to the group injected with siRNA described in Chapter.5, which needed to be under anesthesia for a longer time but the same regimen was used.

ketamine/Domitor® despite the fact that both include α-2 adrenoreceptor agonist in their formulation. Therefore, a dose-dependency study would be advised when using injectable anesthetics.

To conclude, all anesthetics tested resulted in a time-dependent reduction in IOP. The degree and speed of reduction depended on the type of drug used, thus it is very important to characterise the effect that anesthesia would have before designing experiments aiming to determine, for example, the effect of drugs on IOP. Equally important is the technique used to measure IOP. When assessing IOP by rebound tonometry using the commercial TonoLab, one has to take into consideration the limitations of the device, therefore, unless measurements are done immediately after onset of anesthesia, IOP may be to low to be measured. An alternative is to directly measure IOP with a pressure transducer by cannulating the eye with a micro-needle, this way, the range of pressures and accuracy increases. In our case, the pressure transducer used can measure P of 0 - 50 mmHg with an accuracy of $\pm$0.024 mmHg[249].

From what we observed doing these experiments, we now have a better insight on how we should measure IOP in order to account for the effects that anesthetics have on IOP. Despite its limitations, the TonoLab is a good tool to measure IOP because it is not invasive and allows multiple measurement on the same eye, for instance, before and after the application of a drug or during the time course of a treatment. In order to account for the IOP decay, we developed the protocol presented in Chapter.5, where IOP is measured at 3 time points, a linear regression is applied to the data and IOP is defined at a constant time point by interpolation.

Chapter 7

Conclusions

7.1 Summary

In this thesis we examined how outflow facility may be regulated by manipulating physiological processes that control hydraulic conductivity of Schlemm's canal (SC) endothelium. Resistance to aqueous humour (AH) outflow is generated in the vicinity of the juxtacanicular tissue, the inner wall of SC and its basement membrane[210]. We speculate that the inner wall of SC, and particularly pores in the inner wall, plays a key role in outflow resistance generation, thus targeting pore formation should allow to modulate outflow facility.

In Chapter.2, we observed that VEGF is involved in outflow facility regulation. We speculate that TM cells can sense signals (stretch, hypoxia, biochemical products, for instance) and produce VEGF to affect SC in a paracrine manner to modulate the hydraulic conductivity of the inner wall and influence outflow. Our data showed an increase in outflow facility with VEGF perfusions as well as a reduction in facility in response to VEGFR inhibitors, which is consistent with previous work described in the literature regarding vascular permeability and hydraulic conductance. This indicates that modulation of hydraulic conductance of SC endothelium is key to outflow facility regulation. Specifically, we showed that the VEGF-mediated effect on outflow facility is mediated through VEGFR-2 activation and that NO and Rac1 are necessary downstream effectors. Moreover, we showed that VEGF is present within the outflow pathway in mouse eyes by immunohistochemistry staining. This, may explain why repeated treatment with anti-VEGF therapies can result in sustained IOP elevation. Additionally, in Chapter.3, we showed that in mice with glucocorticoid-induced ocular hypertension (OHT) eyes did not respond to VEGF. Therefore, impaired VEGF signaling pathways may contribute towards OHT.

In Chapter.4 we focused on the role of PLVAP in outflow reisistance. We observed that PLVAP heterozygote (*Plvap*$^{+/-}$) mice had significantly lower outflow facility compared to their WT littermates. We speculate that *Plvap*$^{+/-}$ mice have impaired I-pore formation because they are not able to form fenestrae (or "mini-pores") due to the lack of PLVAP. It has been proposed that mini-pores are precursors to the micron-sized I-pores[38]. Moreover, in the outflow pathway, PLVAP is exclusively expressed by SC endothelial cells, which reinforces the idea that modulating SC endothelium is key to outflow

regulation. Perfusions with an actin disrupting drug, such as Latrunculin-B, eliminated the difference in facility between *Plvap*$^{+/-}$ and WT mice, indicating that the increased resistance seen in *Plvap*$^{+/-}$ mice have a cellular origin, instead of being, for example, a physical defect due to genetic modification. Therefore, despite SC cells might not be able to form I-pores, they have the potential to respond to drugs, for instance, by increasing the number of B-pores in response to Latrunculin-B.

In Chapter.5 we targeted tight junctions (TJs) in the SC endothelium. TJs are key regulators of endothelial barrier function. Therefore, the disassembly of TJs should lead to formation of paracellular spaces in the inner wall of SC. Accordingly, the delivery of ZO-1 and tricellulin siRNA into the anterior chamber resulted in an increase in outflow facility and reduction in IOP.

Overall, we presented evidence that by targeting cellular mechanisms involved in the barrier function of SC endothelium, it is possible to modulate outflow facility in mice. It is of great interest to observe that VEGF, well known to induce hydraulic conductance and permeability in vascular endothelia, is involved in the regulation of outflow resistance. Even though we did not visualise pores, we detected changes in outflow facility when targeting proteins involved in the formation of I-pores or B-pores, reinforcing the idea that pores are the path that AH follows to cross the otherwise continuous SC endothelium.

7.2 Future work

This thesis provides insight on how the inner wall of SC regulates outflow. Nevertheless, new questions have risen, which can be addressed in the future.

7.2.1 How is VEGF expression controlled?

We have seen that the outflow pathway responds differently to exogenous $VEGF_{165}a$ and $VEGF_{165}b$. However, we do not know if the balance between this two isoforms controls the dynamism of AH outflow by regulating segmental outflow, for instance. It would be interesting to find out if $VEGF_{165}a$ is expressed more in filtration active areas of SC

than $VEGF_{165}b$ and whether $VEGF_{165}b$ is expressed more in less active areas. It could be possible to generate tracer maps similar to those shown in Chapter.5 and perform protein expression experiments in cells isolated from areas with high and low tracer intensity.

It would also be interesting to discern which factors induce VEGF expression. Possible mechanisms that induce VEGF expression could include: (i) stretch due to increments in IOP in order to release the pressure or (ii) hypoxia, which is well known to promote VEGF expression in other endothelia. These experiments could be done using TM cells in culture by stretching the cells or culture in hypoxic conditions.

7.2.2 How does VEGF affect the ultrastructure of inner wall of SC?

Studies have shown that VEGF induces both fenestration and cell junctions disassembly[90,110]. However, we do not know if both phenomena are responsible for the effect observed in outflow facility. An initial experiment that could be done is to perfuse the eyes of *Plvap*$^{+/-}$ mice with $VEGF_{165}a$ and see if the effect in outflow facility is reduced.

7.2.3 What is the response to long-time exposure to VEGF?

A time course study will give more information about the similarity between SC endothelium and other vascular linings. In mesenteric vessels perfused with VEGF, an initial acute increase in hydraulic conductance followed by a sustained increase has been reported[25]. With the timeframe of a perfusion, we most likely capture the initial acute response but we did not examine the long-term effects of VEGF in outflow facility. To assess this aspect, TM cells in the outflow pathway could be transfected with vectors over-expressing VEGF, this could be particularly interesting with forms of VEGF targeting VEGFR-3, to avoid undesired side effects.

7.2.4 Is the effect seen in DEX-treated mice a representation of POAG?

As we did not measure any change in facility in response to VEGF in DEX-treated mice we proposed that the increase in outflow resistance observed in these mice can be,

in part, due to a malfunction of the VEGF signaling pathway. Because corticoid levels are elevated in POAG patients, it would be interesting to see if the VEGF signaling pathway is also not behaving normally in POAG. We could study the effect of VEGF on SC cells isolated from glaucomatous eyes by perfusing cell monolayers.

7.2.5 Future applications for the iPerfusion system.

All outflow facility measurements performed in this thesis were done using the recently developed iPerfusion system[249], which includes not only a novel methodology to carry out perfusions but also a change in the way we analyze, interpret and present the data. Currently, we have a good characterization of the system for *ex vivo* work on enucleated eyes. Nevertheless, the system can be used *in vivo* for studies where we want to study parameters that are not present in enucleated eyes: AH inflow or unconventional outflow, for instance. Moreover, it is crucial to find a way to have reliable and precise IOP measurements and the iPerfusion can be that tool. Initial attempts to measure IOP using the iPerfusion system are described in Chapter.6 but a refinement of the technique is necessary. From the current experience, changing the anesthesia from injectable to inhaled should improve the repeatability of the measurements and the use of a microscope on an arm flex would facilitate the cannulations. Moreover, to monitor the heart rate of the mouse can be a good way to assess the depth of anesthesia.

Bibliography

[1] Abedi, G., Adelman, R. A. and Salim, S. [2013], 'Incidence and management of elevated intraocular pressure with antivascular endothelial growth factor agents', Semin Ophthalmol .

[2] Achen, M. G., Jeltsch, M., Kukk, E., Makinen, T., Vitali, A., Wilks, A. F., Alitalo, K. and Stacker, S. A. [1998], 'Vascular endothelial growth factor d (vegf-d) is a ligand for the tyrosine kinases vegf receptor 2 (flk1) and vegf receptor 3 (flt4)', Proc Natl Acad Sci U S A **95**(2), 548–53.

[3] Achen, M. G. and Stacker, S. A. [1998], 'The vascular endothelial growth factor family; proteins which guide the development of the vasculature', Int J Exp Pathol **79**(5), 255–65.

[4] Achen, M. G. and Stacker, S. A. [2012], 'Vascular endothelial growth factor-d: signaling mechanisms, biology, and clinical relevance', Growth Factors **30**(5), 283–96.

[5] Adelman, R. A., Zheng, Q. and Mayer, H. R. [2010], 'Persistent ocular hypertension following intravitreal bevacizumab and ranibizumab injections', J Ocul Pharmacol Ther **26**(1), 105–10.

[6] Aihara, M., Lindsey, J. D. and Weinreb, R. N. [2003a], 'Aqueous humor dynamics in mice', Invest Ophthalmol Vis Sci **44**(12), 5168–73.

[7] Aihara, M., Lindsey, J. D. and Weinreb, R. N. [2003b], 'Experimental mouse ocular hypertension: establishment of the model', Invest Ophthalmol Vis Sci **44**(10), 4314–20.

[8] Aihara, M., Lindsey, J. D. and Weinreb, R. N. [2003c], 'Ocular hypertension in mice with a targeted type i collagen mutation', Invest Ophthalmol Vis Sci **44**(4), 1581–5.

[9] Allingham, R. R., de Kater, A. W. and Ethier, R. C. [1996], 'Schlemm 's canal and primary open angle glaucoma: Correlation between schlemm 's canal dimensions and outflow facility', Experimental Eye Research **62**(1), 101–110.

[10] Allingham, R. R., Dekater, A. W., Ethier, C. R., Anderson, P. J., Hertzmark, E. and Epstein, D. L. [1992], 'The relationship between pore density and outflow facility in human eyes', Invest Ophthalmol Vis Sci **33**(5), 1661–1669.

[11] Alm, A. and Nilsson, S. F. [2009], 'Uveoscleral outflow–a review', Exp Eye Res **88**(4), 760–8.

[12] Alvarado, J. A., Betanzos, A., Franse-Carman, L., Chen, J. and Gonzalez-Mariscal, L. [2004], 'Endothelia of schlemm's canal and trabecular meshwork: distinct molecular, functional, and anatomic features', Am J Physiol Cell Physiol **286**(3), C621–34.

[13] Alzet [2015], 'Formulating the test solution'.

[14] Antonetti, D. A., Barber, A. J., Hollinger, L. A., Wolpert, E. B. and Gardner, T. W. [1999], 'Vascular endothelial growth factor induces rapid phosphorylation of tight junction proteins occludin and zonula occluden 1. a potential mechanism for vascular permeability in diabetic retinopathy and tumors', J Biol Chem **274**(33), 23463–7.

[15] Apweiler, R., Bateman, A., Martin, M. J., O'Donovan, C., Magrane, M., Alam-Faruque, Y., Alpi, E., Antunes, R., Arganiska, J., Casanova, E. B., Bely, B., Bingley, M., Bonilla, C., Britto, R., Bursteinas, B., Chan, W. M., Chavali, G., Cibrian-Uhalte, E., Da Silva, A., De Giorgi, M., Fazzini, F., Gane, P., Castro, L. G., Garmiri, P., Hatton-Ellis, E., Hieta, R., Huntley, R., Legge,

D., Liu, W. D., Luo, J., MacDougall, A., Mutowo, P., Nightingale, A., Orchard, S., Pichler, K., Poggioli, D., Pundir, S., Pureza, L., Qi, G. Y., Rosanoff, S., Sawford, T., Shypitsyna, A., Turner, E., Volynkin, V., Wardell, T., Watkins, X., Zellner, H., Corbett, M., Donnelly, M., Van Rensburg, P., Goujon, M., McWilliam, H., Lopez, R., Xenarios, I., Bougueleret, L., Bridge, A., Poux, S., Redaschi, N., Aimo, L., Auchincloss, A., Axelsen, K., Bansal, P., Baratin, D., Binz, P. A., Blatter, M. C., Boeckmann, B., Bolleman, J., Boutet, E., Breuza, L., Casal-Casas, C., de Castro, E., Cerutti, L., Coudert, E., Cuche, B., Doche, M., Dornevil, D., Duvaud, S., Estreicher, A., Famiglietti, L., Feuermann, M., Gasteiger, E., Gehant, S., Gerritsen, V., Gos, A., Gruaz-Gumowski, N., Hinz, U., Hulo, C., James, J., Jungo, F., Keller, G., Lara, V., Lemercier, P., Lew, J., Lieberherr, D., Lombardot, T., Martin, X., Masson, P., Morgat, A., Neto, T., Paesano, S. et al. [2014], 'Activities at the universal protein resource (uniprot)', Nucleic Acids Research **42**(D1), D191–D198.

[16] Aspelund, A., Tammela, T., Antila, S., Nurmi, H., Leppanen, V. M., Zarkada, G., Stanczuk, L., Francois, M., Makinen, T., Saharinen, P., Immonen, I. and Alitalo, K. [2014], 'The schlemm's canal is a vegf-c/vegfr-3-responsive lymphatic-like vessel', J Clin Invest **124**(9), 3975–86.

[17] Baeyens, N., Nicoli, S., Coon, B. G., Ross, T. D., Van den Dries, K., Han, J., Lauridsen, H. M., Mejean, C. O., Eichmann, A., Thomas, J. L., Humphrey, J. D. and Schwartz, M. A. [2015], 'Vascular remodeling is governed by a vegfr3-dependent fluid shear stress set point', Elife **4**.

[18] Bakri, S. J., McCannel, C. A., Edwards, A. O. and Moshfeghi, D. M. [2008], 'Persisent ocular hypertension following intravitreal ranibizumab', Graefes Arch Clin Exp Ophthalmol **246**(7), 955–8.

[19] Bakri, S. J., Pulido, J. S., McCannel, C. A., Hodge, D. O., Diehl, N. and Hillemeier, J. [2009], 'Immediate intraocular pressure changes following intravitreal injections of triamcinolone, pegaptanib, and bevacizumab', Eye (Lond) **23**(1), 181–5.

[20] Balda, M. S. and Anderson, J. M. [1993], 'Two classes of tight junctions are revealed by zo-1 isoforms', Am J Physiol **264**(4 Pt 1), C918–24.

[21] Bàràny, E. H. [1964], 'Simultaneous measurement of changing intraocular pressure and outflow facility in the vervet monkey by constant pressure infusion', Invest Ophthalmol **3**, 135–43.

[22] Bates, D. O. [1998], 'The chronic effect of vascular endothelial growth factor on individually perfused frog mesenteric microvessels', J Physiol **513 (Pt 1)**, 225–33.

[23] Bates, D. O. [2010], 'Vascular endothelial growth factors and vascular permeability', Cardiovasc Res **87**(2), 262–71.

[24] Bates, D. O., Cui, T. G., Doughty, J. M., Winkler, M., Sugiono, M., Shields, J. D., Peat, D., Gillatt, D. and Harper, S. J. [2002], 'Vegf165b, an inhibitory splice variant of vascular endothelial growth factor, is down-regulated in renal cell carcinoma', Cancer Res **62**(14), 4123–31.

[25] Bates, D. O. and Curry, F. E. [1996], 'Vascular endothelial growth factor increases hydraulic conductivity of isolated perfused microvessels', Am J Physiol **271**(6 Pt 2), H2520–8.

[26] Bates, D. O. and Curry, F. E. [1997], 'Vascular endothelial growth factor increases microvascular permeability via a ca(2+)-dependent pathway', Am J Physiol **273**(2 Pt 2), H687–94.

[27] Bates, D. O. and Harper, S. J. [2002], 'Regulation of vascular permeability by vascular endothelial growth factors', Vascular Pharmacology **39**(4-5), 225–237.

[28] Bates, D. O., Hillman, N. J., Williams, B., Neal, C. R. and Pocock, T. M. [2002], 'Regulation of microvascular permeability by vascular endothelial growth factors', J Anat **200**(6), 581–97.

[29] Bazzoni, G. and Dejana, E. [2004], 'Endothelial cell-to-cell junctions: molecular organization and role in vascular homeostasis', Physiol Rev **84**(3), 869–901.

[30] Bazzoni, G., Martinez Estrada, O. and Dejana, E. [1999], 'Molecular structure and functional role of vascular tight junctions', Trends Cardiovasc Med **9**(6), 147–52.

[31] Bearer, E. L. and Orci, L. [1985], 'Endothelial fenestral diaphragms: a quick-freeze, deep-etch study', J Cell Biol **100**(2), 418–28.

[32] Beazley-Long, N., Hua, J., Jehle, T., Hulse, R. P., Dersch, R., Lehrling, C., Bevan, H., Qiu, Y., Lagreze, W. A., Wynick, D., Churchill, A. J., Kehoe, P., Harper, S. J., Bates, D. O. and Donaldson, L. F. [2013], 'Vegf-a165b is an endogenous neuroprotective splice isoform of vascular endothelial growth factor a in vivo and in vitro', Am J Pathol **183**(3), 918–29.

[33] Becker, P. M., Waltenberger, J., Yachechko, R., Mirzapoiazova, T., Sham, J. S., Lee, C. G., Elias, J. A. and Verin, A. D. [2005], 'Neuropilin-1 regulates vascular endothelial growth factor-mediated endothelial permeability', Circ Res **96**(12), 1257–65.

[34] Behzadian, M. A., Windsor, L. J., Ghaly, N., Liou, G., Tsai, N. T. and Caldwell, R. B. [2003], 'Vegf-induced paracellular permeability in cultured endothelial cells involves urokinase and its receptor', FASEB J **17**(6), 752–4.

[35] Bhandari, V., Choo-Wing, R., Chapoval, S. P., Lee, C. G., Tang, C., Kim, Y. K., Ma, B., Baluk, P., Lin, M. I., McDonald, D. M., Homer, R. J., Sessa, W. C. and Elias, J. A. [2006], 'Essential role of nitric oxide in vegf-induced, asthma-like angiogenic, inflammatory, mucus, and physiologic responses in the lung', Proc Natl Acad Sci U S A **103**(29), 11021–6.

[36] Bhatt, K., Gong, H. and Freddo, T. F. [1995], 'Freeze-fracture studies of interendothelial junctions in the angle of the human eye', Invest Ophthalmol Vis Sci **36**(7), 1379–89.

[37] Bill, A. [1966], 'Conventional and uveo-scleral drainage of aqueous humour in the cynomolgus monkey (macaca irus) at normal and high intraocular pressures', Exp Eye Res **5**(1), 45–54.

[38] Bill, A. [1975], 'Blood circulation and fluid dynamics in the eye', Physiol Rev **55**(3), 383–417.

[39] Bill, A. and Phillips, C. I. [1971], 'Uveoscleral drainage of aqueous humour in human eyes', Exp Eye Res **12**(3), 275–81.

[40] Bill, A. and Svedbergh, B. [1972], 'Scanning electron microscopic studies of the trabecular meshwork and the canal of schlemm–an attempt to localize the main resistance to outflow of aqueous humor in man', Acta Ophthalmol (Copenh) **50**(3), 295–320.

[41] Bodor, C., Nagy, J. P., Vegh, B., Nemeth, A., Jenei, A., MirzaHosseini, S., Sebe, A. and Rosivall, L. [2012], 'Angiotensin ii increases the permeability and pv-1 expression of endothelial cells', Am J Physiol Cell Physiol **302**(1), C267–76.

[42] Boussommier-Calleja, A., Bertrand, J., Woodward, D. F., Ethier, C. R., Stamer, W. D. and Overby, D. R. [2012], 'Pharmacologic manipulation of conventional outflow facility in ex vivo mouse eyes', Invest Ophthalmol Vis Sci **53**(9), 5838–45.

[43] Boussommier-Calleja, A., Li, G., Wilson, A., Ziskind, T., Scinteie, O. E., Ashpole, N. E., Sherwood, J. M., Farsiu, S., Challa, P., Gonzalez, P., Downs, J. C., Ethier, C. R., Stamer, W. D. and Overby, D. R. [2015], 'Physical factors affecting outflow facility measurements in mice', Invest Ophthalmol Vis Sci **56**(13), 8331–8339.

[44] Boussommier-Calleja, A. and Overby, D. R. [2013], 'The influence of genetic background on conventional outflow facility in mice', Invest Ophthalmol Vis Sci **54**(13), 8251–8.

[45] Braakman, S. T., Moore, J. E., J., Ethier, C. R. and Overby, D. R. [2015], 'Transport across schlemm's canal endothelium and the blood-aqueous barrier', Exp Eye Res **146**, 17–21.

[46] Braakman, S. T., Pedrigi, R. M., Read, A. T., Smith, J. A., Stamer, W. D., Ethier, C. R. and Overby, D. R. [2014], 'Biomechanical strain as a trigger for pore formation in schlemm's canal endothelial cells', Exp Eye Res **127**, 224–35.

[47] Braakman, S. T., Read, A. T., Chan, D. W., Ethier, C. R. and Overby, D. R. [2015], 'Colocalization of outflow segmentation and pores along the inner wall of schlemm's canal', Exp Eye Res **130**, 87–96.

[48] Bradley, J. M., Vranka, J., Colvis, C. M., Conger, D. M., Alexander, J. P., Fisk, A. S., Samples, J. R. and Acott, T. S. [1998], 'Effect of matrix metalloproteinases activity on outflow in perfused human organ culture', Invest Ophthalmol Vis Sci **39**(13), 2649–58.

[49] Braet, F., De Zanger, R., Jans, D., Spector, I. and Wisse, E. [1996], 'Microfilament-disrupting agent latrunculin a induces and increased number of fenestrae in rat liver sinusoidal endothelial cells: comparison with cytochalasin b', Hepatology **24**(3), 627–35.

[50] Braet, F., Spector, I., De Zanger, R. and Wisse, E. [1998], 'A novel structure involved in the formation of liver endothelial cell fenestrae revealed by using the actin inhibitor misakinolide', Proc Natl Acad Sci U S A **95**(23), 13635–40.

[51] Braga, V. M., Del Maschio, A., Machesky, L. and Dejana, E. [1999], 'Regulation of cadherin function by rho and rac: modulation by junction maturation and cellular context', Mol Biol Cell **10**(1), 9–22.

[52] Brubaker, R. F. [2004], 'Goldmann's equation and clinical measures of aqueous dynamics', Exp Eye Res **78**(3), 633–7.

[53] Buller, C., Johnson, D. H. and Tschumper, R. C. [1990], 'Human trabecular meshwork phagocytosis. observations in an organ culture system', Invest Ophthalmol Vis Sci **31**(10), 2156–63.

[54] Burke, J. A. and Potter, D. E. [1986], 'The ocular effects of xylazine in rabbits, cats, and monkeys', J Ocul Pharmacol **2**(1), 9–21.

[55] Calderone, L., Grimes, P. and Shalev, M. [1986], 'Acute reversible cataract induced by xylazine and by ketamine-xylazine anesthesia in rats and mice', Exp Eye Res **42**(4), 331–7.

[56] Camras, L. J., Sufficool, K. E., Camras, C. B., Fan, S., Liu, H. and Toris, C. B. [2010], 'Duration of anesthesia affects intraocular pressure, but not outflow facility in mice', Curr Eye Res **35**(9), 819–27.

[57] Carson-Walter, E. B., Hampton, J., Shue, E., Geynisman, D. M., Pillai, P. K., Sathanoori, R., Madden, S. L., Hamilton, R. L. and Walter, K. A. [2005], 'Plasmalemmal vesicle associated protein-1 is a novel marker implicated in brain tumor angiogenesis', Clin Cancer Res **11**(21), 7643–50.

[58] Chang, F. W., Burke, J. A. and Potter, D. E. [1985], 'Mechanism of the ocular hypotensive action of ketanserin', J Ocul Pharmacol **1**(2), 137–47.

[59] Chang, J. Y. H., Folz, S. J., Laryea, S. N. and Overby, D. R. [2014], 'Multi-scale analysis of segmental outflow patterns in human trabecular meshwork with changing intraocular pressure', Journal of Ocular Pharmacology and Therapeutics **30**(2-3), 213–223.

[60] Chang, J. Y., Stamer, W. D., Bertrand, J., Read, A. T., Marando, C. M., Ethier, C. R. and Overby, D. R. [2015], 'Role of nitric oxide in murine conventional outflow physiology', Am J Physiol Cell Physiol **309**(4), C205–14.

[61] Chiou, G. C. [1983], 'Effects of alpha 1 and alpha 2 activation of adrenergic receptors on aqueous humor dynamics', Life Sci **32**(15), 1699–704.

[62] Choi, D. Y., Ortube, M. C., McCannel, C. A., Sarraf, D., Hubschman, J. P., McCannel, T. A. and Gorin, M. B. [2011], 'Sustained elevated intraocular pressures after intravitreal injection of bevacizumab, ranibizumab, and pegaptanib', Retina **31**(6), 1028–35.

[63] Civan, M. M. and Macknight, A. D. C. [2004], 'The ins and outs of aqueous humour secretion', Experimental Eye Research **78**(3), 625–631.

[64] Claesson-Welsh, L. [2003], 'Signal transduction by vascular endothelial growth factor receptors', Biochem Soc Trans **31**(Pt 1), 20–4.

[65] Clark, A. F. and Wordinger, R. J. [2009], 'The role of steroids in outflow resistance', Exp Eye Res **88**(4), 752–9.

[66] Cone, F. E., Steinhart, M. R., Oglesby, E. N., Kalesnykas, G., Pease, M. E. and Quigley, H. A. [2012], 'The effects of anesthesia, mouse strain and age on intraocular pressure and an improved murine model of experimental glaucoma', Exp Eye Res **99**, 27–35.

[67] Connolly, D. T., Heuvelman, D. M., Nelson, R., Olander, J. V., Eppley, B. L., Delfino, J. J., Siegel, N. R., Leimgruber, R. M. and Feder, J. [1989], 'Tumor vascular permeability factor stimulates endothelial cell growth and angiogenesis', J Clin Invest **84**(5), 1470–8.

[68] Coon, B. G., Baeyens, N., Han, J., Budatha, M., Ross, T. D., Fang, J. S., Yun, S., Thomas, J. L. and Schwartz, M. A. [2015], 'Intramembrane binding of ve-cadherin to vegfr2 and vegfr3 assembles the endothelial mechanosensory complex', J Cell Biol **208**(7), 975–86.

[69] Costagliola, C., Daniele, A., dell'Omo, R., Romano, M. R., Aceto, F., Agnifili, L., Semeraro, F. and Porcellini, A. [2013], 'Aqueous humor levels of vascular endothelial growth factor and adiponectin in patients with type 2 diabetes before and after intravitreal bevacizumab injection', Exp Eye Res **110**, 50–4.

[70] Crawley, L., Zamir, S. M., Cordeiro, M. F. and Guo, L. [2012], 'Clinical options for the reduction of elevated intraocular pressure', Ophthalmol Eye Dis **4**, 43–64.

[71] Crowston, J. G., Aihara, M., Lindsey, J. D. and Weinreb, R. N. [2004], 'Effect of latanoprost on outflow facility in the mouse', Invest Ophthalmol Vis Sci **45**(7), 2240–5.

[72] Dalvin, L. A. and Fautsch, M. P. [2015], 'Analysis of circadian rhythm gene expression with reference to diurnal pattern of intraocular pressure in mice', Invest Ophthalmol Vis Sci **56**(4), 2657–63.

[73] Danias, J., Kontiola, A. I., Filippopoulos, T. and Mittag, T. [2003], 'Method for the noninvasive measurement of intraocular pressure in mice', Invest Ophthalmol Vis Sci **44**(3), 1138–41.

[74] de Kater, A. W., Melamed, S. and Epstein, D. L. [1989], 'Patterns of aqueous humor outflow in glaucomatous and nonglaucomatous human eyes. a tracer study using cationized ferritin', Arch Ophthalmol **107**(4), 572–6.

[75] Dejana, E., Orsenigo, F. and Lampugnani, M. G. [2008], 'The role of adherens junctions and ve-cadherin in the control of vascular permeability', J Cell Sci **121**(Pt 13), 2115–22.

[76] Desire, L., Bourdin, J., Loiseau, N., Peillon, H., Picard, V., De Oliveira, C., Bachelot, F., Leblond, B., Taverne, T., Beausoleil, E., Lacombe, S., Drouin, D. and Schweighoffer, F. [2005], 'Rac1 inhibition targets amyloid precursor protein processing by gamma-secretase and decreases abeta production in vitro and in vivo', J Biol Chem **280**(45), 37516–25.

[77] Downs, J. C., Burgoyne, C. F., Seigfreid, W. P., Reynaud, J. F., Strouthidis, N. G. and Sallee, V. [2011], '24-hour iop telemetry in the nonhuman primate: implant system performance and initial characterization of iop at multiple timescales', Invest Ophthalmol Vis Sci **52**(10), 7365–75.

[78] Dudek, S. M., Jacobson, J. R., Chiang, E. T., Birukov, K. G., Wang, P., Zhan, X. and Garcia, J. G. [2004], 'Pulmonary endothelial cell barrier enhancement by sphingosine 1-phosphate: roles for cortactin and myosin light chain kinase', J Biol Chem **279**(23), 24692–700.

[79] Duncalf, D. [1975], 'Anesthesia and intraocular pressure', Bull N Y Acad Med **51**(3), 374–81.

[80] Duran, W. N., Breslin, J. W. and Sanchez, F. A. [2010], 'The no cascade, enos location, and microvascular permeability', Cardiovasc Res **87**(2), 254–61.

[81] Ebos, J. M., Bocci, G., Man, S., Thorpe, P. E., Hicklin, D. J., Zhou, D., Jia, X. and Kerbel, R. S. [2004], 'A naturally occurring soluble form of vascular endothelial growth factor receptor 2 detected in mouse and human plasma', Mol Cancer Res **2**(6), 315–26.

[82] Eliceiri, B. P., Paul, R., Schwartzberg, P. L., Hood, J. D., Leng, J. and Cheresh, D. A. [1999], 'Selective requirement for src kinases during vegf-induced angiogenesis and vascular permeability', Mol Cell **4**(6), 915–24.

[83] Ellis, D. Z., Sharif, N. A. and Dismuke, W. M. [2010], 'Endogenous regulation of human schlemm's canal cell volume by nitric oxide signaling', Invest Ophthalmol Vis Sci **51**(11), 5817–24.

[84] Epstein, D. L. and Rohen, J. W. [1991], 'Morphology of the trabecular meshwork and inner-wall endothelium after cationized ferritin perfusion in the monkey eye', Invest Ophthalmol Vis Sci **32**(1), 160–71.

[85] Epstein, D. L., Rowlette, L. L. and Roberts, B. C. [1999], 'Acto-myosin drug effects and aqueous outflow function', Invest Ophthalmol Vis Sci **40**(1), 74–81.

[86] Ergorul, C., Ray, A., Huang, W., Darland, D., Luo, Z. K. and Grosskreutz, C. L. [2008], 'Levels of vascular endothelial growth factor-a165b (vegf-a165b) are elevated in experimental glaucoma', Mol Vis **14**, 1517–24.

[87] Erickson-Lamy, K., Schroeder, A. M., Bassett-Chu, S. and Epstein, D. L. [1990], 'Absence of time-dependent facility increase ("washout") in the perfused enucleated human eye', Invest Ophthalmol Vis Sci **31**(11), 2384–8.

[88] Eriksson, A., Cao, R., Roy, J., Tritsaris, K., Wahlestedt, C., Dissing, S., Thyberg, J. and Cao, Y. [2003], 'Small gtp-binding protein rac is an essential mediator of vascular endothelial growth factor-induced endothelial fenestrations and vascular permeability', Circulation **107**(11), 1532–8.

[89] Eriksson, A. and Svedbergh, B. [1980], 'Transcellular aqueous humor outflow: a theoretical and experimental study', Albrecht Von Graefes Arch Klin Exp Ophthalmol **212**(3-4), 187–97.

[90] Esser, S., Wolburg, K., Wolburg, H., Breier, G., Kurzchalia, T. and Risau, W. [1998], 'Vascular endothelial growth factor induces endothelial fenestrations in vitro', J Cell Biol **140**(4), 947–59.

[91] Ethier, C. R., Coloma, F. M., Sit, A. J. and Johnson, M. [1998], 'Two pore types in the inner-wall endothelium of schlemm's canal', Invest Ophthalmol Vis Sci **39**(11), 2041–2048.

[92] Ethier, C. R., Johnson, M. and Ruberti, J. [2004], 'Ocular biomechanics and biotransport', Annu Rev Biomed Eng **6**, 249–73.

[93] Ethier, C. R., Read, A. T. and Chan, D. [2004], 'Biomechanics of schlemm's canal endothelial cells: Influence on f-actin architecture', Biophysical Journal **87**(4), 2828–2837.

[94] Ethier, C. R., Read, A. T. and Chan, D. W. [2006], 'Effects of latrunculin-b on outflow facility and trabecular meshwork structure in human eyes', Invest Ophthalmol Vis Sci **47**(5), 1991–8.

[95] Ethier, R. C. [2002], 'The inner wall of schlemm's canal', Experimental Eye Research **74**(2), 161–172.

[96] Farquhar, M. G. and Palade, G. E. [1963], 'Junctional complexes in various epithelia', J Cell Biol **17**, 375–412.

[97] Feng, Y., Venema, V. J., Venema, R. C., Tsai, N., Behzadian, M. A. and Caldwell, R. B. [1999], 'Vegf-induced permeability increase is mediated by caveolae', Invest Ophthalmol Vis Sci **40**(1), 157–67.

[98] Ferrara, N. [2001], 'Role of vascular endothelial growth factor in regulation of physiological angiogenesis', Am J Physiol Cell Physiol **280**(6), C1358–66.

[99] Ferrara, N., Gerber, H. P. and LeCouter, J. [2003], 'The biology of vegf and its receptors', Nat Med **9**(6), 669–76.

[100] Fong, T. A., Shawver, L. K., Sun, L., Tang, C., App, H., Powell, T. J., Kim, Y. H., Schreck, R., Wang, X., Risau, W., Ullrich, A., Hirth, K. P. and McMahon, G. [1999], 'Su5416 is a potent and selective inhibitor of the vascular endothelial growth factor receptor (flk-1/kdr) that inhibits tyrosine kinase catalysis, tumor vascularization, and growth of multiple tumor types', Cancer Res **59**(1), 99–106.

[101] Ford, K. M., Saint-Geniez, M., Walshe, T. E. and D'Amore, P. A. [2012], 'Expression and role of vegf-a in the ciliary body', Invest Ophthalmol Vis Sci **53**(12), 7520–7.

[102] Ford, K. M., Saint-Geniez, M., Walshe, T., Zahr, A. and D'Amore, P. A. [2011], 'Expression and role of vegf in the adult retinal pigment epithelium', Invest Ophthalmol Vis Sci **52**(13), 9478–87.

[103] Fu, B. M. and Shen, S. [2004], 'Acute vegf effect on solute permeability of mammalian microvessels in vivo', Microvasc Res **68**(1), 51–62.

[104] Fuchshofer, R., Stephan, D. A., Russell, P. and Tamm, E. R. [2009], 'Gene expression profiling of tgfbeta2- and/or bmp7-treated trabecular meshwork cells: Identification of smad7 as a critical inhibitor of tgf-beta2 signaling', Exp Eye Res **88**(6), 1020–32.

[105] Fukumura, D., Gohongi, T., Kadambi, A., Izumi, Y., Ang, J., Yun, C. O., Buerk, D. G., Huang, P. L. and Jain, R. K. [2001], 'Predominant role of endothelial nitric oxide synthase in vascular endothelial growth factor-induced angiogenesis and vascular permeability', Proc Natl Acad Sci U S A **98**(5), 2604–9.

[106] Furuse, M. [2010], 'Molecular basis of the core structure of tight junctions', Cold Spring Harb Perspect Biol **2**(1), a002907.

[107] Galvagni, F., Pennacchini, S., Salameh, A., Rocchigiani, M., Neri, F., Orlandini, M., Petraglia, F., Gotta, S., Sardone, G. L., Matteucci, G., Terstappen, G. C. and Oliviero, S. [2010], 'Endothelial cell adhesion to the extracellular matrix induces c-src-dependent vegfr-3 phosphorylation without the activation of the receptor intrinsic kinase activity', Circ Res **106**(12), 1839–48.

[108] Garcia, J. G., Liu, F., Verin, A. D., Birukova, A., Dechert, M. A., Gerthoffer, W. T., Bamberg, J. R. and English, D. [2001], 'Sphingosine 1-phosphate promotes endothelial cell barrier integrity by edg-dependent cytoskeletal rearrangement', J Clin Invest **108**(5), 689–701.

[109] Gargiulo, S., Greco, A., Gramanzini, M., Esposito, S., Affuso, A., Brunetti, A. and Vesce, G. [2012], 'Mice anesthesia, analgesia, and care, part i: Anesthetic considerations in preclinical research', ILAR Journal **53**(1), E55–E69.

[110] Gavard, J. and Gutkind, J. S. [2006], 'Vegf controls endothelial-cell permeability by promoting the beta-arrestin-dependent endocytosis of ve-cadherin', Nat Cell Biol **8**(11), 1223–34.

[111] Gharagozloo, N. Z., Relf, S. J. and Brubaker, R. F. [1988], 'Aqueous flow is reduced by the alpha-adrenergic agonist, apraclonidine hydrochloride (alo-2145)', Ophthalmology **95**(9), 1217–1220.

[112] Goel, M., Picciani, R. G., Lee, R. K. and Bhattacharya, S. K. [2010], 'Aqueous humor dynamics: a review', Open Ophthalmol J **4**, 52–9.

[113] Gogat, K., Le Gat, L., Van Den Berghe, L., Marchant, D., Kobetz, A., Gadin, S., Gasser, B., Quere, I., Abitbol, M. and Menasche, M. [2004], 'Vegf and kdr gene expression during human embryonic and fetal eye development', Invest Ophthalmol Vis Sci **45**(1), 7–14.

[114] Gong, H., Ruberti, J., Overby, D., Johnson, M. and Freddo, T. F. [2002], 'A new view of the human trabecular meshwork using quick-freeze, deep-etch electron microscopy', Exp Eye Res **75**(3), 347–58.

[115] Gong, H., Tripathi, R. C. and Tripathi, B. J. [1996], 'Morphology of the aqueous outflow pathway', Microsc Res Tech **33**(4), 336–67.

[116] Good, T. J., Kimura, A. E., Mandava, N. and Kahook, M. Y. [2011], 'Sustained elevation of intraocular pressure after intravitreal injections of anti-vegf agents', Br J Ophthalmol **95**(8), 1111–4.

[117] Grant, W. M. [1951], 'Clinical measurements of aqueous outflow', Am J Ophthalmol **34**(11), 1603–5.

[118] Grant, W. M. [1963], 'Experimental aqueous perfusion in enucleated human eyes', Arch Ophthalmol **69**, 783–801.

[119] Hahnenberger, R. W. [1976], 'Influence of various anesthetic drugs on the intraocular pressure of cats', Albrecht Von Graefes Arch Klin Exp Ophthalmol **199**(2), 179–86.

[120] Hamanaka, T. and Bill, A. [1987], 'Morphological and functional effects of na2edta on the outflow routes for aqueous humor in monkeys', Exp Eye Res **44**(2), 171–90.

[121] He, H., Venema, V. J., Gu, X., Venema, R. C., Marrero, M. B. and Caldwell, R. B. [1999], 'Vascular endothelial growth factor signals endothelial cell production of nitric oxide and prostacyclin through flk-1/kdr activation of c-src', J Biol Chem **274**(35), 25130–5.

[122] Heier, J. S., Brown, D. M., Chong, V., Korobelnik, J. F., Kaiser, P. K., Nguyen, Q. D., Kirchhof, B., Ho, A., Ogura, Y., Yancopoulos, G. D., Stahl, N., Vitti, R., Berliner, A. J., Soo, Y., Anderesi, M., Groetzbach, G., Sommerauer, B., Sandbrink, R., Simader, C., Schmidt-Erfurth, U., View and Groups, V. S. [2012], 'Intravitreal aflibercept (vegf trap-eye) in wet age-related macular degeneration', Ophthalmology **119**(12), 2537–48.

[123] Heimark, R. L., Kaochar, S. and Stamer, W. D. [2002], 'Human schlemm's canal cells express the endothelial adherens proteins, ve-cadherin and pecam-1', Curr Eye Res **25**(5), 299–308.

[124] Herrnberger, L., Ebner, K., Junglas, B. and Tamm, E. R. [2012], 'The role of plasmalemmal vesicle-associated protein (plvap) in endothelial cells of schlemm's canal and ocular capillaries', Experimental Eye Research **105**, 27–33.

[125] Herrnberger, L., Hennig, R., Kremer, W., Hellerbrand, C., Goepferich, A., Kalbitzer, H. R. and Tamm, E. R. [2014], 'Formation of fenestrae in murine liver sinusoids depends on plasmalemma vesicle-associated protein and is required for lipoprotein passage', PLoS One **9**(12), e115005.

[126] Herrnberger, L., Seitz, R., Kuespert, S., Bösl, M. R., Fuchshofer, R. and Tamm, E. R. [2012], 'Lack of endothelial diaphragms in fenestrae and caveolae of mutant plvap-deficient mice', Histochem Cell Biol **138**(5), 709–24.

[127] Heyne, G. W., Kiland, J. A., Kaufman, P. L. and Gabelt, B. T. [2013], 'Effect of nitric oxide on anterior segment physiology in monkeys', Invest Ophthalmol Vis Sci **54**(7), 5103–10.

[128] Hicklin, D. J. and Ellis, L. M. [2005], 'Role of the vascular endothelial growth factor pathway in tumor growth and angiogenesis', J Clin Oncol **23**(5), 1011–27.

[129] Hillman, N. J., Whittles, C. E., Pocock, T. M., Williams, B. and Bates, D. O. [2001], 'Differential effects of vascular endothelial growth factor-c and placental growth factor-1 on the hydraulic conductivity of frog mesenteric capillaries', J Vasc Res **38**(2), 176–86.

[130] Hippenstiel, S., Krull, M., Ikemann, A., Risau, W., Clauss, M. and Suttorp, N. [1998], 'Vegf induces hyperpermeability by a direct action on endothelial cells', Am J Physiol **274**(5 Pt 1), L678–84.

[131] Hnasko, R., Carter, J. M., Medina, F., Frank, P. G. and Lisanti, M. P. [2006], 'Pv-1 labels trans-cellular openings in mouse endothelial cells and is negatively regulated by vegf', Cell Cycle **5**(17), 2021–2028.

[132] Hoang, Q. V., Mendonca, L. S., Della Torre, K. E., Jung, J. J., Tsuang, A. J. and Freund, K. B. [2012], 'Effect on intraocular pressure in patients receiving unilateral intravitreal anti-vascular endothelial growth factor injections', Ophthalmology **119**(2), 321–6.

[133] Hoang, Q. V., Tsuang, A. J., Gelman, R., Mendonca, L. S., Della Torre, K. E., Jung, J. J. and Freund, K. B. [2013], 'Clinical predictors of sustained intraocular pressure elevation due to intravitreal anti-vascular endothelial growth factor therapy', Retina-the Journal of Retinal and Vitreous Diseases **33**(1), 179–187.

[134] Hoeben, A., Landuyt, B., Highley, M. S., Wildiers, H., Van Oosterom, A. T. and De Bruijn, E. A. [2004], 'Vascular endothelial growth factor and angiogenesis', Pharmacol Rev **56**(4), 549–80.

[135] Hofman, P., Blaauwgeers, H. G., Tolentino, M. J., Adamis, A. P., Nunes Cardozo, B. J., Vrensen, G. F. and Schlingemann, R. O. [2000], 'Vegf-a induced hyperpermeability of blood-retinal barrier endothelium in vivo is predominantly associated with pinocytotic vesicular transport and not with formation of fenestrations. vascular endothelial growth factor-a', Curr Eye Res **21**(2), 637–45.

[136] Holmberg, A. [1959], 'The fine structure of the inner wall of schlemm's canal', A.M.A. Archives of Ophthalmology **62**(6), 956–958.

[137] Hornig, C., Barleon, B., Ahmad, S., Vuorela, P., Ahmed, A. and Weich, H. A. [2000], 'Release and complex formation of soluble vegfr-1 from endothelial cells and biological fluids', Lab Invest **80**(4), 443–54.

[138] Hsu, M. Y., Yang, C. Y., Hsu, W. H., Lin, K. H., Wang, C. Y., Shen, Y. C., Chen, Y. C., Chau, S. F., Tsai, H. Y. and Cheng, C. M. [2014], 'Monitoring the vegf level in aqueous humor of patients with ophthalmologically relevant diseases via ultrahigh sensitive paper-based elisa', Biomaterials **35**(12), 3729–35.

[139] Hu, D. N., Ritch, R., Liebmann, J., Liu, Y., Cheng, B. and Hu, M. S. [2002], 'Vascular endothelial growth factor is increased in aqueous humor of glaucomatous eyes', J Glaucoma **11**(5), 406–10.

[140] Ikenouchi, J., Furuse, M., Furuse, K., Sasaki, H., Tsukita, S. and Tsukita, S. [2005], 'Tricellulin constitutes a novel barrier at tricellular contacts of epithelial cells', J Cell Biol **171**(6), 939–45.

[141] Inomata, H., Smelser, G. K. and Bill, A. [1972], 'Aqueous humor pathways through trabecular meshwork and into schlemms canal in cynomolgus monkey (macaca irus)', American Journal of Ophthalmology **73**(5), 760–790.

[142] Ioannidou, S., Deinhardt, K., Miotla, J., Bradley, J., Cheung, E., Samuelsson, S., Ng, Y. S. and Shima, D. T. [2006], 'An in vitro assay reveals a role for the diaphragm protein pv-1 in endothelial fenestra morphogenesis', Proc Natl Acad Sci U S A **103**(45), 16770–5.

[143] Itokawa, T., Nokihara, H., Nishioka, Y., Sone, S., Iwamoto, Y., Yamada, Y., Cherrington, J., McMahon, G., Shibuya, M., Kuwano, M. and Ono, M. [2002], 'Antiangiogenic effect by su5416 is partly attributable to inhibition of flt-1 receptor signaling', Mol Cancer Ther **1**(5), 295–302.

[144] Jia, L., Cepurna, W. O., Johnson, E. C. and Morrison, J. C. [2000], 'Effect of general anesthetics on iop in rats with experimental aqueous outflow obstruction', Invest Ophthalmol Vis Sci **41**(11), 3415–9.

[145] Jin, Y., Wilson, S., Elko, E. E. and Yorio, T. [1991], 'Ocular hypotensive effects of medetomidine and its analogs', J Ocul Pharmacol **7**(4), 285–96.

[146] Johnson, D. H. [2002], 'Glaucoma surgery and aqueous outflow - how does nonpenetrating glaucoma surgery work?', Archives of Ophthalmology **120**(1), 67–70.

[147] Johnson, D. H., Bradley, J. M. and Acott, T. S. [1990], 'The effect of dexamethasone on glycosaminoglycans of human trabecular meshwork in perfusion organ culture', Invest Ophthalmol Vis Sci **31**(12), 2568–71.

[148] Johnson, M. [2006], 'What controls aqueous humour outflow resistance?', Experimental Eye Research **82**(4), 545–557.

[149] Johnson, M. C. and Kamm, R. D. [1983], 'The role of schlemm's canal in aqueous outflow from the human eye', Invest Ophthalmol Vis Sci **24**(3), 320–5.

[150] Johnson, M., Chan, D., Read, A. T., Christensen, C., Sit, A. and Ethier, C. R. [2002], 'The pore density in the inner wall endothelium of schlemm's canal of glaucomatous eyes', Invest Ophthalmol Vis Sci **43**(9), 2950–2955.

[151] Johnson, M., Chan, D., Reed, A. T., Christensen, C., Sit, A. and Ethier, C. R. [2002], 'Glaucomatous eyes have a reduced pore density in the inner wall endothelium of schlemm's canal', Invest Ophthalmol Vis Sci **43**, U1137–U1137.

[152] Johnson, M. and Erickson, K. [2000], Mechanisms and routes of aqueous humor drainage, Vol. 4, W.B Saunders Company, Saunders, Philadelphia, chapter Chapter 193B, Glaucoma, pp. 2577–2595.

[153] Johnson, M., Shapiro, A., Ethier, C. R. and Kamm, R. D. [1992], 'Modulation of outflow resistance by the pores of the inner wall endothelium', Invest Ophthalmol Vis Sci **33**(5), 1670–5.

[154] Johnson, T. V., Fan, S., Camras, C. B. and Toris, C. B. [2008], 'Aqueous humor dynamics in exfoliation syndrome', Arch Ophthalmol **126**(7), 914–20.

[155] Kahook, M. Y. and Ammar, D. A. [2010], 'In vitro effects of antivascular endothelial growth factors on cultured human trabecular meshwork cells', J Glaucoma **19**(7), 437–41.

[156] Kamba, T., Tam, B. Y., Hashizume, H., Haskell, A., Sennino, B., Mancuso, M. R., Norberg, S. M., O'Brien, S. M., Davis, R. B., Gowen, L. C., Anderson, K. D., Thurston, G., Joho, S., Springer, M. L., Kuo, C. J. and McDonald, D. M. [2006], 'Vegf-dependent plasticity of fenestrated capillaries in the normal adult microvasculature', Am J Physiol Heart Circ Physiol **290**(2), H560–76.

[157] Kanehisa, M., Goto, S., Sato, Y., Kawashima, M., Furumichi, M. and Tanabe, M. [2014], 'Data, information, knowledge and principle: back to metabolism in kegg', Nucleic Acids Res **42**(Database issue), D199–205.

[158] Karnezis, T., Shayan, R., Caesar, C., Roufail, S., Harris, N. C., Ardipradja, K., Zhang, Y. F., Williams, S. P., Farnsworth, R. H., Chai, M. G., Rupasinghe, T. W., Tull, D. L., Baldwin, M. E., Sloan, E. K., Fox, S. B., Achen, M. G. and Stacker, S. A. [2012], 'Vegf-d promotes tumor metastasis by regulating prostaglandins produced by the collecting lymphatic endothelium', Cancer Cell **21**(2), 181–95.

[159] Karpinich, N. O. and Caron, K. M. [2014], 'Schlemm's canal: more than meets the eye, lymphatics in disguise', J Clin Invest pp. 1–3.

[160] Kaufman, P. L., Alm, A. and Adler, F. H. P. o. t. e. [2003], Adler's physiology of the eye : clinical application, 10th ed. / edited by paul l. kaufman, albert alm. edn, Mosby, St. Louis ; London. GBA419155 bnb 2783 Previous ed.: 1992. Includes bibliographical references and index.

[161] Kaufman, P. L., True-Gabelt, B. and Erickson-Lamy, K. A. [1988], 'Time-dependence of perfusion outflow facility in the cynomolgus monkey', Curr Eye Res **7**(7), 721–6.

[162] Keck, P. J., Hauser, S. D., Krivi, G., Sanzo, K., Warren, T., Feder, J. and Connolly, D. T. [1989], 'Vascular permeability factor, an endothelial cell mitogen related to pdgf', Science **246**(4935), 1309–12.

[163] Kevil, C. G., Payne, D. K., Mire, E. and Alexander, J. S. [1998], 'Vascular permeability factor/vascular endothelial cell growth factor-mediated permeability occurs through disorganization of endothelial junctional proteins', J Biol Chem **273**(24), 15099–103.

[164] Khurana, A. and Khurana, I. [1998], Anatomy and Physiology of Eye, second edn, CBS Publishers and Distributors Pvt. Ltd., Delhi, India.

[165] Kim, J. E., Mantravadi, A. V., Hur, E. Y. and Covert, D. J. [2008], 'Short-term intraocular pressure changes immediately after intravitreal injections of anti-vascular endothelial growth factor agents', Am J Ophthalmol **146**(6), 930–4 e1.

[166] Kizhatil, K., Ryan, M., Marchant, J. K., Henrich, S. and John, S. W. [2014], 'Schlemm's canal is a unique vessel with a combination of blood vascular and lymphatic phenotypes that forms by a novel developmental process', PLoS Biol **12**(7), e1001912.

[167] Klaassen, I., Hughes, J. M., Vogels, I. M., Schalkwijk, C. G., Van Noorden, C. J. and Schlingemann, R. O. [2009], 'Altered expression of genes related to blood-retina barrier disruption in streptozotocin-induced diabetes', Exp Eye Res **89**(1), 4–15.

[168] Ko, M. K. and Tan, J. C. [2013], 'Contractile markers distinguish structures of the mouse aqueous drainage tract', Mol Vis **19**, 2561–70.

[169] Koch, S. and Claesson-Welsh, L. [2012], 'Signal transduction by vascular endothelial growth factor receptors', Cold Spring Harb Perspect Med **2**(7), a006502.

[170] Koehn, D., Meyer, K. J., Syed, N. A. and Anderson, M. G. [2015], 'Ketamine/xylazine-induced corneal damage in mice', PLoS One **10**(7), e0132804.

[171] Kubo, K., Shimizu, T., Ohyama, S., Murooka, H., Iwai, A., Nakamura, K., Hasegawa, K., Kobayashi, Y., Takahashi, N., Takahashi, K., Kato, S., Izawa, T. and Isoe, T. [2005], 'Novel potent orally active selective vegfr-2 tyrosine kinase inhibitors: synthesis, structure-activity relationships, and antitumor activities of n-phenyl-n'-4-(4-quinolyloxy)phenylureas', J Med Chem **48**(5), 1359–66.

[172] Kwon, Y. H., Fingert, J. H., Kuehn, M. H. and Alward, W. L. [2009], 'Primary open-angle glaucoma', N Engl J Med **360**(11), 1113–24.

[173] Lakshminarayanan, S., Antonetti, D. A., Gardner, T. W. and Tarbell, J. M. [2000], 'Effect of vegf on retinal microvascular endothelial hydraulic conductivity: the role of no', Invest Ophthalmol Vis Sci **41**(13), 4256–61.

[174] Lei, Y., Overby, D. R., Boussommier-Calleja, A., Stamer, W. D. and Ethier, C. R. [2011], 'Outflow physiology of the mouse eye: pressure dependence and washout', Invest Ophthalmol Vis Sci **52**(3), 1865–71.

[175] Leung, D. W., Cachianes, G., Kuang, W. J., Goeddel, D. V. and Ferrara, N. [1989], 'Vascular endothelial growth factor is a secreted angiogenic mitogen', Science **246**(4935), 1306–9.

[176] Li, Y., Ito, N., Suzuki, T., Stechschulte, D. J. and Dileepan, K. N. [1995], 'Dexamethasone inhibits nitric oxide-mediated cytotoxicity via effects on both macrophages and target cells', Immunopharmacology **30**(2), 177–86.

[177] Liu, L., Ammar, D. A., Ross, L. A., Mandava, N., Kahook, M. Y. and Carpenter, J. F. [2011], 'Silicone oil microdroplets and protein aggregates in repackaged bevacizumab and ranibizumab: effects of long-term storage and product mishandling', Invest Ophthalmol Vis Sci **52**(2), 1023–34.

[178] Llobet, A., Gasull, X. and Gual, A. [2003], 'Understanding trabecular meshwork physiology: A key to the control of intraocular pressure?', News in Physiological Sciences **18**, 205–209.

[179] Loukianou, E., Brouzas, D. and Apostolopoulos, M. [2011], 'Sustained ocular hypertension following intravitreal injections of 0.5 mg/0.05 ml ranibizumab', Int Ophthalmol **31**(3), 211–3.

[180] Lu, Z., Overby, D. R., Scott, P. A., Freddo, T. F. and Gong, H. [2008], 'The mechanism of increasing outflow facility by rho-kinase inhibition with y-27632 in bovine eyes', Exp Eye Res **86**(2), 271–81.

[181] Lutjen-Drecoll, E., Futa, R. and Rohen, J. W. [1981], 'Ultrahistochemical studies on tangential sections of the trabecular meshwork in normal and glaucomatous eyes', Invest Ophthalmol Vis Sci **21**(4), 563–73.

[182] Maeda, A., Tsujiya, S., Higashide, T., Toida, K., Todo, T., Ueyama, T., Okamura, H. and Sugiyama, K. [2006], 'Circadian intraocular pressure rhythm is generated by clock genes', Invest Ophthalmol Vis Sci **47**(9), 4050–2.

[183] Mäepea, O. and Bill, A. [1992], 'Pressures in the juxtacanalicular tissue and schlemm's canal in monkeys', Exp Eye Res **54**(6), 879–83.

[184] Mathalone, N., Arodi-Golan, A., Sar, S., Wolfson, Y., Shalem, M., Lavi, I. and Geyer, O. [2012], 'Sustained elevation of intraocular pressure after intravitreal injections of bevacizumab in eyes with neovascular age-related macular degeneration', Graefes Arch Clin Exp Ophthalmol **250**(10), 1435–40.

[185] Matsumoto, T. and Claesson-Welsh, L. [2001], 'Vegf receptor signal transduction', Sci STKE **2001**(112), re21.

[186] McAuliffe-Curtin, D. and Buckley, C. [1989], 'Review of alpha adrenoceptor function in the eye', Eye (Lond) **3 (Pt 4)**, 472–6.

[187] McCarty, G. R. and Schwartz, B. [1991], 'Increased plasma noncortisol glucocorticoid activity in open-angle glaucoma', Invest Ophthalmol Vis Sci **32**(5), 1600–8.

[188] McEwen, W. K. [1958], 'Application of poiseuille's law to aqueous outflow', AMA Arch Ophthalmol **60**(2), 290–4.

[189] McKinnon, S. J., Schlamp, C. L. and Nickells, R. W. [2009], 'Mouse models of retinal ganglion cell death and glaucoma', Exp Eye Res **88**(4), 816–24.

[190] Michel, C. C. and Neal, C. R. [1999], 'Openings through endothelial cells associated with increased microvascular permeability', Microcirculation **6**(1), 45–54.

[191] Millar, J. C., Clark, A. F. and Pang, I. H. [2011], 'Assessment of aqueous humor dynamics in the mouse by a novel method of constant-flow infusion', Invest Ophthalmol Vis Sci **52**(2), 685–94.

[192] Millard, L. H., Woodward, D. F. and Stamer, W. D. [2011], 'The role of the prostaglandin ep4 receptor in the regulation of human outflow facility', Invest Ophthalmol Vis Sci **52**(6), 3506–13.

[193] Miller, J. W., Le Couter, J., Strauss, E. C. and Ferrara, N. [2013], 'Vascular endothelial growth factor a in intraocular vascular disease', Ophthalmology **120**(1), 106–14.

[194] Miller-Kasprzak, E. and Jagodzinski, P. P. [2008], '5-aza-2'-deoxycytidine increases the expression of anti-angiogenic vascular endothelial growth factor 189b variant in human lung microvascular endothelial cells', Biomed Pharmacother **62**(3), 158–63.

[195] Mirakhur, R. K., Elliott, P., Shepherd, W. F. and McGalliard, J. N. [1990], 'Comparison of the effects of isoflurane and halothane on intraocular pressure', Acta Anaesthesiol Scand **34**(4), 282–5.

[196] Moazed, D. [2009], 'Small rnas in transcriptional gene silencing and genome defence', Nature **457**(7228), 413–20.

[197] Monaghan-Benson, E. and Burridge, K. [2009], 'The regulation of vascular endothelial growth factor-induced microvascular permeability requires rac and reactive oxygen species', J Biol Chem **284**(38), 25602–11.

[198] Moseley, H., Grierson, I. and Lee, W. R. [1983], 'Mathematical modelling of aqueous humour outflow from the eye through the pores in the lining endothelium of schlemm's canal', Clin Phys Physiol Meas **4**(1), 47–63.

[199] Moses, R. A. [1977], 'The effect of intraocular pressure on resistance to outflow', Surv Ophthalmol **22**(2), 88–100.

[200] National-Center-for Biotechnology-Information, N. [2015], 'Pubchem bioassay database', https://pubchem.ncbi.nlm.nih.gov/compound/3763section=Top .

[201] Nilsson, S. F. [1997], 'The uveoscleral outflow routes', Eye (Lond) **11 (Pt 2)**, 149–54.

[202] Nonobe, N. I., Kachi, S., Kondo, M., Takai, Y., Takemoto, K., Nakayama, A., Hayakawa, M. and Terasaki, H. [2009], 'Concentration of vascular endothelial growth factor in aqueous humor of eyes with advanced retinopathy of prematurity before and after intravitreal injection of bevacizumab', Retina **29**(5), 579–85.

[203] of Age-related Macular Degeneration Treatments Trials Research Group, C., Martin, D. F., Maguire, M. G., Fine, S. L., Ying, G. S., Jaffe, G. J., Grunwald, J. E., Toth, C., Redford, M. and Ferris, F. L., r. [2012], 'Ranibizumab and bevacizumab for treatment of neovascular age-related macular degeneration: two-year results', Ophthalmology **119**(7), 1388–98.

[204] Oh, H., Takagi, H., Otani, A., Koyama, S., Kemmochi, S., Uemura, A. and Honda, Y. [2002], 'Selective induction of neuropilin-1 by vascular endothelial growth factor (vegf): a mechanism contributing to vegf-induced angiogenesis', Proc Natl Acad Sci U S A **99**(1), 383–8.

[205] Olsson, A. K., Dimberg, A., Kreuger, J. and Claesson-Welsh, L. [2006], 'Vegf receptor signalling - in control of vascular function', Nat Rev Mol Cell Biol **7**(5), 359–71.

[206] Overby, D. R., Bertrand, J., Schicht, M., Paulsen, F., Stamer, W. D. and Lutjen-Drecoll, E. [2014], 'The structure of the trabecular meshwork, its connections to the ciliary muscle, and the effect of pilocarpine on outflow facility in mice', Invest Ophthalmol Vis Sci **55**(6), 3727–36.

[207] Overby, D. R., Bertrand, J., Tektas, O. Y., Boussommier-Calleja, A., Schicht, M., Ethier, C. R., Woodward, D. F., Stamer, W. D. and Lutjen-Drecoll, E. [2014], 'Ultrastructural changes associated with dexamethasone-induced ocular hypertension in mice', Invest Ophthalmol Vis Sci **55**(8), 4922–33.

[208] Overby, D. R. and Clark, A. F. [2015], 'Animal models of glucocorticoid-induced glaucoma', Exp Eye Res **141**, 15–22.

[209] Overby, D. R., Gong, H., Qiu, G., Freddo, T. F. and Johnson, M. [2002], 'The mechanism of increasing outflow facility during washout in the bovine eye', Invest Ophthalmol Vis Sci **43**(11), 3455–64.

[210] Overby, D. R., Stamer, W. D. and Johnson, M. [2009], 'The changing paradigm of outflow resistance generation: towards synergistic models of the jct and inner wall endothelium', Exp Eye Res **88**(4), 656–70.

[211] Overby, D. R., Zhou, E. H., Vargas-Pinto, R., Pedrigi, R. M., Fuchshofer, R., Braakman, S. T., Gupta, R., Perkumas, K. M., Sherwood, J. M., Vahabikashi, A., Dang, Q., Kim, J. H., Ethier, C. R., Stamer, W. D., Fredberg, J. J. and Johnson, M. [2014], 'Altered mechanobiology of schlemm's canal endothelial cells in glaucoma', Proc Natl Acad Sci U S A **111**(38), 13876–81.

[212] Ozmen, A., Unek, G., Kipmen-Korgun, D., Cetinkaya, B., Avcil, Z. and Korgun, E. T. [2015], 'Glucocorticoid exposure altered angiogenic factor expression via akt/mtor pathway in rat placenta', Ann Anat **198**, 34–40.

[213] Park, D. Y., Lee, J., Park, I., Choi, D., Lee, S., Song, S., Hwang, Y., Hong, K. Y., Nakaoka, Y., Makinen, T., Kim, P., Alitalo, K., Hong, Y. K. and Koh, G. Y. [2014], 'Lymphatic regulator prox1 determines schlemm canal integrity and identity', J Clin Invest .

[214] Pattabiraman, P. P., Epstein, D. L. and Rao, P. V. [2013], 'Regulation of adherens junctions in trabecular meshwork cells by rac gtpase and their influence on intraocular pressure', J Ocul Biol **1**(1).

[215] Pederson, J. E. and Toris, C. B. [1987], 'Uveoscleral outflow: diffusion or flow?', Invest Ophthalmol Vis Sci **28**(6), 1022–4.

[216] Pedrigi, R. M., Simon, D., Reed, A., Stamer, W. D. and Overby, D. R. [2011], 'A model of giant vacuole dynamics in human schlemm's canal endothelial cells', Exp Eye Res **92**(1), 57–66.

[217] Peiris-Pages, M. [2012], 'The role of vegf 165b in pathophysiology', Cell Adh Migr **6**(6), 561–8.

[218] Penn, J. S., Madan, A., Caldwell, R. B., Bartoli, M., Caldwell, R. W. and Hartnett, M. E. [2008], 'Vascular endothelial growth factor in eye disease', Prog Retin Eye Res **27**(4), 331–71.

[219] Perkins, E. S. [2015], 'Human eye', Encyclopædia Britannica .

[220] Perkumas, K. M. and Stamer, W. D. [2012], 'Protein markers and differentiation in culture for schlemm's canal endothelial cells', Exp Eye Res **96**(1), 82–7.

[221] Perrin, R. M., Konopatskaya, O., Qiu, Y., Harper, S., Bates, D. O. and Churchill, A. J. [2005], 'Diabetic retinopathy is associated with a switch in splicing from anti- to pro-angiogenic isoforms of vascular endothelial growth factor', Diabetologia **48**(11), 2422–7.

[222] Persson, J. [2010], 'Wherefore ketamine?', Curr Opin Anaesthesiol **23**(4), 455–60.

[223] Peterson, J. A., Tian, B., Geiger, B. and Kaufman, P. L. [2000], 'Effect of latrunculin-b on outflow facility in monkeys', Exp Eye Res **70**(3), 307–13.

[224] Philipp, W., Speicher, L. and Humpel, C. [2000], 'Expression of vascular endothelial growth factor and its receptors in inflamed and vascularized human corneas', Invest Ophthalmol Vis Sci **41**(9), 2514–22.

[225] Pocock, T. M. and Bates, D. O. [2001], 'In vivo mechanisms of vascular endothelial growth factor-mediated increased hydraulic conductivity of rana capillaries', J Physiol **534**(Pt. 2), 479–88.

[226] Qiu, Y., Ferguson, J., Oltean, S., Neal, C. R., Kaura, A., Bevan, H., Wood, E., Sage, L. M., Lanati, S., Nowak, D. G., Salmon, A. H., Bates, D. and Harper, S. J. [2010], 'Overexpression of vegf165b in podocytes reduces glomerular permeability', J Am Soc Nephrol **21**(9), 1498–509.

[227] Quigley, H. A. [2011], 'Glaucoma', Lancet **377**(9774), 1367–77.

[228] Ramos, R. F., Hoying, J. B., Witte, M. H. and Daniel Stamer, W. [2007], 'Schlemm's canal endothelia, lymphatic, or blood vasculature?', J Glaucoma **16**(4), 391–405.

[229] Rao, P. V., Deng, P. F., Kumar, J. and Epstein, D. L. [2001], 'Modulation of aqueous humor outflow facility by the rho kinase-specific inhibitor y-27632', Invest Ophthalmol Vis Sci **42**(5), 1029–37.

[230] Rennel, E. S., Varey, A. H., Churchill, A. J., Wheatley, E. R., Stewart, L., Mather, S., Bates, D. O. and Harper, S. J. [2009], 'Vegf(121)b, a new member of the vegf(xxx)b family of vegf-a splice isoforms, inhibits neovascularisation and tumour growth in vivo', Br J Cancer **101**(7), 1183–93.

[231] Resnikoff, S., Pascolini, D., Etya'ale, D., Kocur, I., Pararajasegaram, R., Pokharel, G. P. and Mariotti, S. P. [2004], 'Global data on visual impairment in the year 2002', Bull World Health Organ **82**(11), 844–51.

[232] Rissanen, T. T., Markkanen, J. E., Gruchala, M., Heikura, T., Puranen, A., Kettunen, M. I., Kholova, I., Kauppinen, R. A., Achen, M. G., Stacker, S. A., Alitalo, K. and Yla-Herttuala, S. [2003], 'Vegf-d is the strongest angiogenic and lymphangiogenic effector among vegfs delivered into skeletal muscle via adenoviruses', Circ Res **92**(10), 1098–106.

[233] Roberts, W. G. and Palade, G. E. [1995], 'Increased microvascular permeability and endothelial fenestration induced by vascular endothelial growth factor', J Cell Sci **108 (Pt 6)**, 2369–79.

[234] Roberts, W. G. and Palade, G. E. [1997], 'Neovasculature induced by vascular endothelial growth factor is fenestrated', Cancer Research **57**(4), 765–772.

[235] Rogers, M. E., Navarro, I. D., Perkumas, K. M., Niere, S. M., Allingham, R. R., Crosson, C. E. and Stamer, W. D. [2013], 'Pigment epithelium-derived factor decreases outflow facility', Invest Ophthalmol Vis Sci **54**(10), 6655–61.

[236] Roh, M. I., Kim, H. S., Song, J. H., Lim, J. B., Koh, H. J. and Kwon, O. W. [2009], 'Concentration of cytokines in the aqueous humor of patients with naive, recurrent and regressed cnv associated with amd after bevacizumab treatment', Retina **29**(4), 523–9.

[237] Rohen, J. W., Futa, R. and Lutjendrecoll, E. [1981], 'The fine-structure of the cribriform meshwork in normal and glaucomatous eyes as seen in tangential sections', Invest Ophthalmol Vis Sci **21**(4), 574–585.

[238] Rosenfeld, P. J., Brown, D. M., Heier, J. S., Boyer, D. S., Kaiser, P. K., Chung, C. Y., Kim, R. Y. and Group, M. S. [2006], 'Ranibizumab for neovascular age-related macular degeneration', N Engl J Med **355**(14), 1419–31.

[239] Saint-Geniez, M., Kurihara, T., Sekiyama, E., Maldonado, A. E. and D'Amore, P. A. [2009], 'An essential role for rpe-derived soluble vegf in the maintenance of the choriocapillaris', Proc Natl Acad Sci U S A **106**(44), 18751–6.

[240] Saint-Geniez, M., Maharaj, A. S., Walshe, T. E., Tucker, B. A., Sekiyama, E., Kurihara, T., Darland, D. C., Young, M. J. and D'Amore, P. A. [2008], 'Endogenous vegf is required for visual function: evidence for a survival role on muller cells and photoreceptors', PLoS One **3**(11), e3554.

[241] Saint-Geniez, M., Maldonado, A. E. and D'Amore, P. A. [2006], 'Vegf expression and receptor activation in the choroid during development and in the adult', Invest Ophthalmol Vis Sci **47**(7), 3135–42.

[242] Sano, K., Katsuta, O., Shirae, S., Kubota, Y., Ema, M., Suda, T., Nakamura, M. and Hirashima, M. [2012], 'Flt1 and flk1 mediate regulation of intraocular pressure and their double heterozygosity causes the buphthalmia in mice', Biochem Biophys Res Commun **420**(2), 422–7.

[243] Santas, A. J., Bahler, C., Peterson, J. A., Filla, M. S., Kaufman, P. L., Tamm, E. R., Johnson, D. H. and Peters, D. M. [2003], 'Effect of heparin ii domain of fibronectin on aqueous outflow in cultured anterior segments of human eyes', Invest Ophthalmol Vis Sci **44**(11), 4796–804.

[244] Satchell, S. C. and Braet, F. [2009], 'Glomerular endothelial cell fenestrations: an integral component of the glomerular filtration barrier', Am J Physiol Renal Physiol **296**(5), F947–56.

[245] Sawada, O., Kawamura, H., Kakinoki, M., Sawada, T. and Ohji, M. [2007], 'Vascular endothelial growth factor in aqueous humor before and after intravitreal injection of bevacizumab in eyes with diabetic retinopathy', Arch Ophthalmol **125**(10), 1363–6.

[246] Schmucker, C. and Schaeffel, F. [2004], 'In vivo biometry in the mouse eye with low coherence interferometry', Vision Res **44**(21), 2445–56.

[247] Segal, O., Ferencz, J. R., Cohen, P., Nemet, A. Y. and Nesher, R. [2013], 'Persistent elevation of intraocular pressure following intravitreal injection of bevacizumab', Isr Med Assoc J **15**(7), 352–5.

[248] Senger, D. R., Galli, S. J., Dvorak, A. M., Perruzzi, C. A., Harvey, V. S. and Dvorak, H. F. [1983], 'Tumor cells secrete a vascular permeability factor that promotes accumulation of ascites fluid', Science **219**(4587), 983–5.

[249] Sherwood, J. M., Reina-Torres, E., Bertrand, J., Barnaby, R. and Overby, D. R. [2016], 'Measurement of outflow facility using iperfusion', PLoS One **11**, e0150694.

[250] Shikata, Y., Birukov, K. G. and Garcia, J. G. [2003], 'S1p induces fa remodeling in human pulmonary endothelial cells: role of rac, git1, fak, and paxillin', J Appl Physiol (1985) **94**(3), 1193–203.

[251] Sit, A. J., Coloma, F. M., Ethier, C. R. and Johnson, M. [1997], 'Factors affecting the pores of the inner wall endothelium of schlemm's canal', Invest Ophthalmol Vis Sci **38**(8), 1517–25.

[252] Sivak-Callcott, J. A., O'Day, D. M., Gass, J. D. and Tsai, J. C. [2001], 'Evidence-based recommendations for the diagnosis and treatment of neovascular glaucoma', Ophthalmology **108**(10), 1767–76; quiz1777, 1800.

[253] Smith, R. S. [2002], Systematic evaluation of the mouse eye : anatomy, pathology, and biomethods, first edn, CRC Press, Boca Raton ; London. editor-in-chief, Richard S. Smith ; co-editors, Simon W.M. John, Patsy M. Nishina, John P. Sundberg ; graphics and artwork by Jennifer L. Smith. Research methods for mutant mice. Includes bibliographical references and index.

[254] Smith, R. S., Zabaleta, A., Savinova, O. V. and John, S. W. [2001], 'The mouse anterior chamber angle and trabecular meshwork develop without cell death', BMC Dev Biol **1**, 3.

[255] Sniegowski, M., Mandava, N. and Kahook, M. Y. [2010], 'Sustained intraocular pressure elevation after intravitreal injection of bevacizumab and ranibizumab associated with trabeculitis', Open Ophthalmol J **4**, 28–9.

[256] Soohoo, J. R., Seibold, L. K. and Kahook, M. Y. [2014], 'The link between intravitreal antivascular endothelial growth factor injections and glaucoma', Curr Opin Ophthalmol **25**(2), 127–33.

[257] Spector, I., Shochet, N. R., Kashman, Y. and Groweiss, A. [1983], 'Latrunculins: novel marine toxins that disrupt microfilament organization in cultured cells', Science **219**(4584), 493–5.

[258] Stamer, W. D. and Acott, T. S. [2012], 'Current understanding of conventional outflow dysfunction in glaucoma', Curr Opin Ophthalmol **23**(2), 135–43.

[259] Stamer, W. D., Braakman, S. T., Zhou, E. H., Ethier, C. R., Fredberg, J. J., Overby, D. R. and Johnson, M. [2015], 'Biomechanics of schlemm's canal endothelium and intraocular pressure reduction', Prog Retin Eye Res **44**, 86–98.

[260] Stamer, W. D., Hoffman, E. A., Luther, J. M., Hachey, D. L. and Schey, K. L. [2011], 'Protein profile of exosomes from trabecular meshwork cells', J Proteomics **74**(6), 796–804.

[261] Stamer, W. D., Lei, Y., Boussommier-Calleja, A., Overby, D. R. and Ethier, C. R. [2011], 'enos, a pressure-dependent regulator of intraocular pressure', Invest Ophthalmol Vis Sci **52**(13), 9438–44.

[262] Stamer, W. D., Read, A. T., Sumida, G. M. and Ethier, C. R. [2009], 'Sphingosine-1-phosphate effects on the inner wall of schlemm's canal and outflow facility in perfused human eyes', Experimental Eye Research **89**(6), 980–988.

[263] Stan, R. V. [2004], 'Multiple pv1 dimers reside in the same stomatal or fenestral diaphragm', Am J Physiol Heart Circ Physiol **286**(4), H1347–53.

[264] Stan, R. V. [2005], 'Structure of caveolae', Biochimica Et Biophysica Acta-Molecular Cell Research **1746**(3), 334–348.

[265] Stan, R. V., Kubitza, M. and Palade, G. E. [1999], 'Pv-1 is a component of the fenestral and stomatal diaphragms in fenestrated endothelia', Proc Natl Acad Sci U S A **96**(23), 13203–7.

[266] Stan, R. V., Tkachenko, E. and Niesman, I. R. [2004], 'Pv1 is a key structural component for the formation of the stomatal and fenestral diaphragms', Mol Biol Cell **15**(8), 3615–30.

[267] Stan, R. V., Tse, D., Deharvengt, S. J., Smits, N. C., Xu, Y., Luciano, M. R., McGarry, C. L., Buitendijk, M., Nemani, K. V., Elgueta, R., Kobayashi, T., Shipman, S. L., Moodie, K. L., Daghlian, C. P., Ernst, P. A., Lee, H. K., Suriawinata, A. A., Schned, A. R., Longnecker, D. S., Fiering, S. N., Noelle, R. J., Gimi, B., Shworak, N. W. and Carriere, C. [2012], 'The diaphragms of fenestrated endothelia: gatekeepers of vascular permeability and blood composition', Dev Cell **23**(6), 1203–18.

[268] Steffan, A. M., Gendrault, J. L. and Kirn, A. [1987], 'Increase in the number of fenestrae in mouse endothelial liver cells by altering the cytoskeleton with cytochalasin b', Hepatology **7**(6), 1230–8.

[269] Stevenson, B. R., Siliciano, J. D., Mooseker, M. S. and Goodenough, D. A. [1986], 'Identification of zo-1: a high molecular weight polypeptide associated with the tight junction (zonula occludens) in a variety of epithelia', J Cell Biol **103**(3), 755–66.

[270] Strickland, L. A., Jubb, A. M., Hongo, J. A., Zhong, F., Burwick, J., Fu, L., Frantz, G. D. and Koeppen, H. [2005], 'Plasmalemmal vesicle-associated protein (plvap) is expressed by tumour endothelium and is upregulated by vascular endothelial growth factor-a (vegf)', J Pathol **206**(4), 466–75.

[271] Suzuki, T., Nakamura, Y., Moriya, T. and Sasano, H. [2003], 'Effects of steroid hormones on vascular functions', Microsc Res Tech **60**(1), 76–84.

[272] Svedbergh, B. [1976], 'Protrusions of the inner wall of schlemm's canal', Am J Ophthalmol **82**(6), 875–82.

[273] Takahashi, H. and Shibuya, M. [2005], 'The vascular endothelial growth factor (vegf)/vegf receptor system and its role under physiological and pathological conditions', Clin Sci (Lond) **109**(3), 227–41.

[274] Takai, Y., Tanito, M. and Ohira, A. [2012], 'Multiplex cytokine analysis of aqueous humor in eyes with primary open-angle glaucoma, exfoliation glaucoma, and cataract', Invest Ophthalmol Vis Sci **53**(1), 241–7.

[275] Tamm, E. R. [2009], 'The trabecular meshwork outflow pathways: Structural and functional aspects', Experimental Eye Research **88**(4), 648–655.

[276] Tamm, E. R., Braunger, B. M. and Fuchshofer, R. [2015], 'Intraocular pressure and the mechanisms involved in resistance of the aqueous humor flow in the trabecular meshwork outflow pathways', Prog Mol Biol Transl Sci **134**, 301–14.

[277] Tamm, E. R. and Fuchshofer, R. [2007], 'What increases outflow resistance in primary open-angle glaucoma?', Survey of Ophthalmology **52**(6, Supplement), S101–S104.

[278] Tamm, E. R.; Kellenberger, A. [2008], Aqueous humour dynamics and Trabecular Meshwork, MIT Press, Cambridge, Massachusetts, chapter 9, pp. 129 – 133.

[279] Tamm, E. R. and Lutjen-Drecoll, E. [1996], 'Ciliary body', Microsc Res Tech **33**(5), 390–439.

[280] Taraboletti, G., D'Ascenzo, S., Giusti, I., Marchetti, D., Borsotti, P., Millimaggi, D., Giavazzi, R., Pavan, A. and Dolo, V. [2006], 'Bioavailability of vegf in tumor-shed vesicles depends on vesicle burst induced by acidic ph', Neoplasia **8**(2), 96–103.

[281] The-AGIS-investigators [2000], 'The advanced glaucoma intervention study (agis): 7. the relationship between control of intraocular pressure and visual field deterioration.the agis investigators', Am J Ophthalmol **130**(4), 429–40.

[282] Tian, B., Kaufman, P. L., Volberg, T., Gabelt, B. T. and Geiger, B. [1998], 'H-7 disrupts the actin cytoskeleton and increases outflow facility', Arch Ophthalmol **116**(5), 633–43.

[283] Tille, J. C., Wang, X., Lipson, K. E., McMahon, G., Ferrara, N., Zhu, Z., Hicklin, D. J., Sleeman, J. P., Eriksson, U., Alitalo, K. and Pepper, M. S. [2003], 'Vascular endothelial growth factor (vegf) receptor-2 signaling mediates vegf-c(deltandeltac)- and vegf-a-induced angiogenesis in vitro', Exp Cell Res **285**(2), 286–98.

[284] Tischer, E., Mitchell, R., Hartman, T., Silva, M., Gospodarowicz, D., Fiddes, J. C. and Abraham, J. A. [1991], 'The human gene for vascular endothelial growth factor. multiple protein forms are encoded through alternative exon splicing', J Biol Chem **266**(18), 11947–54.

[285] Tong, J. P., Chan, W. M., Liu, D. T., Lai, T. Y., Choy, K. W., Pang, C. P. and Lam, D. S. [2006], 'Aqueous humor levels of vascular endothelial growth factor and pigment epithelium-derived factor in polypoidal choroidal vasculopathy and choroidal neovascularization', Am J Ophthalmol **141**(3), 456–62.

[286] Toris, C. B., Camras, C. B. and Yablonski, M. E. [1999], 'Acute versus chronic effects of brimonidine on aqueous humor dynamics in ocular hypertensive patients', American Journal of Ophthalmology **128**(1), 8–14.

[287] Tripathi, R. C. [1977], 'Pathologic anatomy in the outflow pathway of aqueous humour in chronic simple glaucoma', Exp Eye Res **25 Suppl**, 403–7.

[288] Tripathi, R. C., Li, J. P., Tripathi, B. J., Chalam, K. V. and Adamis, A. P. [1998], 'Increased level of vascular endothelial growth factor in aqueous humor of patients with neovascular glaucoma', Ophthalmology **105**(2), 232–237.

[289] Tseng, J. J., Vance, S. K., Della Torre, K. E., Mendonca, L. S., Cooney, M. J., Klancnik, J. M., Sorenson, J. A. and Freund, K. B. [2012], 'Sustained increased intraocular pressure related to intravitreal antivascular endothelial growth factor therapy for neovascular age-related macular degeneration', J Glaucoma **21**(4), 241–7.

[290] Tzima, E., Irani-Tehrani, M., Kiosses, W. B., Dejana, E., Schultz, D. A., Engelhardt, B., Cao, G., DeLisser, H. and Schwartz, M. A. [2005], 'A mechanosensory complex that mediates the endothelial cell response to fluid shear stress', Nature **437**(7057), 426–31.

[291] Underwood, J. L., Murphy, C. G., Chen, J., Franse-Carman, L., Wood, I., Epstein, D. L. and Alvarado, J. A. [1999], 'Glucocorticoids regulate transendothelial fluid flow resistance and formation of intercellular junctions', Am J Physiol **277**(2 Pt 1), C330–42.

[292] Uniprot [2015], 'Vascular endothelial growth factor a', http://www.uniprot.org/uniprot/P15692 .

[293] van der Merwe, E. L. and Kidson, S. H. [2014], 'The three-dimensional organisation of the post-trabecular aqueous outflow pathway and limbal vasculature in the mouse', Exp Eye Res **125**, 226–35.

[294] van Wetering, S., van Buul, J. D., Quik, S., Mul, F. P., Anthony, E. C., ten Klooster, J. P., Collard, J. G. and Hordijk, P. L. [2002], 'Reactive oxygen species mediate rac-induced loss of cell-cell adhesion in primary human endothelial cells', J Cell Sci **115**(Pt 9), 1837–46.

[295] van Wetering, S., van den Berk, N., van Buul, J. D., Mul, F. P., Lommerse, I., Mous, R., ten Klooster, J. P., Zwaginga, J. J. and Hordijk, P. L. [2003], 'Vcam-1-mediated rac signaling controls endothelial cell-cell contacts and leukocyte transmigration', Am J Physiol Cell Physiol **285**(2), C343–52.

[296] Veilleux-Lemieux, D., Castel, A., Carrier, D., Beaudry, F. and Vachon, P. [2013], 'Pharmacokinetics of ketamine and xylazine in young and old sprague-dawley rats', J Am Assoc Lab Anim Sci **52**(5), 567–70.

[297] Vouret-Craviari, V., Bourcier, C., Boulter, E. and van Obberghen-Schilling, E. [2002], 'Distinct signals via rho gtpases and src drive shape changes by thrombin and sphingosine-1-phosphate in endothelial cells', J Cell Sci **115**(Pt 12), 2475–84.

[298] Walford, G. and Loscalzo, J. [2003], 'Nitric oxide in vascular biology', J Thromb Haemost **1**(10), 2112–8.

[299] Walsh, M. M., Yi, H., Friedman, J., Cho, K. I., Tserentsoodol, N., McKinnon, S., Searle, K., Yeh, A. and Ferreira, P. A. [2009], 'Gene and protein expression pilot profiling and biomarkers in an experimental mouse model of hypertensive glaucoma', Exp Biol Med (Maywood) **234**(8), 918–30.

[300] Waltenberger, J., Claesson-Welsh, L., Siegbahn, A., Shibuya, M. and Heldin, C. H. [1994], 'Different signal transduction properties of kdr and flt1, two receptors for vascular endothelial growth factor', J Biol Chem **269**(43), 26988–95.

[301] Wang, J. W., Zhou, M. W., Zhang, X., Huang, W. B., Gao, X. B., Wang, W., Chen, S., Zhang, X. Y., Ding, X. Y. and Jonas, J. B. [2015], 'Short-term effect of intravitreal ranibizumab on intraocular concentrations of vascular endothelial growth factor-a and pigment epithelium-derived factor in neovascular glaucoma', Clin Experiment Ophthalmol **43**(5), 415–21.

[302] Wang, W. H., Millar, J. C., Pang, I. H., Wax, M. B. and Clark, A. F. [2005], 'Noninvasive measurement of rodent intraocular pressure with a rebound tonometer', Invest Ophthalmol Vis Sci **46**(12), 4617–21.

[303] Wang, W., Merrill, M. J. and Borchardt, R. T. [1996], 'Vascular endothelial growth factor affects permeability of brain microvessel endothelial cells in vitro', Am J Physiol **271**(6 Pt 1), C1973–80.

[304] Whitlock, N. A., McKnight, B., Corcoran, K. N., Rodriguez, L. A. and Rice, D. S. [2010], 'Increased intraocular pressure in mice treated with dexamethasone', Invest Ophthalmol Vis Sci **51**(12), 6496–503.

[305] Whittles, C. E., Pocock, T. M., Wedge, S. R., Kendrew, J., Hennequin, L. F., Harper, S. J. and Bates, D. O. [2002], 'Zm323881, a novel inhibitor of vascular endothelial growth factor-receptor-2 tyrosine kinase activity', Microcirculation **9**(6), 513–22.

[306] Winkler, N. S. and Fautsch, M. P. [2014], 'Effects of prostaglandin analogues on aqueous humor outflow pathways', J Ocul Pharmacol Ther **30**(2-3), 102–9.

[307] Wisniewska-Kruk, J., Hoeben, K. A., Vogels, I. M., Gaillard, P. J., Van Noorden, C. J., Schlingemann, R. O. and Klaassen, I. [2012], 'A novel co-culture model of the blood-retinal barrier based on primary retinal endothelial cells, pericytes and astrocytes', Exp Eye Res **96**(1), 181–90.

[308] Wisniewska-Kruk, J., Klaassen, I., Vogels, I. M., Magno, A. L., Lai, C. M., Van Noorden, C. J., Schlingemann, R. O. and Rakoczy, E. P. [2014], 'Molecular analysis of blood-retinal barrier loss in the akimba mouse, a model of advanced diabetic retinopathy', Exp Eye Res **122C**, 123–131.

[309] Witmer, A. N., van Blijswijk, B. C., van Noorden, C. J., Vrensen, G. F. and Schlingemann, R. O. [2004], 'In vivo angiogenic phenotype of endothelial cells and pericytes induced by vascular endothelial growth factor-a', J Histochem Cytochem **52**(1), 39–52.

[310] Woolard, J., Wang, W. Y., Bevan, H. S., Qiu, Y., Morbidelli, L., Pritchard-Jones, R. O., Cui, T. G., Sugiono, M., Waine, E., Perrin, R., Foster, R., Digby-Bell, J., Shields, J. D., Whittles, C. E., Mushens, R. E., Gillatt, D. A., Ziche, M., Harper, S. J. and Bates, D. O. [2004], 'Vegf165b, an inhibitory vascular endothelial growth factor splice variant: mechanism of action, in vivo effect on angiogenesis and endogenous protein expression', Cancer Res **64**(21), 7822–35.

[311] Wu, H. M., Huang, Q., Yuan, Y. and Granger, H. J. [1996], 'Vegf induces no-dependent hyperpermeability in coronary venules', Am J Physiol **271**(6 Pt 2), H2735–9.

[312] WuDunn, D. [2009], 'Mechanobiology of trabecular meshwork cells', Experimental Eye Research **88**(4), 718–723.

[313] Yan, D. B., Trope, G. E., Ethier, C. R., Menon, I. A. and Wakeham, A. [1991], 'Effects of hydrogen peroxide-induced oxidative damage on outflow facility and washout in pig eyes', Invest Ophthalmol Vis Sci **32**(9), 2515–20.

[314] Yang, S. and Zhang, L. [2004], 'Glucocorticoids and vascular reactivity', Curr Vasc Pharmacol **2**(1), 1–12.

[315] Yannuzzi, N. A., Patel, S. N., Bhavsar, K. V., Sugiguchi, F. and Freund, K. B. [2014], 'Predictors of sustained intraocular pressure elevation in eyes receiving intravitreal anti-vascular endothelial growth factor therapy', Am J Ophthalmol **158**(2), 319–327 e2.

[316] Zachary, I. and Gliki, G. [2001], 'Signaling transduction mechanisms mediating biological actions of the vascular endothelial growth factor family', Cardiovasc Res **49**(3), 568–81.

[317] Zhang, Y., Davidson, B. R., Stamer, W. D., Barton, J. K., Marmorstein, L. Y. and Marmorstein, A. D. [2009], 'Enhanced inflow and outflow rates despite lower iop in bestrophin-2-deficient mice', Invest Ophthalmol Vis Sci **50**(2), 765–70.

[318] Zhou, Y., Grinchuk, O. and Tomarev, S. I. [2008], 'Transgenic mice expressing the tyr437his mutant of human myocilin protein develop glaucoma', Invest Ophthalmol Vis Sci **49**(5), 1932–9.

[319] Zode, G. S., Sharma, A. B., Lin, X., Searby, C. C., Bugge, K., Kim, G. H., Clark, A. F. and Sheffield, V. C. [2014], 'Ocular-specific er stress reduction rescues glaucoma in murine glucocorticoid-induced glaucoma', J Clin Invest **124**(5), 1956–65.

Appendix I: Representative elecrophoresis gel for PLVAP transgenic mice genotyping.

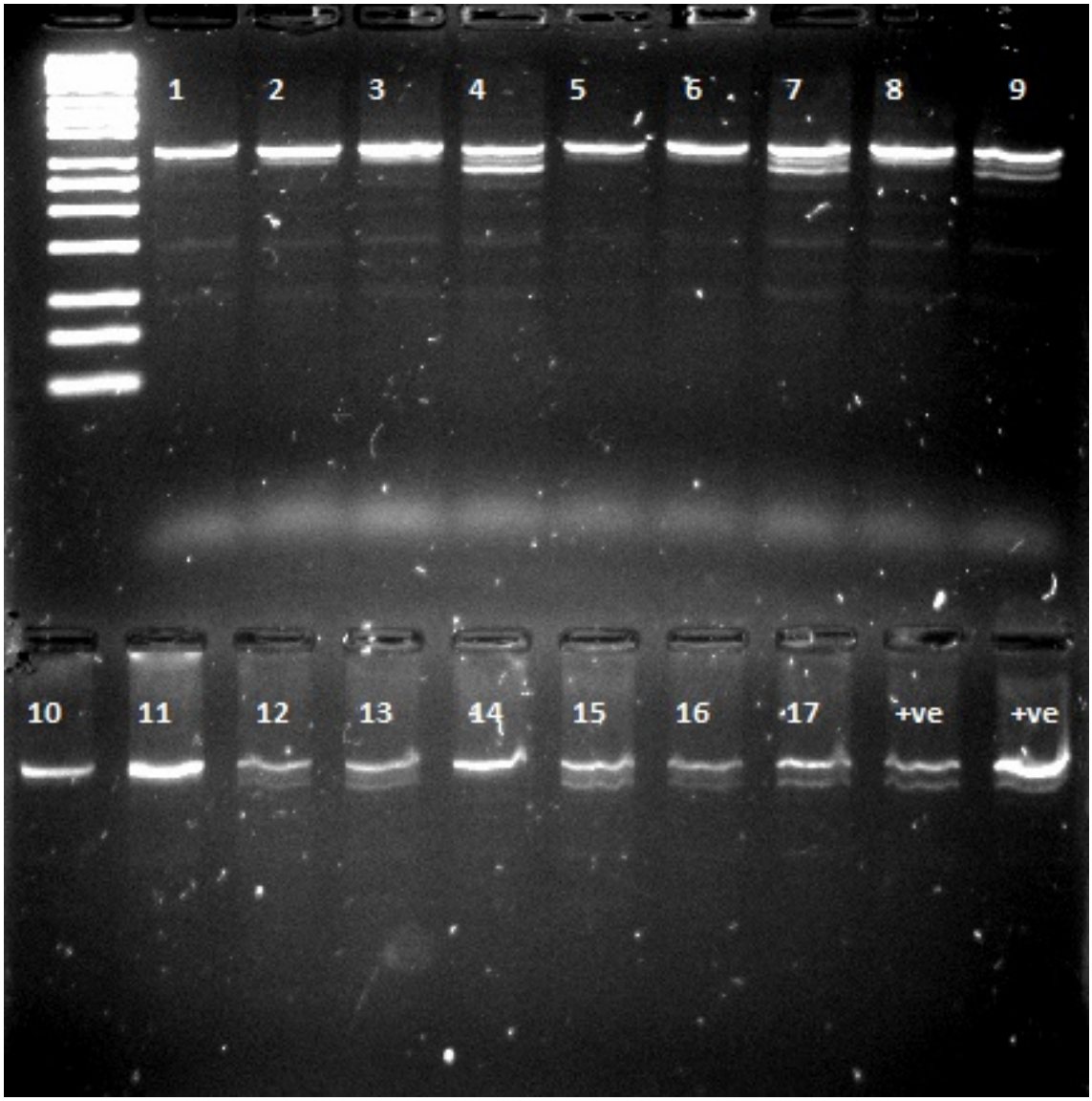


Figure 7.1: Representative gel electrophoresis for PLVAP transgenic mice genotyping. Each line represents one mouse, 1 band corresponds to *Plvap*$^{+/+}$ mice while 2 bands correspond to *Plvap*$^{+/-}$.

Appendix II: Permission Documents for Reprint.

De: **ukcustomerservice** ukcustomerservice@britannica.co.uk
Tema: (REINA-TORRES, Esther) Britannica [AM]
Data: 26 d'octubre de 2015, 13:33
Per a: Reina Torres, Ester e.reina-torres12@imperial.ac.uk

U

Dear Ester Reina-Torres

Thank you for your e-mail.

You can reproduce any image that has the Encyclopaedia Britannica credit attributed to it within your thesis as long as you cite the source of the image correctly. We provide citation option with all of the articles and images.

Kind regards

Britannica Customer Service

If you can include any previous message history in your reply it will speed up the time it takes to reply.

We hope that this is of some help to you. If you require further assistance with this, please do not hesitate to contact us on 0800 282433 or +44 207 500 7843 for customers outside the UK.

Encyclopædia Britannica (UK) Ltd
Registered in England and Wales: Number 3830890

From: Reina Torres, Ester [e.reina-torres12@imperial.ac.uk]
Sent: 20 October 2015 14:18
To: enquiries - General Enquiries at Britannica.co.uk
Subject: Reproduction of one of your figures

Dear Sir/Madam,

I write to you because I want to include one of the images in the Encyclopædia Britannica ("eye, human: horizontal section") in my PhD thesis and I was wondering if it is necessary to have some kind of permission for reproduction from you or citing the source is enough.

Thank you very much in advance.

Kind regards,

Ester Reina-Torres
.....

Ester Reina-Torres - PhD Student
Department of Bioengineering
Imperial College London
South Kensington Campus
London SW7 2AZ

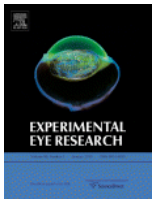
Figure 7.2: Permission for reproduction Figure.1.1



Figure 7.3: Permission for reproduction Figure.1.2

Copyright Clearance Center RightsLink®

Home | Account Info | Help | Live Chat



Title: The Inner Wall of Schlemm's Canal
Author: C. Ross Ethier
Publication: Experimental Eye Research
Publisher: Elsevier
Date: February 2002

Copyright © 2002 Elsevier Science Ltd. All rights reserved.

Logged in as:
Ester Reina
LOGOUT

Order Completed

Thank you very much for your order.

This is a License Agreement between Ester Reina-Torres ("You") and Elsevier ("Elsevier"). The license consists of your order details, the terms and conditions provided by Elsevier, and the payment terms and conditions.

Get the printable license.

License Number	3770841284069
License date	Dec 16, 2015
Licensed content publisher	Elsevier
Licensed content publication	Experimental Eye Research
Licensed content title	The Inner Wall of Schlemm's Canal
Licensed content author	C. Ross Ethier
Licensed content date	February 2002
Licensed content volume number	74
Licensed content issue number	2
Number of pages	12
Type of Use	reuse in a thesis/dissertation
Portion	figures/tables/illustrations
Number of figures/tables /illustrations	1
Format	both print and electronic
Are you the author of this Elsevier article?	No
Will you be translating?	No
Original figure numbers	1
Title of your thesis/dissertation	Enhancing hydraulic conductivity of Schlemm's canal endothelium as a potential treatment for glaucoma
Expected completion date	Jan 2016
Estimated size (number of pages)	170
Elsevier VAT number	GB 494 6272 12
Permissions price	0.00 USD
VAT/Local Sales Tax	0.00 USD / 0.00 GBP
Total	0.00 USD

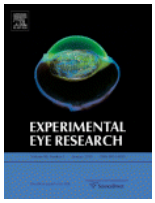
ORDER MORE... CLOSE WINDOW

Copyright © 2015 Copyright Clearance Center, Inc. All Rights Reserved. Privacy statement. Terms and Conditions.
Comments? We would like to hear from you. E-mail us at customercare@copyright.com

Figure 7.4: Permission for reproduction Figure.1.3

Copyright Clearance Center RightsLink®

Home Account Info Help Live Chat



Title: A model of giant vacuole dynamics in human Schlemm's canal endothelial cells

Author: Ryan M. Pedrigi,David Simon,Ashley Reed,W. Daniel Stamer,Darryl R. Overby

Publication: Experimental Eye Research

Publisher: Elsevier

Date: January 2011

Copyright © 2010 Elsevier Ltd. All rights reserved.

Logged in as:
Ester Reina
LOGOUT

Order Completed

Thank you very much for your order.

This is a License Agreement between Ester Reina-Torres ("You") and Elsevier ("Elsevier"). The license consists of your order details, the terms and conditions provided by Elsevier, and the payment terms and conditions.

Get the printable license.

License Number	3770840867894
License date	Dec 16, 2015
Licensed content publisher	Elsevier
Licensed content publication	Experimental Eye Research
Licensed content title	A model of giant vacuole dynamics in human Schlemm's canal endothelial cells
Licensed content author	Ryan M. Pedrigi,David Simon,Ashley Reed,W. Daniel Stamer,Darryl R. Overby
Licensed content date	January 2011
Licensed content volume number	92
Licensed content issue number	1
Number of pages	10
Type of Use	reuse in a thesis/dissertation
Portion	figures/tables/illustrations
Number of figures/tables /illustrations	1
Format	both print and electronic
Are you the author of this Elsevier article?	No
Will you be translating?	No
Original figure numbers	1
Title of your thesis/dissertation	Enhancing hydraulic conductivity of Schlemm's canal endothelium as a potential treatment for glaucoma
Expected completion date	Jan 2016
Estimated size (number of pages)	170
Elsevier VAT number	GB 494 6272 12
Permissions price	0.00 USD
VAT/Local Sales Tax	0.00 USD / 0.00 GBP
Total	0.00 USD

ORDER MORE... CLOSE WINDOW

Copyright © 2015 Copyright Clearance Center, Inc. All Rights Reserved. Privacy statement. Terms and Conditions.
Comments? We would like to hear from you. E-mail us at customercare@copyright.com

Figure 7.5: Permission for reproduction Figure.1.4

Copyright Clearance Center RightsLink®

My Orders My Library My Profile

Welcome e.reina-torres12@imperial.ac.uk Log out | Help

My Orders > Orders > All Orders

License Details

Thank you very much for your order.

This is a License Agreement between Ester Reina ("You") and Elsevier ("Elsevier"). The license consists of your order details, the terms and conditions provided by Elsevier, and the payment terms and conditions.

Get the printable license.

License Number	3770841063185
License date	Dec 16, 2015
Licensed Content Publisher	Elsevier
Licensed Content Publication	Experimental Eye Research
Licensed Content Title	Biomechanical strain as a trigger for pore formation in Schlemm's canal endothelial cells
Licensed Content Author	Sietse T. Braakman,Ryan M. Pedrigi,A. Thomas Read,James A.E. Smith,W. Daniel Stamer,C. Ross Ethier,Darryl R. Overby
Licensed Content Date	October 2014
Licensed content volume number	127
Licensed content issue number	n/a
Number of pages	12
Type of Use	reuse in a thesis/dissertation
Portion	figures/tables/illustrations
Number of figures/tables/illustrations	1
Format	both print and electronic
Are you the author of this Elsevier article?	No
Will you be translating?	No
Original figure numbers	3
Title of your thesis/dissertation	Enhancing hydraulic conductivity of Schlemm's canal endothelium as a potential treatment for glaucoma
Expected completion date	Jan 2016
Estimated size (number of pages)	170
Elsevier VAT number	GB 494 6272 12
Price	0.00 USD
VAT/Local Sales Tax	0.00 USD / 0.00 GBP
Total	**0.00 USD**

BACK

Copyright © 2015 Copyright Clearance Center, Inc. All Rights Reserved. Privacy statement . Terms and Conditions . Comments? We would like to hear from you. E-mail us at customercare@copyright.com

Figure 7.6: Permission for reproduction Figure.1.5

De: **Debbie Chin** dchin@arvo.org
Tema: RE: Permission for reproduction in PhD thesis
Data: 30 de desembre de 2015, 18:11
Per a: Reina Torres, Ester e.reina-torres12@imperial.ac.uk

DC

Dear Ester Reina-Torres,

Permission is hereby granted to reprint the following figures in your PhD thesis for Imperial College London:

Figure 5 from Bhatt K, Gong H, Freddo TF. Freeze-fracture studies of interendothelial junctions in the angle of the human eye. Invest Ophthalmol Vis Sci. 1995;36:1379-1389.

Figure 1 from Overby D, Gong H, Qiu G, Freddo TF, Johnson M. The mechanism of increasing outflow facility during washout in the bovine eye. Invest Ophthalmol Vis Sci. 2002;43:3455-3464.

A reprint of this material must include full article citations and acknowledge ARVO as the copyright holder.

Best regards,

Debbie Chin
ARVO Journals

Figure 7.7: Permission for reproduction Figure.1.6a and Figure.1.7



My Orders | My Library | My Profile

Welcome e.reina-torres12@imperial.ac.uk Log out | Help

My Orders > Orders > All Orders

License Details

Thank you very much for your order.

This is a License Agreement between Ester Reina ("You") and Elsevier ("Elsevier"). The license consists of your order details, the terms and conditions provided by Elsevier, and the payment terms and conditions.

Get the printable license.

License Number	3770841063185
License date	Dec 16, 2015
Licensed Content Publisher	Elsevier
Licensed Content Publication	Experimental Eye Research
Licensed Content Title	Biomechanical strain as a trigger for pore formation in Schlemm's canal endothelial cells
Licensed Content Author	Sietse T. Braakman,Ryan M. Pedrigi,A. Thomas Read,James A.E. Smith,W. Daniel Stamer,C. Ross Ethier,Darryl R. Overby
Licensed Content Date	October 2014
Licensed content volume number	127
Licensed content issue number	n/a
Number of pages	12
Type of Use	reuse in a thesis/dissertation
Portion	figures/tables/illustrations
Number of figures/tables/illustrations	1
Format	both print and electronic
Are you the author of this Elsevier article?	No
Will you be translating?	No
Original figure numbers	3
Title of your thesis/dissertation	Enhancing hydraulic conductivity of Schlemm's canal endothelium as a potential treatment for glaucoma
Expected completion date	Jan 2016
Estimated size (number of pages)	170
Elsevier VAT number	GB 494 6272 12
Price	0.00 USD
VAT/Local Sales Tax	0.00 USD / 0.00 GBP
Total	**0.00 USD**

BACK

Copyright © 2015 Copyright Clearance Center, Inc. All Rights Reserved. Privacy statement . Terms and Conditions . Comments? We would like to hear from you. E-mail us at customercare@copyright.com

Figure 7.8: Permission for reproduction Figure.1.6b

Copyright Clearance Center RightsLink®

Home | Account Info | Help | Live Chat



Title: Vascular endothelial growth factor in eye disease

Author: J.S. Penn,A. Madan,R.B. Caldwell,M. Bartoli,R.W. Caldwell,M.E. Hartnett

Publication: Progress in Retinal and Eye Research

Publisher: Elsevier

Date: July 2008

Copyright © 2008 Elsevier Ltd. All rights reserved.

Logged in as:
Ester Reina-Torres
Account #: 3000983546
LOGOUT

Order Completed

Thank you very much for your order.

This is a License Agreement between Ester Reina-Torres ("You") and Elsevier ("Elsevier"). The license consists of your order details, the terms and conditions provided by Elsevier, and the payment terms and conditions.

Get the printable license.

License Number	3774130745202
License date	Dec 22, 2015
Licensed content publisher	Elsevier
Licensed content publication	Progress in Retinal and Eye Research
Licensed content title	Vascular endothelial growth factor in eye disease
Licensed content author	J.S. Penn,A. Madan,R.B. Caldwell,M. Bartoli,R.W. Caldwell,M.E. Hartnett
Licensed content date	July 2008
Licensed content volume number	27
Licensed content issue number	4
Number of pages	41
Type of Use	reuse in a thesis/dissertation
Portion	figures/tables/illustrations
Number of figures/tables /illustrations	1
Format	both print and electronic
Are you the author of this Elsevier article?	No
Will you be translating?	No
Original figure numbers	1
Title of your thesis/dissertation	Enhancing hydraulic conductivity of Schlemm's canal endothelium as a potential treatment for glaucoma
Expected completion date	Jan 2016
Estimated size (number of pages)	170
Elsevier VAT number	GB 494 6272 12
Permissions price	0.00 GBP
VAT/Local Sales Tax	0.00 GBP / 0.00 GBP
Total	0.00 GBP

ORDER MORE... CLOSE WINDOW

Copyright © 2015 Copyright Clearance Center, Inc. All Rights Reserved. Privacy statement. Terms and Conditions.
Comments? We would like to hear from you. E-mail us at customercare@copyright.com

Figure 7.9: Permission for reproduction Figure.1.8